



MARMARA UNIVERSITY
INSTITUTE FOR GRADUATE STUDIES
IN PURE AND APPLIED SCIENCES



**ULTRAFAST SPIN DYNAMICS IN DILUTED
MAGNETIC SEMICONDUCTOR
NANOSTRUCTURES**

MUHAMMET ARUCU

Ph.D. THESIS

Department of Physics

Thesis Supervisor

Prof. Dr. Şahin AKTAŞ

Thesis Second Supervisor

Prof. Dr. Roy W. Chantrell

ISTANBUL, 2015



MARMARA UNIVERSITY
INSTITUTE FOR GRADUATE STUDIES
IN PURE AND APPLIED SCIENCES



**ULTRAFAST SPIN DYNAMICS IN DILUTED
MAGNETIC SEMICONDUCTOR
NANOSTRUCTURES**

MUHAMMET ARUCU

(721213701)

Ph.D. THESIS

Department of Physics

Thesis Supervisor

Prof. Dr. Şahin AKTAŞ

Thesis Second Supervisor

Prof. Dr. Roy W. Chantrell

MARMARA UNIVERSITY
INSTITUTE FOR GRADUATE STUDIES
IN PURE AND APPLIED SCIENCES

Muhammet ARUCU, a Doctor of Philosophy student of Marmara University Institute for Graduate Studies in Pure and Applied Sciences, defended his thesis entitled “Ultrafast Spin Dynamics in Diluted Magnetic Semiconductor Nanostructures”, on **June 16, 2015** and has been found to be satisfactory by the jury members.

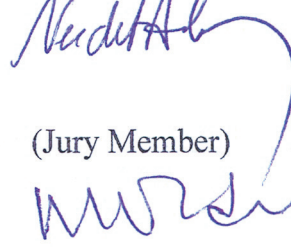
Jury Members

Prof.Dr. Şahin AKTAŞ
Marmara University

(Advisor)


Prof. Dr. Necdet ASLAN
Yeditepe University

(Jury Member)



Assoc.Prof.Dr. Mustafa ÖZDEMİR
Turkish Atomic Energy Authority

(Jury Member)



Assoc.Prof.Dr. Lütfi ARDA
Bahçeşehir University

(Jury Member)



Assist.Prof.Dr. Cihat BOYRAZ
Marmara University

(Jury Member)

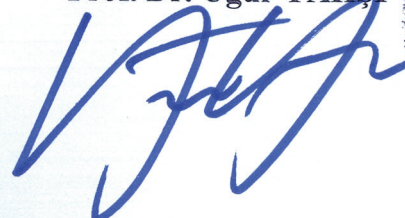


APPROVAL

Marmara University Institute for Graduate Studies in Pure and Applied Sciences Executive Committee approves that Muhammet ARUCU be granted the degree of **Doctor of Philosophy** in **Department of Physics, Physics Program** on **03.07.2015** . (Resolution no: **2015/14-02**)

Director of the Institute

Prof. Dr. Uğur YAHSI





...dedicated this thesis to my beloved wife and my parents.

Declaration

I hereby declare that the contents of this dissertation are original and have not been submitted in whole or in part for consideration for any other degree or qualification in this, or any other university. Otherwise stated, this dissertation is my original work and contains nothing but the outcome of the work done in collaboration with Professor Roy Chantrell's Computational Magnetism group of University of York. This dissertation contains no fewer than 35,000 words including appendices, bibliography, tables and equations and has fewer than 80 figures.

Muhammet Arucu

June 2015

Acknowledgements

First of all, I would especially like to thank my PhD. supervisor Prof.Dr. Şahin Aktaş from Marmara University-Turkey and Prof.Dr. Roy W. Chantrell from University of York-UK for their enthusiasm in guiding my thesis, which have been inspirational and helpful. Without their support, not only in academics but also in my personal life in Ağrı, Istanbul, York as a Ph.D. graduate student, I could have never advanced during my PhD. studies. I have benefited tremendously from the many opportunities provided to me. It is a great pleasure to express my gratitude that going to University of York for a part of my graduate research is one of my best decisions.

Second, I would like to thank a genius post-doc, Dr. Richard Evans as well, who have been very generous to mentor me for all the information about computer programming, code writing, spin dynamics. I would especially like to thank him about VAMPIRE package program, which played an important role in the success of my PhD. research. With his patience, motivation and friendship, I have accomplished completing this thesis. His enthusiasm in doing research as a physicist have been a magnificent reference to me in my future academic life.

I would also like to extend my sincere acknowledgement to another genius post-doc, Dr. Thomas Ostler, who helped me a lot in proofreading, mentoring and guidance during writing of this thesis.

I must thank all the members of York computational magnetism group: Dr. Joseph Baker, Dr. Ramon Cuadrado, Mr. Matthew Ellis, Mr. Sergiu Ruta, Mr. Andrea Meo, Mr. Sam Westmoreland, Mr. Razvan Ababei and others for their invaluable help and suggestions.

I would also like to express my gratitude to my co-workers Dr. İlhan Yavuz, İzzet Paruğ Duru, and others from Marmara University and Ağrı Ibrahim Çeçen University.

Furthermore, I would like to thank Miss Claire Sayers, the editorial assistant of Professor Roy Chantrell, for official affairs and correspondences, FEMTOMAG summer school leader Prof.Dr. Theo Rasing and his research team at Radboud University-Nijmegen for giving lectures on femto-second magnetism.

I would also like to thank Marmara University-Turkey, Council of Higher Education-Turkey, University of York-UK, Radboud University-Netherlands and Turkish Petrol Foundation-Turkey for financial support.

Finally, I would like to thank my beloved wife, Damla, who has been encouraging and supportive in many ways throughout my graduate studies. I would like to extend my gratitude to my parents for their financial and moral supports in my entire educational life.

Özet

Seyreltilmiş manyetik yarı iletken (DMS) manyetik bir malzemedir, ki o manyetik toprak elementleri ve geçiş metallerin yarı iletken malzemeye katılanmasıdır. Bu tür yeni nesil elektronik malzemelerde kullanılan DMS malzemeler spin elektronuğunun temelidir. Bu yüzden ferromanyetik yarı iletken malzemeler oda sıcaklığının üstünde Curie sıcaklığına (T_c) sahiptir ve ideal bir spintronik aygıttır. Nobel Ödüllü dev magnetorezistansın (GMR) keşfinden beri, elektronun spini mikroelektronik alanında önemi gittikçe artmaktadır. Hatta kuantum bilgisayarlar spintronik arařtırmalarındaki öneminden dolayı, kuantum kriptografi, kuantum iletişim alanlarında spintronik uygulamaların birçok arařtırmacı için ilham kaynağı olmuştur. Ancak, DMS oda sıcaklığı ferromanyetizması akademik arařtırmalarda hala tartışmalıdır. Bu nedenle, biz bu tezde DMS'lerin manyetik özelliklerini detaylı olarak inceledik.

Spintronik olarak bilinen yeni nesil elektronik cihazların sektörünün hızlı gelişmesi eğilimindedir. Bu yeni nesil cihazlar veri aktarım hızı, dijital depolama, güç tüketimi, sensörler, optoelektronik, fotovoltaik gibi özellikler bakımından elektronik ağıtlar için önemli avantajlara sahiptir. Bu tür seyreltilmiş manyetik yarı iletkenler yeni bir sınıf Spintronik (Spin + elektronik) malzeme olarak tarif edilmektedir. Bu malzemeler geçiş metali veya toprak grubu elementleri ile katkılıandığında farklı manyetik özellikler gösterebilirler. Bu malzemeler periyodik cetvelde II-VI grubunda (ZnO, ...) veya III-V grubunda (GaAs, ...) yer alır. Şimdiye kadar en çok çalışılan DMS malzeme III-V grubu (Ga,Mn)As elementleridir. Daha sonra, (Zn,TM)O materyalleri detaylı olarak incelenmiştir ($TM : Mn, Ni, Co$). Bu tezdeki amacımız, yukarıda verilen bilgiler ışığında geçiş metalinin (TM) ZnO kristal

malzemesine katkılayıp bu malzemenin manyetik özelliklerini inceleyerek yeni teori yöntemler geliştirmek.

Bu tezde (Zn,TM)O tabanlı malzemelerin manyetik özellikleri, yeni teknoloji uygulamaları için nanometre boyutlarında malzemeye sıcaklık, manyetik ve lazer atma etkisi altında incelenmiştir. Çalışmamızda Co katkılı ZnO kristali farklı parametrelere göre veya uygulanan harici manyetik alan altında ferromanyetik, paramanyetik, superparamanyetik, antiferromanyetik ve spin camı gibi davranışlar göstermiştir. Bu örnekler $x \approx 0.3$ için $Zn_{1-x}Co_xO$ sıfır alanda (ZFC) and alanda soğutulmuş (FC) malzeme 20 K civarında sırasıyla spin camı ve süperparamanyetik özellik göstermiştir. Küçük x değerleri için, CoZnO ferromanyetik, büyük x değerleri için ise antiferromanyetik özellik göstermiştir.

Bu çalışmada, York Üniversitesi hesaplamalı fizik manyetizma grubu tarafından geliştirilen yüksek performanslı atomistik simulasyon programı VAMPIRE yazılım paketi kullanıldı[1]. Tez çalışmamızı üç kategoride sınıflandırabiliriz. Çalışmalara başlamadan önce, ilk olarak, ZnO wurtzite kristal yapısının kodu C++ programlama dilinde yazıldı. Daha sonra, Ruderman-Kittel-Kasuya-Yosida (RKKY) etkileşimi kullanarak, atomlar arası değiş tokuş etkileşimleri incelendi. İkinci olarak, bu yapılar için, Landau-Lifshitz-Gilbert (LLG) spin hareket denklemi ile Monte Carlo ve Heun yöntemi kullanılarak 5 nm, 10 nm ve 20 nm gibi farklı boyutlarda ve parametrelerde sistemlerin manyetik özelliklerini araştırdık. Üçüncü olarak, farklı Co katkı oranlarında ZnO kristal yapılarına lazer kaynaklarının etkisi incelendi. Son olarak da, sonuçların önemli kısımları yorumlanarak bu çalışmanın sonuçları ve yeni uygulamaları tartışıldı.

Abstract

A dilute magnetic semiconductor(DMS) is a magnetic material where a part of the host cations are replaced by magnetic ions of rare earths or transition metals. These leads to localized magnetic moments in the semiconductor materials. Therefore DMS is the key materials for spin electronics where not only charge but also spin of electrons are used for electronic devices. Since the discovery of giant magnetoresistance(GMR) resulting of Nobel Prize, the spin of the electron has drawn attention in the field of microelectronics. Although spintronics research lead to quantum computers, quantum cryptography, and quantum communications, closer spintronic applications have inspired many researchers. Ferromagnetic semiconductors with Curie temperature (T_c) above room temperature are ideal as spintronics devices. However, the origin of room temperature ferromagnetism in DMS is still controversial in the literature. In this thesis we examined their feasibility in terms of magnetic properties.

New generation of electronic devices known as spintronic has lead to the rapid developing field of industry. These new generation devices have significant advantages over conventional electronics in properties such as speed, digital storage, power consumption, sensors, optoelectronics, photovoltaics. By taking into account the properties of magnetics with that of semiconductors, the new class of materials known as dilute magnetic semiconductors are described as spintronic (spin+electronic) materials. These materials depend on a quantity of transition metal or rare earth atoms which can exhibit different magnetic properties. Generally, these materials is located in II-VI group (ZnO, ...) or III-V group (GaAs, ...) in the periodic table. The most widely studied DMS is (Ga,Mn)As which has been well characterized using standard III-V manufacturing techniques in industry field for further

technology. Subsequently, (Zn,TM)O materials were intensively investigated. The goal of this thesis was to develop novel theory methods to understand the properties of transition metal (TM) ions ($TM = Mn, Ni, Co$) doped ZnO.

In this thesis the properties of (Zn,TM)O based systems are studied in relation to the material dimensions, temperature effect, magnetic effect, laser pulse effect in nanometre length scales for new technology applications. Samples of Co doped ZnO crystals showed ferromagnetic, paramagnetic, superparamagnetic, antiferromagnetic and spin glass behaviour with the magnetic element doped and different external magnetic field. Zero field cooled (ZFC) and field cooled magnetization displaying around 20 K at a blocking temperature. Magnetic properties of the Co doped ZnO samples were found at different anisotropy value along the different crystallographic axes and different external applied field. $Zn_{1-x}Co_xO$ samples for $x \approx 0.3$ show superparamagnetic and spin glass behaviour at temperatures around 20 K respectively. The measured magnetization of these samples was proportional the Co content in the samples. For small x values, CoZnO ferromagnetic, for large values of x showed the antiferromagnetic properties.

In the our studies was used VAMPIRE software package for magnetic properties which is high performance code, developed by The University of York, Department of Physics Computational Magnetism Group for our investigations [1]. Vampire is a free, open source software package which makes atomistic simulations of magnetic materials available to both theoretical and experimental researchers. We can classify into three categories the these studies. Firstly, we created ZnO wurtzite crystal structure writing C++ code. Later, using Ruderman-Kittel-Kasuya-Yosida (RKKY) interaction we obtained the nearest neighbour interaction of ZnO that this have different sizes like 5 nm, 10 nm and 20 nm. Secondly, for these structures, we investigated the magnetic properties of these systems using Monte Carlo Method and Heun Method described by the Landau-Lifshitz-Gilbert(LLG) equation which the equation of motion for spins. Thirdly, we researched laser induced spin dynamics for the different Co doped ZnO crystal structures. Finally, a summary and a short outlook is given the of most important results and discuss some new applications or questions arising from the conclusions of this work.

Table of contents

List of Abbreviations	xv
List of Symbols	xvii
List of figures	xix
List of tables	xxi
1 INTRODUCTION	1
1.1 History of Magnetism	1
1.2 Exchange Integral in Magnetism	2
1.3 Classification of Magnetic Materials	3
1.4 Research Motivation	8
1.5 Magnetic Properties	11
1.6 Thesis Outline	17
1.7 Summary	17
2 ATOMISTIC SPIN MODELS	19
2.1 Theoretical Background	19
2.1.1 Classical Spin Hamiltonian	20
2.1.2 Heisenberg Spin Hamiltonian	20
2.2 Monte Carlo Methods	24
2.3 Spin Dynamics	25
2.3.1 Landau-Lifshitz-Gilbert Langevin Equation	27
2.3.2 LLG-Stochastic Spin Dynamics	32
2.3.3 LLG-Atomistic Spin Dynamics	32
2.4 Ultrafast Spin Dynamics	33
2.5 Summary	35

3	ATOMISTIC SPIN MODEL OF DILUTED MAGNETIC SEMICONDUCTORS	37
3.1	Background of Diluted Magnetic Semiconductors	37
3.2	Spintronic Applications of Diluted Magnetic Semiconductors	39
3.3	II–VI and III–V Compound Semiconductors	40
3.3.1	Crystal Structure of Zinc Oxide-ZnO	42
3.4	Exchange Interactions between Local Spins-RKKY	45
3.4.1	Model Description	46
3.4.2	Spin Glass	50
3.5	Ground State Spin Configuration	53
3.6	Correlations between Spin Magnetic Moments	54
3.7	Role of the Anisotropy	56
3.8	Summary	57
4	SIMULATIONS OF DILUTED MAGNETIC SEMICONDUCTORS	59
4.1	Theoretical Background	59
4.2	Magnetization Measurements	60
4.2.1	Magnetization Calculations Depending on Temperature	61
4.2.2	Zero Field Cooled and Field Cooled Magnetization	62
4.2.3	Hysteresis Calculations	70
4.3	Summary	73
5	LASER DYNAMICS IN MAGNETISM	75
5.1	Introduction	75
5.2	Research Motivation of Ultrafast Dynamics in DMS	76
5.3	Laser Induced Spin Dynamics	78
5.4	Demagnetization	80
5.5	Reversal in a Field	82
5.6	Ultrafast Spin Dynamics in DMS	83
5.7	Two Temperature Model	85
5.8	Summary	87
6	CONCLUSIONS AND OUTLOOK	89
6.1	Overview	89
6.1.1	Spintronic Applications	90
6.2	Computational Methods and Test Simulations	91
6.3	Magnetic Properties of Transition Metal Doped ZnO	91
6.3.1	Time Scales of Magnetization Dynamics	92

6.3.2	Ultrafast Magnetization	93
6.4	Demagnetization at Transition Metal Doped ZnO	94
Appendix A		95
A.1	Code's Development and Properties	95
A.2	Table of Parameters Used for Simulations	95
A.3	Code	96
A.4	Input and Material File Examples for Simulations	102
References		105

List of Abbreviations

AFM	Antiferromagnetic	ASD	Atomistic Spin Dynamics
ASD	Atomistic spin dynamics	BCC	Body centered cubic
CVD	Chemical vapor deposition	DFT	Density functional theory
DMS	Dilute magnetic semiconductor	DRAM	Dynamic random access memory
FC	Field-Cooled	FCC	Face centered cubic
FET	Field-effect transistors	FM	Ferromagnetic
GMR	Giant magnetoresistance	H	Applied field
HAMR	Heat Assisted Magnetic Recording	H_c	Coercivity
HCP	Hexagonal cubic package	L	Orbital moment of electrons
LED	light-emitting diodes	LLB	Landau-Lifshitz-Bloch
LLG	Landau-Lifshitz-Gilbert	M	Magnetisation
M_r	Remanence magnetisation	M_s	Saturation magnetisation
MC	Monte Carlo	MOKE	Magneto Optical Kerr Effect
MRAM	Magnetoresistive random access memory	PVD	Physical vapor deposition
RE	Rare Earth	RKKY	Ruderman-Kittel-Kasuya-Yosida
RT	Room temperature	S	Spin moment of electrons
SC	Simple cubic	SEM	Scanning electron microscope
SD	Spin dynamics	SG	Spin glass
SKKR	screened Korringa-Kohn-Rostoker	SPM	Superparamagnetic
SRAM	Static random access memory	T_e	Electrons temperatures
T_l	Lattice temperature	TM	Transition Metal
VSM	Value stream mapping	WZ	Wurtzite
XPS	X-ray photoelectron spectroscopy	ZB	Zincblend
ZFC	Zero-Field-Cooled		

List of Symbols

α	Alpha
β	Beta
π	Pi
χ	Chi
λ	Effective damping parameter
C_e	Electron heat capacity
C_l	Lattice heat capacity
H_{eff}	Effective field
J_{ij}	Exchange integral between spins i and j
T_c	Curie temperature
T_N	Neel temperature
T_B	Blocking temperature
M	Scalar magnetisation
B	Flux density
H	Hamiltonian
H_c	Coercive field
J	Total angular momentum
S	Spin angular momentum
L	Angular momentum
τ	Torque
k_F	Fermi wave factor
μ	Magnetic moment
k_B	Boltzmann constant
S	Spin number
T	Temperature
T_e	Electron temperature
T_l	Phonon/lattice temperature
G	Electron lattice coupling factor
g	Landé g-factor
e	Electron charge
m_e	Electron mass
c	Speed of light

List of figures

1.1	Schematic magnetization temperature phase diagram	4
1.2	Hysteresis curves of ferromagnetism, paramagnetism and supermagnetism .	6
1.3	Flow diagram of different magnetism types	8
1.4	ZnO general hexagonal wurtzite crystal structure	10
1.5	Comparison of susceptibility and M-H behaviour	13
1.6	Zero field cooled and field cooled magnetization curves	15
1.7	Typical hysteresis loops for ferromagnetic magnet	16
2.1	Visualisation of spin exchange interaction	21
2.2	Visualisation of damped and precession in spin dynamics	30
2.3	Schematic illustration of the spin dynamics	31
2.4	Time-scale of ultrafast spin dynamics	34
3.1	Representation of diluted magnetic semiconductors	38
3.2	Diagram of Curie temperatures computed within the Zener model for various semiconductors	41
3.3	Magnetic polarons and magnetic phase diagram for dilute ferromagnetic semiconductors.	42
3.4	A schematic of the structure of ZnO wurtzite crystal structure	43
3.5	Crystal visualization of DMS structures according to doping concentration .	44
3.6	Schematic representation RKKY exchange interactions among atomistic spin	45
3.7	Oscillatory part of Ruderman-Kittel-Kasuya-Yosida interaction	47
3.8	Ferromagnet, spin-glass/paramagnetic and antiferromagnetic phases diagram	49
3.9	Ruderman-Kittel-Kasuya-Yosida interactions distance dependence in non- magnetic metals	50
3.10	Used actual neighbour interactions from our simulations of ZnO	51
3.11	Schematic representation of the random spin structure of a spin glass	52
3.12	Ground-state spin configuration of an antiferromagnet	53
3.13	Visualization of antiferromagnetic ground state magnetic structure	54
4.1	General visulation of Co doped ZnO used our the calculations	60
4.2	Curie temperature of some ferromagnetic materials	61
4.3	Magnetization measurements of Co doped ZnO at different concentration .	62
4.4	Zero field cooled and field cooled magnetization measurements	63

4.5	Effect of uniaxial anisotropy in magnetization behaviour	65
4.6	Ferromagnetic properties of CoZnO at low density and temperature	66
4.7	The zero field cooled magnetizations of $Zn_{0.98}Co_{0.02}O$ at different size	67
4.8	Temperature dependence of field cooled magnetizations for different size of CoZnO	67
4.9	Crystal visualization of DMSs $Co_{0.3}Zn_{0.7}O$ spin glass properties	68
4.10	Paramagnetic spin direct visulation zero field cooling and field cooling measurements	69
4.11	Antiferromagnetic ground state visulation doping zero field cooled and field cooled magnetization measurements of CoO	70
4.12	The hysteresis loops of the CoZnO thin films with different cobalt concentrations	71
4.13	The hysteresis loops of the CoZnO thin films with different external applied field	72
4.14	Effects of uniaxial anisotropy constant on hysteresis curves	73
5.1	The flow diagram of ultrafast spin dynamics	76
5.2	Schematic representation of ultrafast spin dynamics	78
5.3	Schematic representation of laser-induced magnetization dynamics	79
5.4	Schematic illustration of a conventional magnetization-temperature diagram and the effect of laser	80
5.5	Schematic summary of ultrafast magnetization dynamics	81
5.6	Time-resolved ultrafast demagnetisation in Nickel	82
5.7	Crystal visualization of $Co_{0.3}Zn_{0.7}O$ magnetic reversal behaviour	83
5.8	Laser pulse calculations of CoZnO	84
5.9	Two temperature model calculations of CoZnO	84
5.10	Laser pulse calculations of CoZnO	85
5.11	Temperature-time behaviour using two temperature model calculations of Ni	86
5.12	Temperature-time behaviour using Two Temperature Model (TTM) calculations of CoZnO	87
6.1	Schematic representation of spintronic devices illustrated dependent as electronic, optic and magnetic devices	90
6.2	Characteristic times scales of magnetization dynamics	93

List of tables

1.1	Crystal structure and magnetic moments of the some ferromagnetic materials, and their Curie temperature	14
1.2	Crystal structure and magnetic moments of the some antiferromagnetic materials, and their Neel temperature	14
3.1	Some ferromagnetic behaviour of oxide materials with Curie temperature above room temperature	41
3.2	Some Fermi wave vector constant according to different doping concentrations	49
A.1	Used physical parameters for CoZnO in this thesis	95

Chapter 1

INTRODUCTION

1.1 History of Magnetism

Magnetism is class of physical phenomena paramount important in the modern age discovered by the ancient Greek philosopher Aristotle in 600 BC. Electric currents and magnetic moments of elementary particles generate a magnetic field. In nature all materials are affected to some extent by a magnetic field. During last 150 years there has been extensive research attention by a large number of scientists since invention of electricity towards understanding the relationship between electricity and magnetism. Therefore, there are many in digital information storage, high tech devices, computers etc. Indeed, we live in world where electromagnetic phenomena form the basis of modern industrialized society. Magnets have huge advancements of science and technology in areas of research in condensed matter physics. It means that the development of novel approaches to the study of magnetic materials for new applications.

Until the first half of the 20th century, most permanent magnets were made from steel such as $Fe_{65}Co_{35}$. Steel magnets for permanent magnet applications are unused at the present time. $L1_0$ magnets such as PtCo and Fe_3O_4 materials were used in the past as a permanent magnets. Recently, hexagonal ferrites such as $BaFe_{12}O_{19}$ have been widely used to produce cheaper magnets, since the anisotropy of Fe_3O_4 is low. However, most high performance magnets are made from rare-earth transition metals such as $Nd_2Fe_{14}B$. So, the most important magnets are hard (NdFeB) or soft (Permalloy) or specialized, eg. magnetic recording.

To understand the history of magnetism, we have to look at the magnetic moment of atoms. Two sources of magnetism occur by the orbital angular and the intrinsic spin moment. The magnetisation is described as the sum of all the spin moments. Each individual electron within an atom has an angular momentum 'L', associated with its orbital motion, and spin angular momentum 'S'. These phrase described as the below.

$$\begin{aligned}\vec{\mu}_L &= -\beta\vec{L} \\ \vec{\mu}_S &= -2\beta\vec{S}\end{aligned}\tag{1.1}$$

Where β is the Bohr magneton. Even if the magnetic moment μ is fixed, it is given by

$$\vec{\mu} = -\beta(\vec{L} + 2\vec{S})\tag{1.2}$$

So far some information about the magnetism is given. Now, I will be introduced important properties of magnetic materials and their applications.

1.2 Exchange Integral in Magnetism

Exchange integral, J , which arises from Heisenberg's theory of ferromagnetism. Two nearby atoms have unpaired electrons which they are the electron spins have parallel or antiparallel affects. This quantum mechanical effect called the exchange interaction. As a result, in ferromagnetic materials, nearest neighbour spins tend to align in the same direction. Transition metal doped semiconductor oxides have Ruderman-Kittel-Kasuya-Yosida (RKKY) interactions. Or we consider the stability of the long-range magnetic order interactions. It is a phenomenon of significance in the study of spintronic materials.

1.3 Classification of Magnetic Materials

What is the significance of the different magnetic order? The best way to introduce the different types of magnetism with different applied field and effect. This may be surprising, however all materials is magnetic in periodic table. Magnetic properties of some materials are much more magnetic than others. The main distinguish properties in materials is interaction between atomic magnetic moments. Sometimes this can be very strong interaction between atomic moments. Therefore, materials have different magnetic properties, which can be classified as the following.

Diamagnetism

Diamagnetism is a weak form of magnetism that is appears in all materials and exhibited by a substance in the presence of an externally applied magnetic field. The magnetization of a diamagnetic material is proportional to the applied magnetic field and they have a negative and quite weak relative susceptibility. It is generally a weak effect in most materials, although superconductors display a strong effect. This effect is explored by nanoscale spin electronic devices. Many metals and most non-metals are diamagnetic in nature[2, 3]. Bismuth and Carbon Graphite are the strongest diamagnetic materials in the periodic table.

Paramagnetism

Paramagnetism is a weak form of magnetism which displays magnetic properties only with applied magnetic field. Also it depend on temperature for magnetic systems. In the absence of an external field, the magnetic moments are oriented randomly. Many metals and non-metals are paramagnetic, such as some transition metal, some rare earth metal and gas etc. For example Aluminum and Copper are classified paramagnetic metals. Actually, ferromagnets become paramagnetic above the Curie temperature T_c as well, where a material's spontaneous magnetisation disappears. Few materials such as Fe, Ni, and Co have high Curie temperature, and shown paramagnetic properties above their Curie temperature as ferromagnetic materials. Diamagnetic atoms have only paired electrons, however paramagnetic atoms, which can be

made magnetic, have at least one unpaired electron. A paramagnetic electron is an unpaired electron. The unpaired electrons of paramagnetic atoms realign in under an external magnetic fields.

Ferromagnetism

Ferromagnetic materials have a spontaneous magnetization, even in the absence of an external magnetic field. It is well known that despite the spontaneous magnetization property. They approach magnetic saturation as the field strength continues to increase. Ferromagnets contain spontaneously magnetized magnetic domains. Actually the domains can orient randomly so as to produce a demagnetised state. The magnetization of ferromagnets disappears above

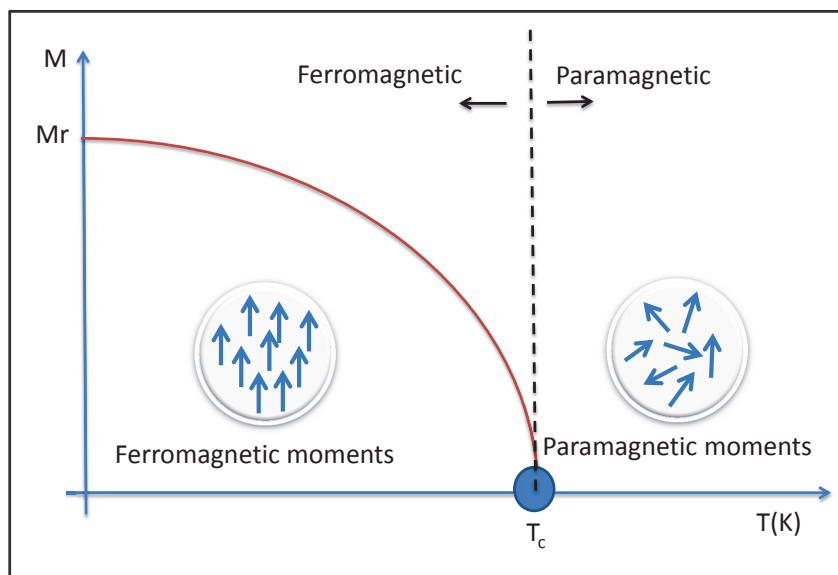


Fig. 1.1 Schematic magnetization(M) temperature(T) phase diagram. Temperature dependence of the spontaneous magnetization and M_r is remanence magnetization point. Magnetization which a substance possesses in the absence of an applied magnetic field.

Curie temperature T_c , they become paramagnetic Fig-1.1. Scientifically, we can think that ferromagnets are considered a subclass of paramagnetic materials. Examples of ferromagnetic materials are transition metals such as Iron-Fe body-centered cubic, Cobalt-Co close-packed hexagonal or face-centered cubic, Nickel-Ni face centered cubic. Also alloys involving some transition metal doped oxides and rare-earth elements (Gd, Dy) are well-known ferromagnets.

Extensive investigations of the magnetic properties of ferromagnetic materials have been made. The investigations have been both scientific and commercial and both experimental and theoretical.

Fig-1.1 shows that for temperatures $T > T_c$ ferromagnetic materials behave paramagnetically. However, for $T < T_c$, this figure a ferromagnetic relationship is shown between the saturation magnetization M_r and the temperature T . For example, the Curie temperatures of the some ferromagnetic metals which are Iron, Cobalt and Nickel, are 1044 K, 1388 K and 628 K, respectively [2].

Superparamagnetism

Superparamagnetism is a form of magnetism, which has small ferromagnetic or ferrimagnetic properties, and has Blocking temperature below the Curie or Neel temperature [4]. In particular small nanoparticles, magnetization can randomly flip direction with the effect of temperature. Without external magnetic field ($H=0$ T), the time used to measure the magnetization of the nanoparticles takes longer comparing with the Neel relaxation time. Their magnetization appears to be in around average zero tesla. In general, ferromagnetic or ferrimagnetic material tend to a paramagnetic state above its Curie temperature. However superparamagnetism is different from this standard state since it consist of below the Curie temperature of the material. Magnetic moment has generally two stable orientations in terms of nanoparticle's magnetic anisotropy. The stable orientations define the nanoparticle's so called "easy axis". The mean time between two flips is called the Neel relaxation time τ_N and is given by the following Neel-Arrhenius equation.

$$\tau_N = \tau_0 \exp\left(\frac{K \cdot V}{k_B T}\right) \quad (1.3)$$

where τ_N is the average length of time that it is nanoparticle's magnetization. τ_0 is a length of time, its typical value is among 10^{-9} and 10^{-10} second. K is the nanoparticle's magnetic anisotropy energy and V its volume. $K \cdot V$ is the energy barrier associated with the magnetization moving. k_B is the Boltzmann constant. T is the temperature.

Blocking temperature: Magnetization of superparamagnetic nanoparticle is measured with the measurement time (τ_m). For $\tau_m \gg \tau_N$, the magnetization of the nanoparticle will change a few times and as a result the average magnetization will be zero when the magnetization is measured. For $\tau_m \ll \tau_N$, however, the magnetization of the nanoparticle will not change, thus the magnetization would be the initial instantaneous magnetization of the measurement. For $\tau_m = \tau_N$ condition, the nanoparticle transitions from superparamagnetism state to the blocked state. The measurement time is maintained with varying temperature, thus the function varies from superparamagnetism state to the blocked state with varying temperature. T for which $\tau_m = \tau_N$ is the so-called blocking temperature:

$$T_B = \frac{K.V}{k_B \ln\left(\frac{\tau_m}{\tau_0}\right)}. \quad (1.4)$$

Some magnetic properties of superparamagnets in such as zero field cooled(ZFC) and field cooled(FC) magnetization curves, hysteresis curves exhibit characteristic behaviour and can be explained by simple theories assuming coherent rotation of the magnetisation. Superparamagnetic behaviour varies with respect to the system size. When the systems size is increased, superparamagnetic behaviour in ZFC/FC is observed.

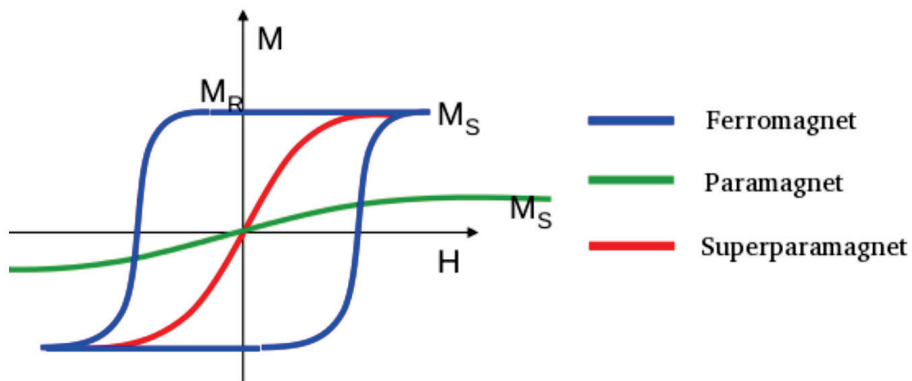


Fig. 1.2 Hysteresis curves of ferromagnetism, paramagnetism and supermagnetism. Ferromagnetic curves has coercive field, but paramagnet and superparamagnet haven't coercive field.

There are many practical applications of superparamagnetic materials like heat transfer and damping. Therefore, superparamagnetic materials have unique properties in term of their

magnetic sizes. Superparamagnetic materials consist of individual (single) magnetic domains of elements (or compounds) that have ferromagnetic properties in bulk. Their magnetic susceptibility is between that of ferromagnetic and paramagnetic materials. Hysteresis curves of ferromagnetic, paramagnetic and superparamagnetic materials are shown in Fig.1.2.

Antiferromagnetism

Anti parallel aligned spins consist of coupled magnetic moments, whose exchange integral J is, in contrast to ferromagnets, negative. According to the J parameter, ferromagnetism and antiferromagnetism are classified. Critic temperature points are called the Curie temperature, T_c , in ferromagnetism and Neel temperature, T_N , in antiferromagnetism. Antiferromagnetism is an arrangement of antiparallel aligned spins on different sublattices. That is, above T_N , for antiferromagnetic materials the antiparallel arrangement of the moments disappears. There is no antiferromagnetic ordering above the Neel temperature. Below the Neel temperature both sublattices possess a zero spontaneous magnetization. This spontaneous antiparallel magnets have small conductivity. Above Neel temperature, the spins become randomly orientated and the susceptibility, measure of the ability of a material to be magnetized, decreases as the temperature is increased. The Neel temperature of some ferromagnetic compound oxides materials are MnO-120K, FeO-190K, CoO-290K and NiO-525K [2]. Also some metals are antiferromagnetic such as Cr is well known antiferromagnetic material. Ferromagnetism and antiferromagnetism can generally be classified by the sign of the exchange constant that couples the magnetic moment.

Ferrimagnetism

Ferrites are Fe_2O_3 derivatives exhibit a kind of magnetism known as ferrimagnetism that is in some ways similar to both ferromagnetism and antiferromagnetism such as oxides and FeGd. Ferrites are generally ferrimagnetic. However, not all ferrimagnetics are ferrites. For example, $DyCo_5$ is a ferrimagnet but it is not a ferrite. In these materials, atomic spin moment ions are situated on two different types of lattice sites. But, one of the resultant magnetizations on the two lattice sites is stronger than the other. Because of this, magnetization is not

totally zero. In fact, ferrimagnetic materials are sometimes defined as ferromagnets. If the magnetic moments of the ions on the two different sites are not equal, this material can be called ferrimagnetic. Above T_c , ferromagnetic and ferrimagnetic materials are paramagnetic. In summary, properties of all these magnetic materials for our studies are illustrated as a flow diagram at Fig. 1.3.

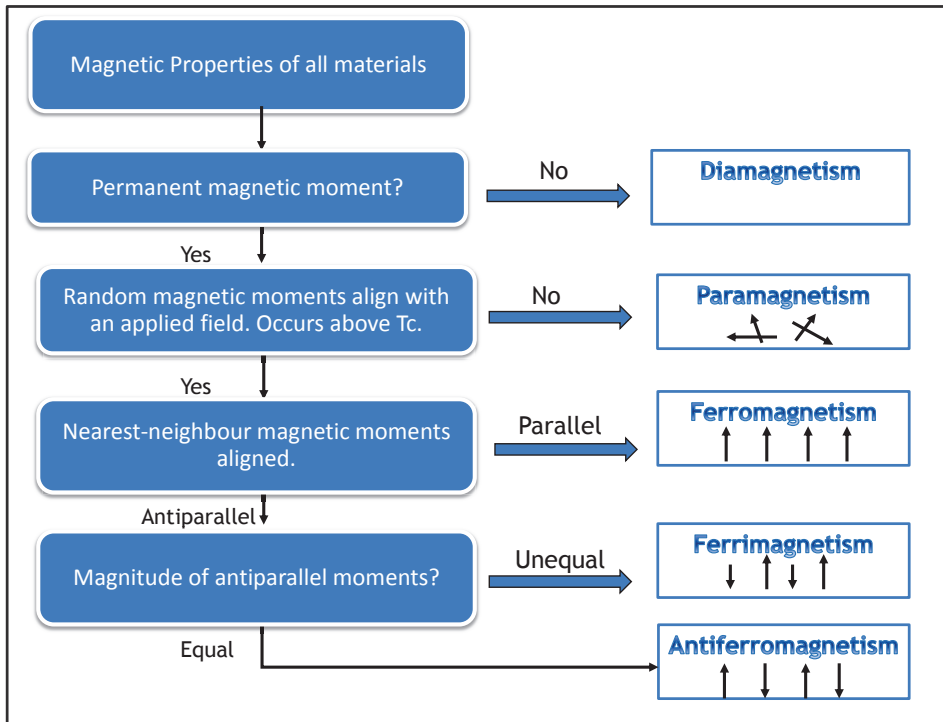


Fig. 1.3 Flow diagram of different magnetism types. This figure illustrates permanent magnetization and alignment of magnetic moments for some of the principal classes of magnetism. Random alignment of magnetic moments defines paramagnets, ferromagnets exhibit parallel alignment of magnetic moments. Even if antiferromagnets exhibit antiparallel alignment of magnetic moments. Diamagnetic has no magnetic moment.

1.4 Research Motivation

Although magnetism has been a topic of research for technological devices since the discovery of electricity in the 1800's, it was first investigated experimentally and theoretically in the beginning 1960's for storage of digital information. With the rising demand for magnetic storage, billions of dollars are spent each year on storage. The research area of magnetism

both in fundamental science and device physics - has enabled the magnetic storage industry for technological advances.

Magnetic semiconductors generally desired from compatibility with silicon electronics and spin polarized currents. The materials are commonly known as semimagnetic semiconductors or diluted magnetic semiconductors. Their importance have been interesting for fundamental science and applications. In term of using technology, magnetic data storage has been widely used over the last decades in computer and audiovisual modern technology such as video cassette recorders, iPods and MP3 players, magnetic tapes, high-definition camcorder, hard drives, computer hard disks, and credit/debit cards, magnetic memory devices of near future and so on. In that market, there are some physical problems such as read-ability, write-ability and thermal stability of data in storage industry. Because of technological requirements there has been constant drive in the magnetic recording industry to improve the capacity and speed performance of their products recently. The aim of the magnetic recording industry market is to increase the capacity of the media, and requires reduction in the sizes of the bits. Bits consist of a number of magnetic grains which are single domains. The first hard disk devices had a few hundred bits on one square inch of magnetic material. Whereas current disks have hundreds of billions of bits.

Computer bytes are recorded magnetically on very small segments of the storage disk. Each bit of digital storage data is recorded on a corresponding magnetic 'bit' on storage media. In terms of data density, these are be directly connected to disk possessing a number of Megabits (Mb), Gigabits (Gb) and Terabit(Tb) per square inch. The main problem with reducing the bit size is magnetic stability, since at very high density each bit consists of only a few particles. in order to achieve our goal the highest bit density for this reason requires the use of particles of only a few nanometres in diameter, referred to as grains [5]. Among today's new technologies is Seagate's Heat Assisted Magnetic Recording (HAMR) that a magnetic storage technology for hard drives beyond $1Tbit/inc^2 = 60TB$, and its bit sizes $25nm \times 25nm = 650nm^2$. For example 1TB hard disk costs \$375 in 2007, 1TB hard disk US\$70 in 2015. The resources spend billions U.S. dollars per year. As the bit size becomes

smaller at the hard disk technology, the information recording speed must also become faster. As a result of this, as the size increases, the price is also increased.

Among inorganic materials, metal oxides such as ZnO play a fundamental role in developing new devices in terms of chemical and physical properties. These materials have suitable synthesis and analysis techniques, and are experimentally used Sol gel, Chemical vapor deposition (CVD), Value stream mapping (VSM), Physical vapor deposition (PVD), X-ray photoelectron spectroscopy (XPS), Scanning electron microscope (SEM) etc. for optical, catalytic, magnetic and electrical properties. Zinc oxide from the II-IV semiconductor group has a wide band gap and has become one of the most important materials in research due to its wide application with various transition metal dopants. The II-VI Diluted Magnetic Semiconductors have attracted considerable attention. Because the spin-dependent magnetic properties can be suitable in low dimension systems for example spin based magnetic devices. ZnO and compounds with transition metal ions are one of the most candidates for room-temperature ferromagnetism of DMS.

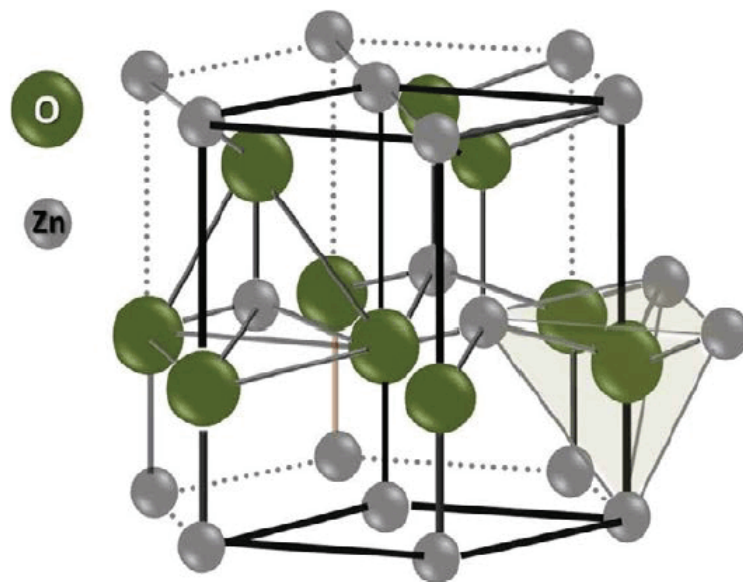


Fig. 1.4 ZnO general hexagonal wurtzite crystal structure consist of Zinc and Oxygen

In light of information in above, modelling of magnetic materials is necessary to provide understanding for complex components and particles such as those used in hard disks. The

standard method of modelling magnetic materials has been used to better understand the behaviour of magnetic materials with a number of physical variables. There exist many models for example ab-initio, LLG, micromagnetic, Stoner-Wohlfarth et atc. In recent years micromagnetics has become a primary tool in understanding the behaviour of magnetic materials. However, the essential problem when extending micromagnetics into the nanoscale is one of length scale. The problem is due to the breakdown of the model because calculation of interactions are not computational feasible for magnetization behaviour at the atomic level. Furthermore, to solve these problems essentially atomistic models based on exchange calculated using the Heisenberg model is used. The atomistic model has successfully been used to describe the response of materials to ultrafast magnetisation pulses and to model the Heat Assisted Magnetic Recording (HAMR) process [6, 7].

Ultrafast laser pulses present a new area for the magnetic data storage technology. With the recent developments of femtosecond lasers in the study of magnetisation dynamics, the study of ultrafast magnetization (spin) dynamics has become one of the most active fields of magnetism for both scientific and technological area. The timescale offered by femtosecond laser pulses, suggests the possibility of reduction of the magnetization reversal time and consequently memory devices. Therefore, we have mainly focused our studies have concentrated on investigating the ultrafast dynamics of DMS.

1.5 Magnetic Properties

Magnetization and Magnetic Susceptibility

Magnetization is a normalized moment (Am^2 in SI unit). There exists an approximately linear relationship between magnetization M and applied field H . This is only true for small fields - overall the dependence of M on H is highly non-linear. In order to describe whether a material is magnetic or not, we need to investigate the material's magnetic behaviour under an applied field. This often uses the magnetic susceptibility, where the ferromagnetic order disappear at above (T_c) critic temperature, and the material becomes paramagnetic in the atomic moments of a few Bohr magnetons. The magnetic susceptibility of a material generally symbolized by

χ . The magnetization of a paramagnetic material per unit applied field which is equal to the applied magnetic field strength, ratio of the magnetization M defined at Eq. 1.6;

$$M = \frac{N\mu_0 g^2 J(J+1)\mu_B^2 H}{3k_B T} \quad (1.5)$$

where μ_B is Bohr magneton, μ_0 is permeability of free space, N is Avogadro's number, g-factor is the Lande factor, and k_B is Boltzmann constant.

$$\chi = \frac{M}{H} \Rightarrow \chi = \frac{N\mu_0 g^2 J(J+1)\mu_B^2}{3k_B T} = \frac{C}{T} \quad (1.6)$$

$\vec{J} = \vec{L} + \vec{S}$: total angular momentum = total orbital angular momentum + total spin angular momentum. χ is a dimensionless quantity. Above T_c the Curie temperature, the moments are aligned randomly, net magnetization is zero. In this region the material is paramagnetic, and its susceptibility is given by

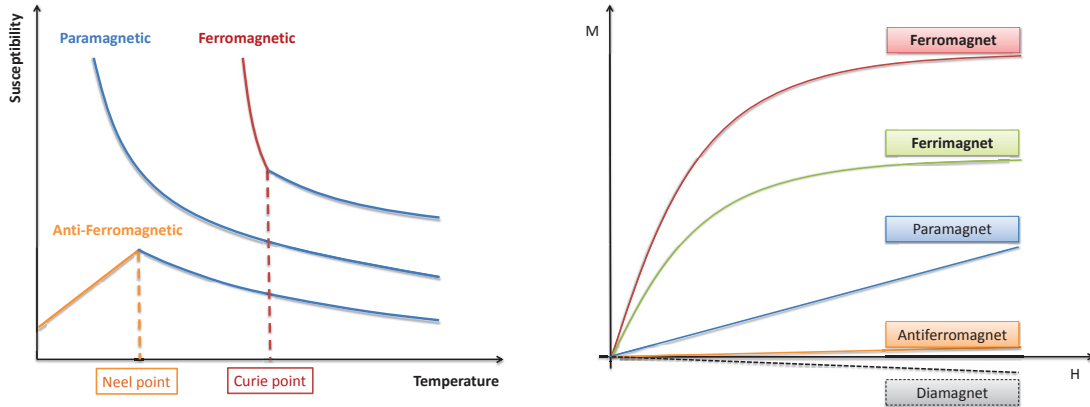
$$\chi = \frac{C}{(T - T_c)} \quad (1.7)$$

which is called as Curie-Weiss law. Where C is known as the Curie constant and T_c is the Curie temperature. The permeability $\mu = 1 + \chi$ is very close to 1 and magnetic susceptibility very close to zero for paramagnetic and diamagnetic materials. For ferromagnetic materials, these values are very large. In Fig.1.5a the Curie and Neel point was shown as the critical temperature for ferromagnetic and anti-ferromagnetic materials, respectively.

The magnetization of diamagnetic materials is negative, since its magnetisation arises from a weak induced magnetic moment. The susceptibility of antiferromagnetic materials above the Neel point and ferromagnetic materials above the Curie point show the transition from antiferromagnetic to paramagnetic behaviour, according to the Curie-Weiss law.

Magnetic induction is associated with magnetic flux and applied magnetic field strength. In fact, strength of the field is known as the magnetic field strength, magnetic field intensity, is given by

$$B = \mu_0 (H + M) \quad (1.8)$$



(a) Susceptibility curves of magnetic materials (b) Behaviour of magnetization and applied field

Fig. 1.5 Comparison of susceptibility-temperature and magnetization(M)-applied field(H)

where μ_0 is the permeability of free space. The permeability μ is defined as follows.

$$B = \mu_0 (1 + \chi) H = \mu_0 \mu_r H = \mu H \quad \text{or,} \quad \mu = \frac{dB}{dH}. \quad (1.9)$$

Susceptibility can also be calculated in terms of magnetisation fluctuations

$$\chi = N \frac{\langle M^2 \rangle - \langle M \rangle^2}{T} \quad (1.10)$$

where N is the number of the magnetic transition metal atoms in diluted magnetic semiconductors.

Temperature Dependence of the Magnetisation

The spontaneous magnetisation and anisotropy energy of ferromagnetic materials are temperature dependent. For bulk magnetic systems the temperature dependence of spontaneous magnetization at low temperatures is described by Bloch's Law as the following:

$$M(T) = M(0) \left[1 - \left(\frac{T}{T_c} \right)^{3/2} \right] \quad (1.11)$$

where $M(0)$ is the spontaneous magnetization at absolute zero temperature. Spontaneous magnetization decreases at higher temperatures due to the increasing excitation of spin waves.

At high temperature

$$M(T) \propto (T - T_c)^\beta \quad (1.12)$$

where β is a critical exponent. The exponent is 0.34, 0.51 for Fe and Ni respectively. We can generally categorize material behaviour in terms of temperature as Ferromagnetic, Antiferromagnetic and Paramagnetic. Curie and Neel temperature of some ferromagnetic and antiferromagnetic materials shown in Table 1.1 and 1.2.

Material	Crystal Structure	μ_B	T_c (K)
Iron(Fe)	BCC	2.2	1043
Cobalt(Co)	HCP or BCC	1.7	1388
Nickel(Ni)	FCC or HCP	0.6	633
Gadolinium(Gd)	HCP	7.0	293
Dysprosium(Dy)	HCP	10.5	88

Table 1.1 Crystal structure and magnetic moments of the some ferromagnetic materials, and their Curie temperature

Material	Crystal Structure	μ_B	T_N (K)
Manganese Oxide(MnO)	FCC	4.7	116
Iron Oxide(FeO)	FCC	3.3	198
Cobalt Oxide(CoO)	FCC	3.6	291
Nickel Oxide(NiO)	FCC	1.8	525

Table 1.2 Crystal structure and magnetic moments of the some antiferromagnetic materials, and their Neel temperature

Zero Field Cooling and Field Cooling Magnetisation

The magnetization measurements are different in a small applied field for a ferromagnet, an antiferromagnet and a spin glass. These magnetic behaviour is one of the characteristic

features of a spin glass. Both Zero Field Cooling (ZFC) and Field Cooling (FC) case is measured during in small external applied field range 0-1 Tesla. Detailed information about this subject was given in section 1.3 (superparamagnetism)

- Zero Field Cooling (ZFC): The samples generally are lowered to 0 K from high temperature, for example 300 K, without applying a magnetic field $H=0$ Tesla. Thus, this situation is called the ZFC during cooling.
- Field Cooling (FC): The samples are lowered to 0 K from from high temperature, as applying a magnetic field of $H=0.1$ Tesla or 1 Tesla. Thus, this situation is called the FC during cooling.

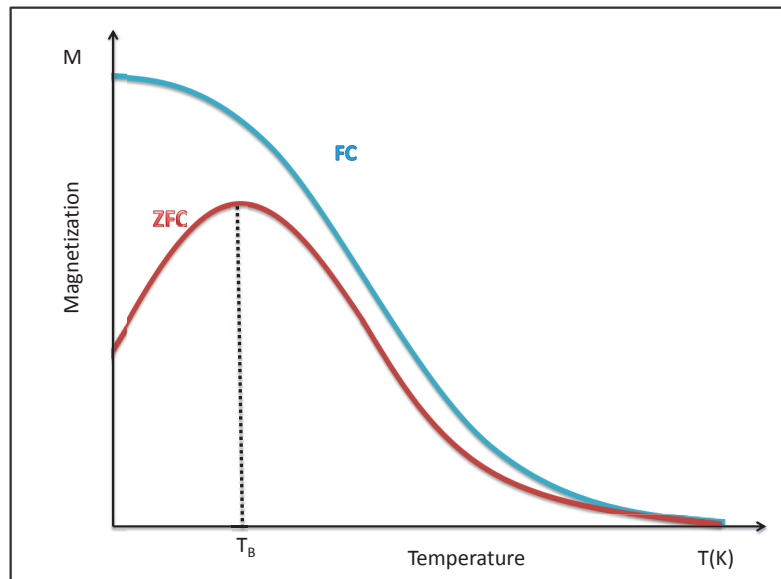


Fig. 1.6 The field dependence of temperature of the zero-field-cooled (ZFC) and field-cooled(FC) magnetization curve of a magnetic nanoparticle system. The relationship between field-cooled and zero-field-cooled show magnetic properties os system. T_B : Blocking temperature which under this point material show superparamagnetic properties with applied field. Without field, this materials show spin glass properties.

Magnetization Hysteresis

An important aspect of magnetism is hysteresis, and is a important feature of ferromagnetic materials in magnetism. Determination of hysteresis loops is obtained by measuring the

magnetisation of a ferromagnetic material while the magnetic field is varied. If a magnetic material is magnetized in a strong magnetic field, it preserves a significant amount of magnetism after the magnetic field is reduced to zero, it has a high remanance at high anisotropy. The phenomenon is known as magnetic hysteresis that gives the relation between the magnetization and the applied field for recording media devices. A hysteresis loop is illustrated schematically as following in Fig.1.7. In this figure M_s , M_r and H_c are the saturation magnetization, remanance magnetization, coercive field, respectively. They described by the hysteresis loop are often used to characterize the magnetic properties of materials. The magnetization that is retained when the applied field is removed is called the remanence of the material, and is an important factor in permanent magnets. It is assumed that the material

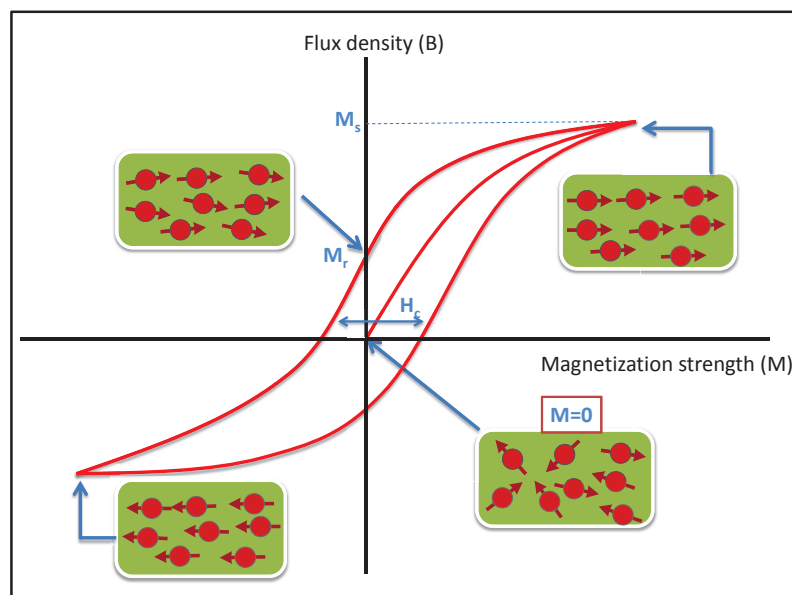


Fig. 1.7 Typical hysteresis loops for ferromagnetic magnet as a function of applied field

is initially in a demagnetized state in the Fig.1.7. When a field is applied, the magnetization of material increases until the saturation point is reached. The plot of B versus M is known as the magnetization or hysteresis curves.

The most fascinating aspect of the hysteresis loop is the coercivity. It describes the stability of the permanent state and constitute the classification of magnets into hard magnetic materials (permanent magnets), semi hard materials (storage media), and soft magnetic mate-

rials. Permanent magnets have a wide range of applications for example used electromotors, loudspeakers, data storage, microphones, hard-disk drives, and as toys.

1.6 Thesis Outline

In this chapter, the history and application of magnetism, a general overview of the magnetic properties like rare earth (RE), and transition metals (TM) were given. After this introductory chapter, we describe spin models such as micromagnetic model and the Landau-Lifshitz-Gilbert and ultrafast dynamic for the properties of magnetic material and also other methods in chapter-2. After that, we describe the written codes in order to understand RKKY theory for diluted magnetic systems in chapter-3. We obtained a lot of magnetic properties such as the magnetization dependence on temperature, zero field cooling and field cooling magnetization measurement, hysteresis calculations using VAMPIRE with our RKKY code in chapter-4. In chapter-5, laser pulse induced demagnetization dynamics in diluted magnetic systems is investigated. Finally, we give a written summary of our result and discuss further work. We discuss applications of this work in industry for applications.

In particular, a comparison between the newest information technology and write data with a laser pulse is given. That is, we have focused magnetic behaviour of diluted magnetic semiconductor using many parameter in this thesis. In this study main aim to develop new classes of magnetic oxide materials, to examine the structure relationships of these novel materials, to develop a essential understanding of magnetism at nanometer length scales and to fabricate spin devices based on these materials.

1.7 Summary

Magnetic materials are a very important class of materials in terms of many electrical and electromechanical devices such as electromagnets, electric motors, generators, transformers, magnetic storage such as hard disks. Therefore, magnetism has been increasing in importance following recent developments in ultrafast magnetic measurements which promise practical

implementation, ultrafast magnetic recording, etc. Recording rates could exceed today's rates by at least 2 orders of magnitude. However, the applicability of this phenomenon is hindered by fundamental problems. In particular, some fundamental issues must be addressed.

- What are the needs of modern day for magnetism and its technological applications used many devices?
- What is the role of temperature, applied field, size and its important for spintronics devices?
- Is it feasible to study the fundamentals of magnetization dynamics? At the femtosecond and picosecond timescale, behaviour of magnetization reversal of recording media.
- Hard disk drives have significant advantages for storage of data. Nowadays, they are embedded in many digital devices such as personal computers, laptops, workstation computers, digital video recorders and automotive vehicles. How can we use the physics of ultrafast magnetism to improve these devices?

Chapter 2

ATOMISTIC SPIN MODELS

2.1 Theoretical Background

The main emphasis in the previous chapter was to introduce the history of magnetism, the principal properties of magnetic materials and magnetism types. In this chapter we will discuss the computational modeling methods in magnetism, such as Monte Carlo, Langevin dynamics using VAMPIRE atomistic spin modelling software. Atomistic spin modelling of magnetic materials at the atomic scale introduces the detailed physics and allows the simulation of complex effects such as exchange energy, uniaxial anisotropy, applied field, ultrafast laser induced spin dynamics, and micro-structural effects [8]. Therefore, behaviour of magnetic materials have many application in data storage industry, atomistic magnetic modelling has been introduced and developed to a high standard and improved computer method.

Traditionally, micro-magnetic simulations have been of increased in spin dynamics. However the method has several restrictions, for example it is limited to long length scales of several nm. Micro-magnetism describes the behaviour of the magnetic systems on a length scale greater than the atomic scale. An atomistic spin model can cope with these limitations treating the spins at the atomic level, in order to give information the detailed magnetic properties, and to be able to simulate ultrafast spin dynamics, with finite temperature and complex spin structures such as antiferromagnet and spin glass.

2.1.1 Classical Spin Hamiltonian

In this section, we focus on the magnetic dipole moment per atom, the spontaneous magnetization, the exchange energy, the magnetocrystalline anisotropy, applied field and dipolar energy. Heisenberg model takes into account the interaction of the nearest neighbour atoms in magnetic systems. The Ising model, proposed by Ernst Ising[9], describes an ordered array of atoms with magnetic dipole moments called spins. Hamiltonian of such system is

$$H = - \sum_{\langle i,j \rangle} J_{ij} S_i S_j - h \sum_i S_i \quad (2.1)$$

where $S_i = \pm 1$ is an Ising spin variable, h is a applied magnetic field, J_{ij} is an interaction constant between spins.

The moment of magnetic solids arise from partly filled inner electron shells of transition metal atoms. Most important are the iron series from transition metal elements (3d elements) Fe, Co and Ni, and the rare-earth or 4f elements, such as Nd, Gd and Dy. There are two sources of the atomic magnetic moment " μ " associated with the orbital motion of the electrons (orbital moment "L") and the electron spin (spin moment "S"). The exchange interaction was discovered by Heisenberg in 1926, the phenomena being central to the magnetic ordering of atomic spin moments in the magnetic materials. The Heisenberg spin model contains all the possible magnetic interactions in a suitable formalism which can be used to investigate a number of situations at the at the basic level. The fundamental part of the model is the Spin Hamiltonian which describe the energetics of the magnetic system.

2.1.2 Heisenberg Spin Hamiltonian

The Heisenberg spin Hamiltonian " H " can be written as a sum of energy terms which including an exchange interaction " E_{exc} " between an atomic spin moment and neighbouring moments, external applied magnetic fields " E_{ext} ", magnetocrystalline energy " E_{ani} ", dipole-dipole interaction " E_{dip} ". The Spin Hamiltonian is generally written in the form:

$$H = E_{exc} + E_{ani} + E_{ext} + E_{dip} \quad (2.2)$$

where the terms in Eq.2.2 are Exchange, Anisotropy, Zeeman (external field) and dipole field.

Exchange Energy

Exchange interactions is heart of the phenomenon and most important term in the spin Hamiltonian (sometimes called Heisenberg exchange) equation (Eq.2.3) in ferromagnetic materials come from the spins behaviour, which tend to align the atomic spin moments. In ferromagnetic metals as identified that the exchange interaction tend to very strong alignment of spin moments to their neighbours. The total of exchange energy for each atom, i , is described by the sum over all neighbouring atomic spin moments.

Apart from mentioned exchange interaction, Zeeman interaction, crystalline anisotropies play an important role in magnetic systems. The strength of the anisotropies and Zeeman interaction determines the equilibrium orientation of the spin moments. Crystalline anisotropies can be uniaxial, cubic or surface.

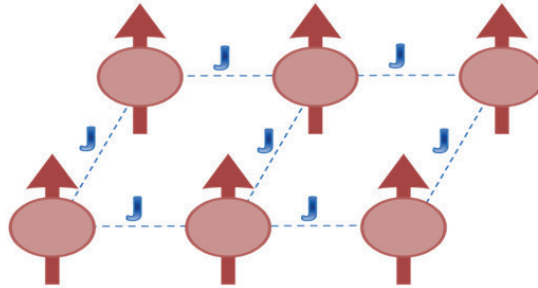


Fig. 2.1 Visualisation of spin exchange interaction between an atomic spin moment. This exchange interaction was shown Eq.3.2 for our system

$$E_{exchange} = - \sum_{i \neq j} J_{ij} S_i \cdot S_j \quad (2.3)$$

where J_{ij} is the exchange constant or exchange integral between a spin " i " and its nearest neighbouring spin " j ", that is depending on the distance between atoms. S_i is local spin moment and S_j is spin moments of the neighbour. The calculation of exchange integral can be complicated, but can be determined from the experimental value of T_c . If the two electrons

are on the same direction, exchange integral positive in Fig.2.1. J_{ij} exchange constant for atomistic model given by [8]

$$J_{ij} = \frac{3k_B T_c}{\epsilon z} \quad (2.4)$$

where k_B is the Boltzmann constant, T_c is the Curie temperature and z is the number of nearest neighbours. This equation give just relative between J_{ij} with T_c . T_c can be shown the changeable according to the behavior ferromagnetic or antiferromagnetic materials. In fact, this J_{ij} equation is general a expression. ϵ is correction factor which depend on crystal structure and coordination number. If you want to use diluted magnetic systems you should use RKKY interaction in magnetism. We will be discussed RKKY interaction in chapter-3. Therefore, J_{ij} is very important for magnetic systems.

Magnetocrystalline Energy

The main source of magnetocrystalline anisotropy is the indirect interaction of the spin with the crystallographic lattice in terms of spin-orbit coupling and orbit-lattice coupling [10]. There are different sources of anisotropy which are shape anisotropy, stress anisotropy and exchange anisotropy. Magnetocrystalline anisotropy, is sometimes called crystalline anisotropy energy. One of the most common basic parameters in a magnetic system is the magnetic anisotropy term. We used as uniaxial single ion anisotropy in this thesis. It makes preference for spin moments to align with particular crystallographic axes, easy axis for positive anisotropy constant, d_e . Each of the two opposite directions is the minimum of energy, therefore the spins will align in either direction throughout the easy axis. Of course, there are other anisotropy terms for example surface anisotropies and shape anisotropies could also be considered. However we preferred uniaxial single ion anisotropy. The anisotropy energy, " E_{ani} ", has been given in the form below

$$E_{ani} = k_u (S_i \cdot d_e)^2 \quad (2.5)$$

where " k_u " is the single-ion anisotropy constant per atom, and " e " the easy axis. Magnetocrystalline energy is an intrinsic property. Its magnetization process is different when the field is applied along different crystallographic directions.

External Energy(Zeeman Energy)

Primarily known as the Zeeman effect(energy) named after the Dutch physicist Pieter Zeeman, the applied energy is the effect of external magnetic field on the magnetic spin moment. For the investigation of hysteresis curves we must include the contribution of external field to the system energy. The Zeeman energy ," E_{app} " , has form in the following:

$$E_{app} = |\mu_s|H_{app}.S_i \quad (2.6)$$

where, μ_s is the individual value of the magnetic moment and H_{app} is applied magnetic field.

Dipolar Energy

The magnetic dipolar coupling energy is a long range interaction between two magnetic dipoles. The dipolar energy (sometimes called magnetostatic or demagnetising energy) between a spin moment S_i and S_j has the form in Eq.2.7. This arises from law of sustainability of flux. The value of the dipolar field associated with the size and shape of individual moments, demagnetizing field, ferromagnetic domains, etc. Since many materials order at higher temperatures, magnetic dipolar interactionis generally small at these temperatures. Nevertheless, it is important to write the spin Hamiltonianincluding the dipolar term which is important at low temperatures. Inthis case, dipolar energy is given by:

$$E_{dipolar} = -\frac{\mu_s^2 \cdot \mu_0}{4\pi a^3} \sum_{i \neq j} \frac{3(S_i \cdot r_{ij})(r_{ij} \cdot S_j) - (S_i \cdot S_j)}{(r_{ij})^3} \quad (2.7)$$

where $r_{ij} \approx 1\text{\AA}$ is the distance between two magnetic dipoles. μ_0 magnetic moment, $\mu_s \approx \mu_B$ spin magnetic moment or Bohr magneton.

Total Energy

In summary, we described classical spin Hamiltonian using Monte Carlo method for magnetic systems. If we combine exchange energy, magnetocrystalline, zeeman energy and dipolar energy; general classical spin Hamiltonian can be written as the following:

$$H = - \underbrace{\sum_{i \neq j} J_{ij} S_i \cdot S_j}_{\text{Exchange}} + \underbrace{d_e (S_i \cdot e)^2}_{\text{Uniaxial}} + \underbrace{|\mu_s| H_{app} \cdot S_i}_{\text{Zeeman}} + \underbrace{\frac{\mu_s^2 \cdot \mu_0}{4\pi a^3} \sum_{i \neq j} \frac{3(S_i \cdot r_{ij})(r_{ij} \cdot S_j) - (S_i \cdot S_j)}{(r_{ij})^3}}_{\text{Dipolar}} \quad (2.8)$$

2.2 Monte Carlo Methods

In order to understand spin systems, there are a wide number of possible computational techniques. One of these techniques is the Monte Carlo(MC) simulation method, which is a powerful class of algorithms that is used not only in physics but also in other fields like material science, engineering, chemistry, economies, and risk analysis in a lot of different fields. Monte Carlo simulation method is not suitable for time dependent phenomena properties. It is useful large scale sampling statistically. However it is difficult to devise structural perturbations.

Monte Carlo methods are not only suitable for studying classical many particle systems, but also dealing with the more general problem of calculating high dimensional integrals. In fact, they are generally used for solving physical and mathematical problems. These method are principal used in apparent problem classes such as optimization, numerical integration, generation of probability distribution. Therefore, apart from MC, there are different simulation methods include molecular dynamics, Brownian dynamics, Langevin Dynamics etc. However, for some our simulations, we used the Monte Carlo method and Langevin dynamics to the systematic study of the magnetic behaviour of nanoparticles and nanoparticle assemblies. At a particular temperature, T, the partition function in a canonical

ensemble function is given by

$$\text{Canonical ensemble} \Rightarrow Z = \int e^{\frac{H}{k_B T}} dx \quad (2.9)$$

the average energy, specific heat, average magnetization and magnetic susceptibility are given by

$$\text{Average energy} \Rightarrow E = \frac{\langle H \rangle_T}{N}, \quad (2.10)$$

$$\text{Specific heat} \Rightarrow C_V = \frac{\langle E^2 \rangle - \langle E \rangle^2}{k_B T^2}, \quad (2.11)$$

$$\text{Average magnetization} \Rightarrow M = \frac{\langle \sum_i^N S_i \rangle_T}{N}, \quad (2.12)$$

$$\text{Magnetic susceptibility} \Rightarrow \chi = \frac{\langle M^2 \rangle - \langle M \rangle^2}{k_B T^2}. \quad (2.13)$$

All these phase can be valuated via the canonical function in Monte Carlo method for magnetic systems. Metropolis algorithm was used for Monte Carlo method. The Metropolis algorithm generates a random walk of points distributed according to a required probability distribution.

2.3 Spin Dynamics

Up to now, we have mentioned a Monte Carlo simulation method to calculate Hamiltonian energy of magnetic materials. This method is useful to find the equilibrium configurations for a magnetized materials though it can not ne used to describe dynamics effect. Because of this we need to apply spin dynamics (SD) or Langevin dynamics.

Langevin dynamics which numerical technique as well for random numbers and play an essential role to magnetic systems. This system is for long time trajectories and to calculations is necessary high central processing unit(CPU). Atomistic simulations of spin dynamics have been presented by several groups in the past as methodological and computational

[8, 11–13]. In this thesis, apart from Monte Carlo method, we also investigated spin dynamics simulations in diluted magnetic systems. In this section, we will be discuss spin dynamics using the LLG equation of motion.

The applications in magnetic storage and information technology are one of the key motivations for the importance of magnetism. For applications, magnetic recording speed at which magnetic bits can be recorded. A main question is, fundamentally how fast angular momentum can be reversed. Therefore, we need to examine the dynamics of angular momentum, and this system generally called spin dynamics. Recently, for requirements of highest speed and density storage elements, energy loss, has accelerated the investigation of magnetization dynamics. Because of this, we used Langevin Dynamics to calculate precessional behaviour of spins in terms of technology speed, energy loss, spin dynamics applications. In particular it is mostly not possible to observe the precession of a single electron spin. Therefore for the macro spin approximation is used to describe the precession of magnetization. According to quantum mechanics, Schrödinger equation is connect with the spin operator,"S", and spin Hamiltonian,"H". In this case the time derivation of spin with the Hamiltonian,H, the equation of motion given by

$$i\hbar \frac{d}{dt} \langle S \rangle = \langle [S, H] \rangle \quad (2.14)$$

where Hamiltonian depend on external applied field.

$$H = -\frac{g\mu_B}{\hbar} S \cdot B \quad \iff \quad B = \mu_0 H \quad (2.15)$$

With the commutator relations

$$[S_x, S_y] = i\hbar S_z, \quad [S_y, S_z] = i\hbar S_x, \quad [S_z, S_x] = i\hbar S_y \quad (2.16)$$

$$[S, H] = -\frac{g\mu_B}{\hbar} \begin{pmatrix} B_y S_z - B_z S_y \\ B_z S_x - B_x S_z \\ B_x S_y - B_y S_x \end{pmatrix} \quad (2.17)$$

Equation of motion is for single spin as the following from quantum mechanics.

$$\frac{d}{dt}\langle S \rangle = -\frac{g\mu_B}{\hbar}(\langle S \rangle \times B) \quad (2.18)$$

2.3.1 Landau-Lifshitz-Gilbert Langevin Equation

The fundamental description of spin dynamics associate the interaction of magnetic moments with magnetic fields. Most spin(magnetization) dynamics simulations are connected with the Landau-Lifshitz-Gilbert equation of motion. Spin dynamics are based on proposed by Landau and Lifshitz [14] in 1935, and added a specific form for the damping by Gilbert [15] in 1955. That is, Gilbert added a specific form for the damping. We will given both Landau-Lifshitz and Gilbert equations as a model for magnetization dynamics. The magnetic torque equation which between external magnetic field " \mathbf{H} " and magnetic moment " \mathbf{M} " given by

$$\vec{\tau} = \vec{M} \times \vec{H}. \quad (2.19)$$

The interaction of a magnetic moment with an external magnetic field gives rise to a magnetic torque as the above. τ depend on both magnetic moment and field directions obvious from the equation. This both the classical equation limit and in reality the magnetization is damped.

Precession of Spin

Einstein and de Haas described relation between magnetism and angular momentum in 1915. The angular momentum in magnetism can be described as identical to the angular momentum of a rotating object, as viewed in classical mechanics. So, it is clear that a magnetic moment is naturally related to its angular momentum " L ". According to quantum mechanics theory, the angular momentum of electron connected with a magnetic moment, " M ", is

$$M = -\gamma L \quad (2.20)$$

where γ is the gyromagnetic ratio of moment and material's parameter dependent. It equal

$$\gamma = \frac{g \cdot e}{2m_e \cdot c} \quad (2.21)$$

g is the Landé g -factor, e is the electron charge, m_e is the electron mass, and c is the speed of light. The various forms of the Eq.2.21 have been often seen in micromagnetics models. In particular, this equation use behaviour of magnetic elements according to the time. The precessional motion of a magnetic moment, in the absence of damping is described by the torque equation in Eq.2.19. The torque is the change of the moment with time ($\tau = \frac{dL}{dt}$). We can combine Eq. 2.20 using Newton's rotational motion of for angular momentum as the following:

$$\vec{\tau} = \frac{d\vec{L}}{dt} = -\vec{M} \times \vec{H} \quad (2.22)$$

Then, when Eq.2.20 and 2.22 are combined magnetic moment can be rewritten as:

$$\frac{d\vec{M}}{dt} = -\gamma \left[\vec{M}(t) \times \vec{H}(t) \right]. \quad (2.23)$$

This is the equation of motion of a magnetic moment in an external magnetic field. The spins not only respond to the external magnetic field but also they are affected the other contributions such as the anisotropy and magnetic dipole interaction. All these interactions are called effective field H_{eff} . The effective field is given by

$$\vec{H}_{eff} = \vec{H}_{exc} + \vec{H}_{ani} + \vec{H}_{app} + \vec{H}_{demag} + \dots \quad (2.24)$$

where H_{exc} is the exchange field, H_{ani} is the anisotropy field, H_{app} is the external applied field, H_{demag} is the demagnetization field and others(magnetostatic coupling field, ampere field, thermal field). Except for external applied field, all other contributions depend on properties of material. Basically, this important model was derived by Landau and Lifshitz(1935) [14] which constitutes a precession equation Eq.2.23, in which includes the presence of quantum

mechanical effects. In that case, Eq.2.23 can be written as:

$$\frac{d\vec{M}}{dt} = -\gamma \left[\vec{M}(t) \times \vec{H}_{eff}(t) \right]. \quad (2.25)$$

Damping of the Precession

Experientially it is observed that the magnetization does not precession, however it's motion is damped. We deal with the theory magnetization dynamics known as the Gilbert damping parameter. This additional term tends to force the magnetization M to turn towards the direction of the effective field. Therefore, Landau and Lifshitz added a damping term in the equation of motion of spin. This term describes the relaxation of magnetization to a stable energy minimum in spin dynamic. New equation form in the below:

$$\frac{d\vec{M}}{dt} = \underbrace{-\gamma(\vec{M} \times \vec{H}_{eff})}_{\text{Precession}} - \underbrace{\gamma \frac{\alpha_{LL}}{|\vec{M}|} \vec{M} \times (\vec{M} \times \vec{H}_{eff})}_{\text{Damping}} \quad (2.26)$$

where α_{LL} is dimensionless constant which called the Landau damping constant, reveals the energy loss speed in the ferromagnetic material. First part is precession, second part is damping term in spin dynamics. α_{LL} is less than 0.1, sometimes it can be 0.01 [8]. This value usually use for Fe, Co, Ni transition metals or alloys. However, in ferromagnetic oxides or ferrites, the this process (α_{LL}) is smaller. The last equation is the Landau–Lifshitz equation which describes the motion in terms of gyromagnetic precession model. Thereafter, Gilbert mentioned to add as precession damping at much larger time and length scales for rotation of the magnetization [15]. Thus, Landau–Lifshitz Gilbert's equation was written in following the form:

$$\frac{d\vec{M}}{dt} = -\gamma(\vec{M} \times \vec{H}_{eff}) - \frac{\alpha_G}{|\vec{M}|} \vec{M} \times \frac{d\vec{M}}{dt} \quad (2.27)$$

This is called as LLG equation. Multiplying both sides of Eq.2.27 by $\vec{M} \times$ gives,

$$\vec{M} \times \frac{d\vec{M}}{dt} = -\gamma \vec{M} \times (\vec{M} \times \vec{H}_{eff}) - \frac{\alpha_G}{|\vec{M}|} \vec{M} \times \left(\vec{M} \times \frac{d\vec{M}}{dt} \right) \quad (2.28)$$

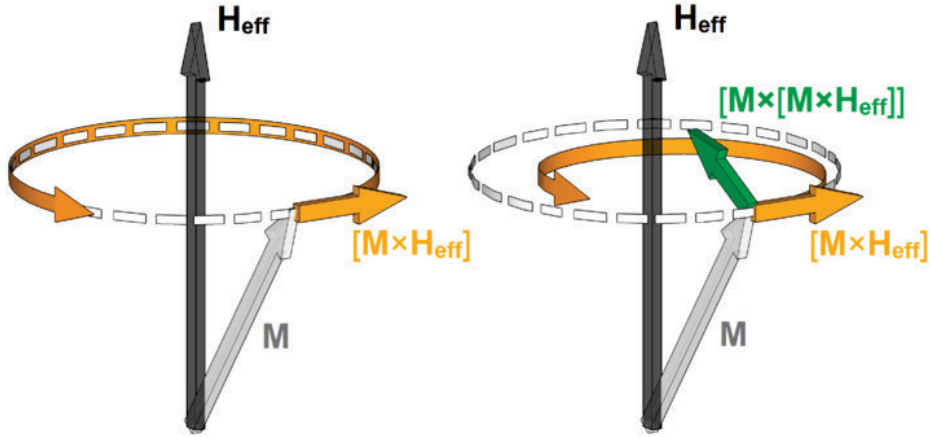


Fig. 2.2 Visualisation of damped and precession in spin dynamics. Precession of the magnetization with an external magnetic field. Undamped gyromagnetic precession (left). Damped gyromagnetic precession (right) from taken ref[16].

Using the vector identity,

$$\vec{A} \times (\vec{B} \times \vec{C}) = (\vec{A} \cdot \vec{C})\vec{B} - (\vec{A} \cdot \vec{B})\vec{C} \quad (2.29)$$

the second term in Eq.2.28 can be rewritten as:

$$\vec{M} \times \frac{d\vec{M}}{dt} = -|\gamma|\vec{M} \times (\vec{M} \times \vec{H}_{eff}) - \alpha_G |\vec{M}| \frac{d\vec{M}}{dt}. \quad (2.30)$$

If we substitute this result in Eq.2.28 and take $|\vec{M}|=1$, we obtain the Landau–Lifshitz–Gilbert (LLG) equation

$$\frac{d\vec{M}}{dt} = -\frac{\gamma}{1 + \alpha_G^2} \left[\vec{M} \times \vec{H}_{eff} - \frac{\alpha_G}{|\vec{M}|} \vec{M} \times (\vec{M} \times \vec{H}_{eff}) \right]: \quad (2.31)$$

In the Landau-Lifshitz model and the LLG model, the relationship between γ and λ is given below:

$$\gamma = \frac{\gamma_L}{1 + \alpha^2}, \quad \lambda = \frac{\gamma_L \alpha}{1 + \alpha^2} = \gamma_L \alpha. \quad (2.32)$$

Therefore, γ is the gyromagnetic ratio related to the phenomenological Gilbert damping factor α_G in the LLG equation and it's unit $T^{-1}sn^{-1}$. Thus, the equation of motion for mag-

netic moments is always called the LLG equation (Eq. 2.31) in micromagnetic simulations. It is dependent on spin-electron, spin-phonon etc coupling and material. Magnetization dynamics is described where the first term and second term are called as precessional and Gilbert coefficient, respectively, in the Eq. 2.32. In this thesis we examined the effect of damping factor on doping of cobalt in ZnO.

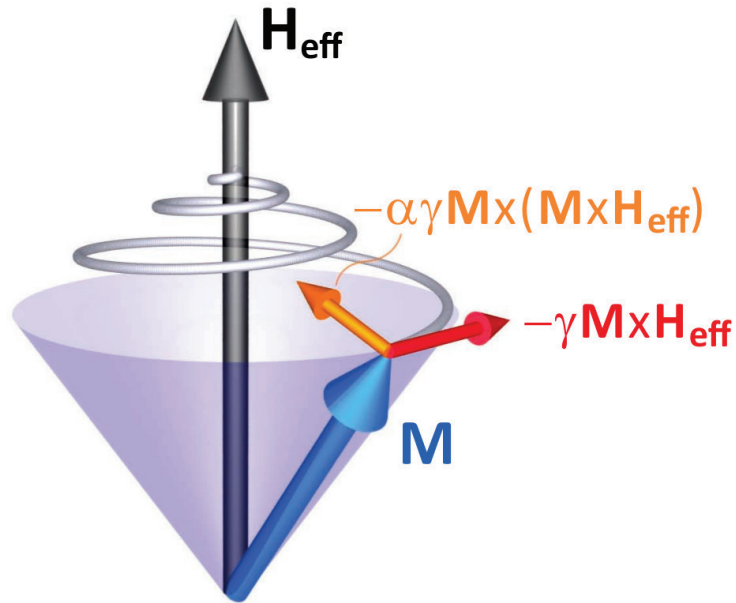


Fig. 2.3 Schematic illustration of the spin dynamics described by the Landau-Lifshitz equation Eq.2.26 taken from ref [17]. The magnetization M precesses throughout the effective magnetic field H_{eff} . A small damping rotation gradually aligns the magnetization with the effective field.

In both magnetization reversal processes described above, there is a relation to the angular momentum of a magnetic moment. A magnetic system with a very small angular momentum is a feasible candidate for a faster magnetization reversal. Thus, in order to transfer the magnetic moment from consistent configuration to another, it takes a time of about 0.1-1 ns. This is a reversal time quite slow for the current demand for a faster data storage device on new technology. The effective field Hamiltonian was determined the dynamics of the magnetic moment as above Eq. 2.24

2.3.2 LLG-Stochastic Spin Dynamics

If we take into account possibility for thermal fluctuations, we should add to Eq. 2.24 stochastic field term ζ suggested by Brown [18] using Langevin equation approach [19].

$$\vec{H}_{eff}(t) = -\frac{\partial \mathcal{H}(t)}{\partial \vec{m}} + \vec{\zeta}(t, T) \quad (2.33)$$

where, Hamiltonian \mathcal{H} contains only exchange and anisotropy. At first, Langevin dynamics simulations in micro size for magnetism were introduced by Chantrell and Lyberatos [20] and further developed by a number of groups [21–24]

$$\frac{(1 + \alpha^2)\mu_s}{\gamma} \frac{d\vec{M}}{dt} = -\vec{M} \times \left[\frac{\partial \mathcal{H}(t)}{\partial \vec{M}} - \zeta(\vec{t}, T) + \alpha_G \vec{M} \times \left(\frac{\partial \mathcal{H}(t)}{\partial \vec{M}} - \vec{\zeta}(t, T) \right) \right] \quad (2.34)$$

where the thermal field ζ has the noise properties for magnetic materials.

$$\langle \zeta_i = 0 \rangle, \quad \langle \zeta_i(0)\zeta_j(t) \rangle = 2 \frac{k_B T \alpha}{\gamma |M|} \delta_{ij} \delta(t); \quad i = x, y, z \quad (2.35)$$

However, the atomistic simulations of the spin dynamics based on the micromagnetic LLG equation, which are not suitable for high temperatures.

2.3.3 LLG-Atomistic Spin Dynamics

Equation of motion for the atomic spins is given in terms of the atomistic Landau-Lifshitz-Gilbert (LLG) equation. The Atomistic spin dynamics (ASD) which include the Langevin fields have been describe as the magnetic moment at each lattice site by a classical spin vector. Atomistic simulation of magnetic materials has become an essential tool in understanding the processes and behaviour of magnetic nanomaterials. Recently, Atomistic models of

magnetic materials have been studying by a lot of scientist [5, 8, 25–27]. The dynamics of each normalized magnetic moment is described as the following:

$$\frac{(1 + \lambda^2)}{\gamma} \frac{d\vec{S}_i}{dt} = -\vec{S}_i \times \left[\frac{\partial \mathcal{H}(t)}{\partial s_i} - \vec{\zeta}_i(t, T) + \lambda S_i \times \left(\frac{\partial \mathcal{H}(t)}{\partial s_i} - \vec{\zeta}_i(t, T) \right) \right] \quad (2.36)$$

where the thermal field ζ_i is written again as:

$$\langle \zeta_i = 0 \rangle, \quad \langle \zeta_i(0) \zeta_j(t) \rangle = 2 \frac{\lambda k_B T}{|\gamma|} \delta_{ij} \delta(t); \quad i = x, y, z. \quad (2.37)$$

The most successful application of magnetism is spintronic devices that it is read heads in hard drives based on Giant Magneto Resistance (GMR). Therefore spintronic devices will play an important role in the future since the dimensions of the devices continues has developed with semiconductor technology.

2.4 Ultrafast Spin Dynamics

The dynamic aspects of a magnetic system are often described as magnetization dynamics or spin dynamics. The non-equilibrium of spin dynamics is magnetization processes that is time dependent, even if the external magnetic field remains constant. The samples are studied in dynamic magnetisation behaviour on the sub-picosecond timescale. Moreover soft magnetic materials exhibit hysteresis losses at high-frequency, and the longterm thermal stability of stored information is important in magnetic recording. Relaxation times shown differences one nanosecond or less in materials for high-frequency applications. Because of this, ultrafast dynamics properties of materials connected with magnetization, anisotropy and time are carried out on very small length scales, especially less than 1 nm [28–30].

In recent years, importance of ultrafast spin dynamics have been increasing in term of relationship among spins, relaxation dynamics of electrons, the lattice dynamics and demagnetization [1, 8, 31, 32]. The relaxation rates are connected with the strength of the coupling between these three energies. Femtosecond laser pulses are able to excite

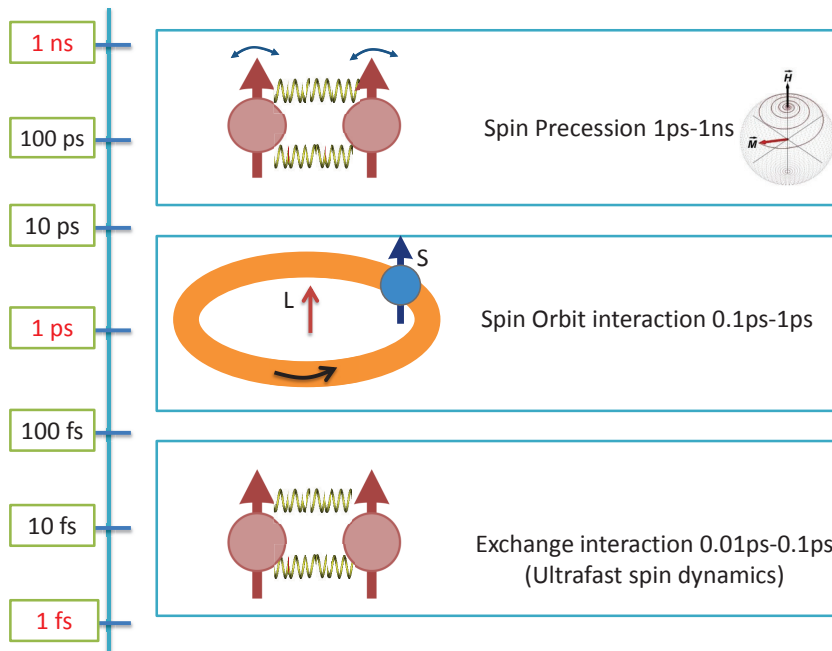


Fig. 2.4 Time-scale of ultrafast spin dynamics

in the magnetic material, on a time scale of the exchange interaction. These observations such laser induced demagnetization of a magnetic material [33], magnetic anisotropy [34, 35], magnetization reversal [36] have been demonstrated. It become important area of spin dynamics to a new technology such as time resolved X-ray, XMCD and TeraHertz (picosecond) probing. Recently, GdFeCo ferrimagnetic alloy materials have showed that ultrafast laser pulses can cause the material to reverse via the inverse Faraday effect [37–41]. The best important relaxation time should be between 10-100 femtoseconds.

On the one end of the scale or around ps, we find the relaxation time in magnetic data storage. On the other end of the time scale, we are faced with ultrafast energy and angular momentum transfer processes in magnetic systems on a time scale of 10^{-14} s. These processes are related to non-equilibrium electron distributions and are held responsible for an extremely fast decay of the magnetic order, for example, after a highly power laser pulse. In the intermediate time regime between 10^{-3} and 10^{-12} sn we find a wealth of different dynamical processes. These range from relatively slow phenomena, such as magnetization loses and

after-effects, to fast mechanisms, which determine the technological limits of magnetization reversal such as domain wall propagation, and coherent rotation.

2.5 Summary

Summarizing, atomic spin models have great important properties of magnetic materials for micro-magnetic models in industry and modern technology. So, we examined Monte Carlo method and LLG-Langevin dynamics for the best compare, due to unique magnetic properties suitable and magnetic recording. After Monte Carlo method, we described the spin dynamic model for damped gyromagnetic precession, described by the Landau-Lifshitz-Gilbert equations. Spin magnetic momentum of electrons relationship with angular momentum through the gyromagnetic ratio was discussed. The most fundamental properties of magnetization dynamics is Gilbert damping constant. In this chapter, the basic Monte Carlo and Heun method theoretically are described.

Chapter 3

ATOMISTIC SPIN MODEL OF DILUTED MAGNETIC SEMICONDUCTORS

3.1 Background of Diluted Magnetic Semiconductors

In this chapter we examined the magnetic properties of diluted magnetic semiconductors (DMS) in order to understanding theoretically according to some properties. The DMS simultaneously exhibit semiconducting properties and are typically either paramagnetic or ferromagnetic order. Therefore, they shown ideal candidates for compare in semiconductor spintronic devices. Particularly, ferromagnetic semiconductors were intensively studied after from middle of 20th century. Therefore, in this chapter we will present the most important features that distinguish a DMS.

Diluted magnetic semiconductors combine a non-magnetic semiconductor with a transition metal (TM) dopant such as Cr, Mn, Fe, Co, Ni and Cu. Also, DMS known as semi-magnetic semiconductors are a wide range of materials. DMS are identified generally as II-VI (ZnO, ZnS, ZnTe etc) and III-V (GaAs, InP GaN, etc) semiconductors and transition metal alloys, especially containing manganese. Research interests in these DMS compounds are mainly aimed towards novel spintronics (spin+electronics) applications [42]. Spintronics devices is a new technology that transforms reading and writing information by spin rather than by electron charge. These materials have magnetic Curie temperatures above room tem-

perature, which they both n- and p-type materials for direct use in semiconducting junction applications [43, 44].

Room temperature ferromagnetism in transition metal doped ZnO theoretically has been developed by Dietl et al [45] who used a theory originally developed for metals by Zener [46]. Some investigations exhibit ferromagnetic properties both theoretically and experimentally which these n-type ZnO doped with Fe, Co, or Ni [47, 48], ZnO doped with small Co doped ZnO near room temperature [49]. Sometimes, according to some parameter ZnO doped with Cr, Ni, or Mn did not show ferromagnetism. Because of this, the development of semiconductor spintronic material is still a very active in the research field. Many scientist have still studies in this area both experimentally and theoretically.

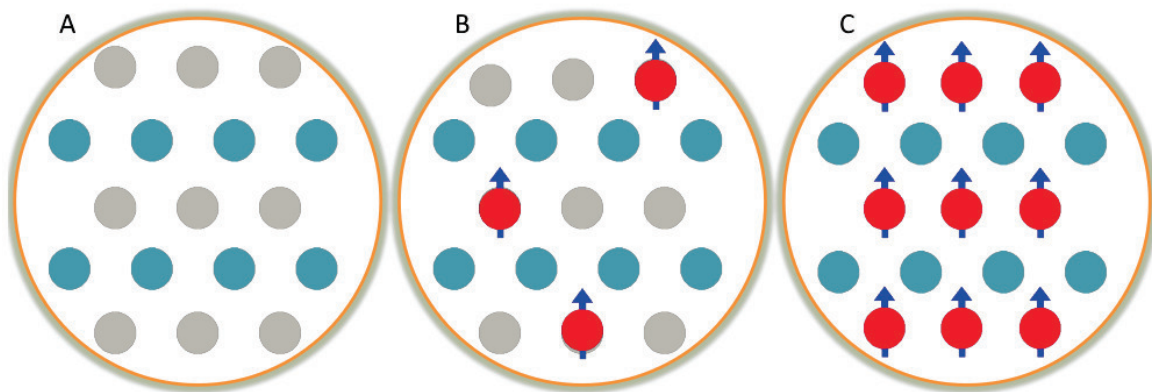


Fig. 3.1 Representation of diluted magnetic semiconductors. Fig-A: Schematic of a non-magnetic semiconductor material consisting of cations and anions, B: a diluted magnetic semiconductor in which some of the non-magnetic cations, C: a magnetic semiconductor in which the magnetic cations form an ordered crystalline array

Diluted magnetic semiconductors have possible material parameters such as the band gap and the lattice constant. The lattice parameters of the DMS crystals has allow to new researchers to grow of quantum wells and super-lattices in order to investigate new magnetic effects [50, 51]. The presence of magnetic ions in DMS are associated with semiconductor properties. The Curie temperature and many other magnetic properties connect with material's properties such as the temperature dependence of the anisotropy and magnetization.

3.2 Spintronic Applications of Diluted Magnetic Semiconductors

Spintronics is a novel technology based on usage of spins as information units. The invention of spin electronics or spintronics discovered by Igor *et al* in 1988 [52]. Spintronics is a novel technology based on usage of spins as information technology with the discovery of the giant magnetoresistance (GMR) which is Nobel Prize in Physics was awarded to Albert Fert and Peter Grünberg in 2007. Modern technologies are frequently developed as parallel or directly with industry through the development of structures of the best materials. Revolution of electronics like quantum computing that spintronics devices have been growing constantly in search for suitable materials to achieve scientists [53, 54]. Generally, magnetic properties of these materials are effect by with the magnetic field, electron defects, the energy states of the electrons, strong applied field. These applications of spintronics materials is listed at below.

- Efficient electrical injection of spin-polarized carriers into semiconductors.
- Spin transistors for low energy consumption at mobile applications like lifetimes in the device like semiconductor nanophysics and optics.
- Mechanisms of ferromagnetism in DMS materials in terms of technological applications like data storage.
- Determination of Curie temperature above room temperature. Effective control and usage of the spin system.

DMS are sensitive pieces of electronic equipment, which known as a piezoelectric material. N-type materials are group V elements in the periodic table which they have a larger electron concentration than hole concentration such as arsenide (As) or phosphorus (P). P-type materials are group III elements like boron (B), aluminium (Al) or iridium (Ir) and they have a larger hole concentration than electron concentration opposed to n-type semiconductors. In addition to all the mentioned characteristics properties which are p-n type ZnO or GaAs with Mn, Co, Ni, V and Fe have sometimes ferromagnetic properties be important for spintronics

applications. Magnetic semiconductors exhibit both ferromagnetism and semiconductor properties. Electronic materials are based on the control of charge carriers, but the magnetic semiconductors would also allow the control of spin position which is an important property for spintronics applications. While many magnetic materials such as magnetite, are also semiconductors. Moreover some materials are more magnetic according to properties of materials. For example diluted magnetic semiconductors are less magnetic due to non-magnetic spins. Off course, this situation depend on many factor such as temperature and magnetic field.

3.3 II–VI and III–V Compound Semiconductors

Diluted magnetic semiconductors generally can be categorized into two groups which these groups are II-VI and III-V semiconductor materials. A number of groups have also studied the effect of transition metal doping of II-VI (ZnO, ZnS, etc) and III-V (GaAs, GaN, etc) semiconductors due to their potentials in spintronic applications. II-VI and III-V group semiconductors which paramagnetic compounds have the most studied DMS materials [45, 55]. They have a high degree of solubility for the magnetic element. Most DMS materials was studied to spintronic applications have low T_c values [56, 57]. In particular, the T_c of $Ga_{1-x}Mn_xAs$ has been reported. Moreover all the experimental measurements and theoretical calculations shown ferromagnetic properties.

Zinc oxide based diluted magnetic semiconductors are one of the most important materials for spintronic materials and devices. In 2000, room temperature ferromagnetism in Mn-doped p-type GaN and ZnO was predicted by Dietl *et. al* using Zener model [46]. Later, these predictions were soon experimentally confirmed for both materials [58, 59]. Then, several other materials were reported such as Co/Cr/Mn doped AlN [60] and Mn-doped GaP [61]. In addition DMS compounds doped with a few percent of magnetic ions they shown ferromagnetic order some temperature T_c [62–64]. The differences between the III-V and II-VI materials are solubility of transition metals in Fig.3.2. Ferromagnetism has firstly been observed in Mn doped InAs [66] and GaAs [67] the Curie temperatures T_c which these

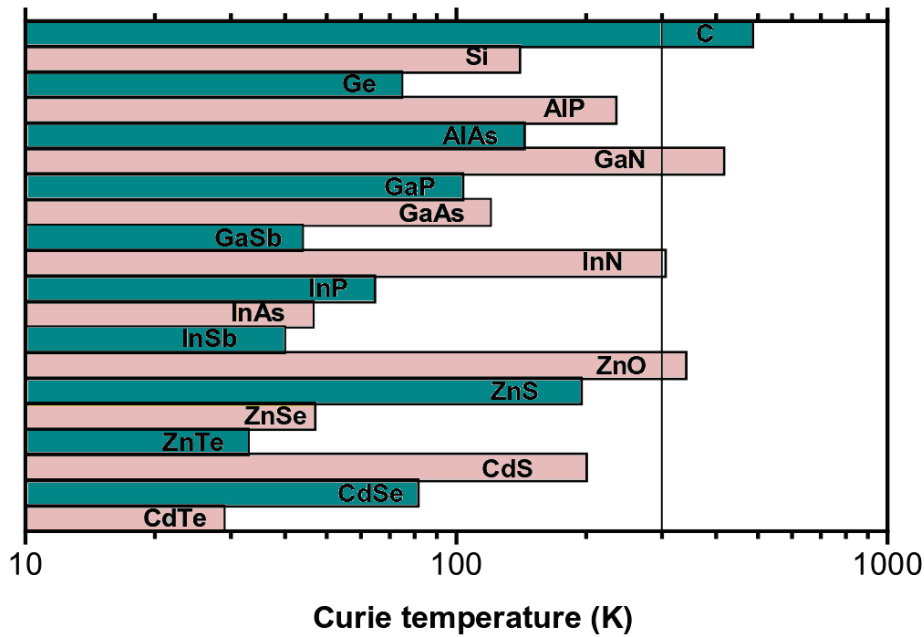


Fig. 3.2 Diagram of Curie temperatures computed within the Zener model for various semiconductors taken from ref[65]

are still well below room temperature (RT). However ferromagnetism has been predicted for wide band gap transition metal doped semiconductors such as ZnO:TM or GaN:TM at room temperature [46] (TM:Transition metal). These materials have been still studies extensively during the last few years. Intensive studies have shown that DMS containing transition metals, such as iron, cobalt, nickel in the literature. Over the past decade, III-V

Material	Doping	Moment(μ_B)	T_c (K)	References
V-ZnO	15%	0.5	>350	Saeki et al. [68]
Mn-ZnO	2.2%	0.16	>300	Sharma et al. [59]
Fe-ZnO	5%	0.75	550	Han et al. [69]
Cu-ZnO	1%	0.75	550	Han et al. [69]
Co-ZnO	10%	2.0	280-300	Ueda et al. [49]
Ni-ZnO	0.9%	0.06	>300	Radovanovic and Gamelin [70]

Table 3.1 Some ferromagnetic behaviour of oxide materials with T_c above room temperature

ferromagnetic DMS have been attracting attention by most scientists in terms of nature of

$Ga_{1-x}Mn_xAs$ and $Ga_{1-x}Mn_xN$. However, some II-VI DMS structures have been shown both ferromagnetic and antiferromagnetic properties in the some papers [71, 72]. Though some papers have been shown spin glass properties [73]. Curie temperature of some oxide materials were shown in Table 3.1. Therefore, we have been focuses to transition metal doped II-VI, III-V semiconductors and alloys to understanding of their general properties. General magnetic phase diagram for dilute ferromagnetic semiconductors shown by [57] in Fig.3.3. So, recently spin dynamics studies in nanostructure diluted magnetic semiconductors are given exciting in terms of technologic requirement [74–79]. We have investigated the properties the electronic structure and magnetism of II–VI DMS systems.

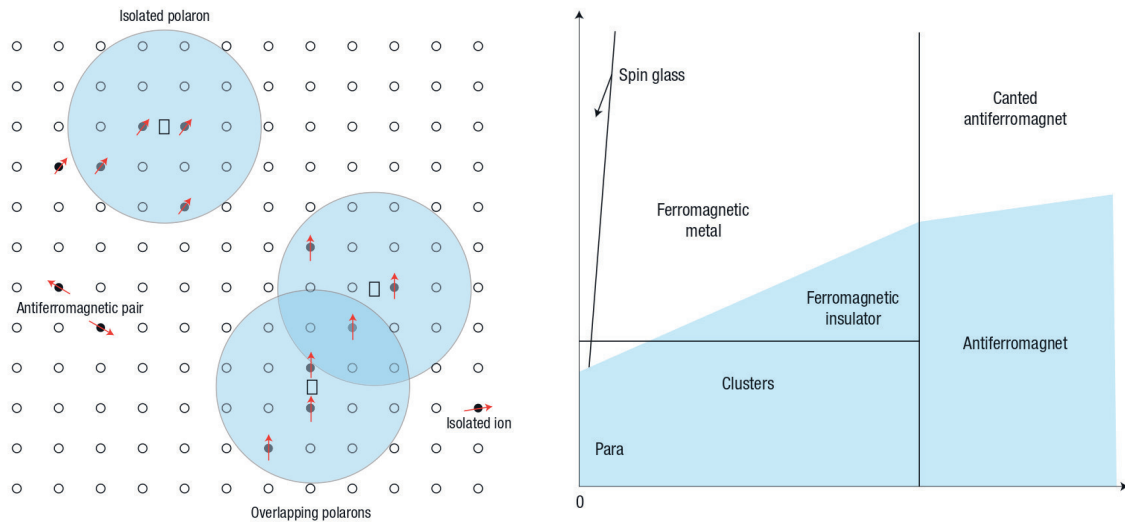


Fig. 3.3 Magnetic polarons and magnetic phase diagram which are interactions between electrons and atoms in a solid material for dilute ferromagnetic semiconductors. Figures represent (left) magnetic polarons (right) magnetic phase diagram for dilute ferromagnetic semiconductors taken from ref [57].

3.3.1 Crystal Structure of Zinc Oxide-ZnO

The crystal structures of ZnO, the II-VI semiconductor, has a cubic rocksalt structure, (wurtzite hexagonal structure or hexagonal zinc-blende structure). They are in the band-gap energy group with energy $E \approx 3.4eV$ and show higher breakdown voltages, lower noise generation

and operation at high-power. The most important features of zinc oxide used in industry listed as follows:

- Most important applications of zinc oxide is rubber industry, ceramic and glass compositions. Zinc oxide is not magnetic. However ferrites has magnetic properties which they oxide ferrite compositions.
- Zinc oxide has the largest exciton binding energy and optical gain reported based semiconductor manufacturing.
- ZnO is one of the hardest materials in II-VI compound semiconductors due to the lasers, light-emitting diodes (LED), optoelectronic, some diodes, field-effect transistors (FET), microwave semiconductor technologies.
- ZnO is one of the hardest materials in II-VI compound semiconductors due to the higher melting point and energy. The component elements of zinc oxide are low cost and can be easily grown at low temperatures.

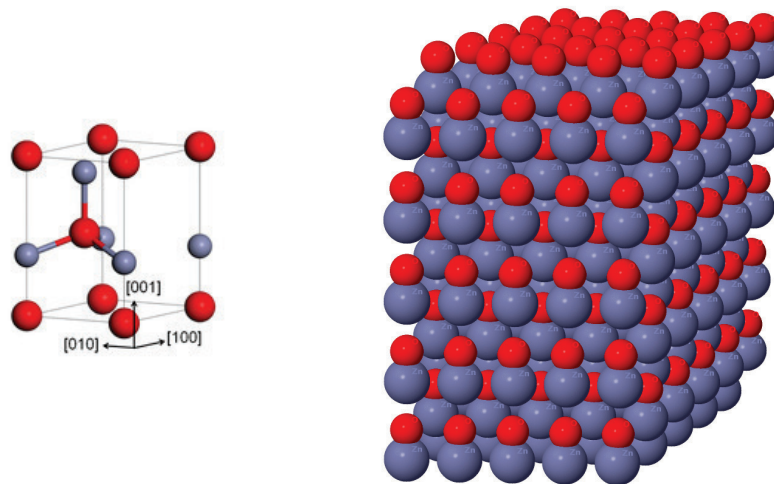


Fig. 3.4 A schematic of the structure of ZnO wurtzite crystal structure. Crystal visualization of ZnO structures used in the calculations $5 \times 5 \times 5$ ZnO wurtzite crystal structure. The blue and red spheres stand for Zn and O atoms, respectively

In order to understanding this systems, firstly, we created ZnO crystal structure. Pure ZnO which consists of Zn and O hexagonal wurtzite structure. In this thesis, the lattice

constants of ZnO hexagonal unit cell are $a=b=3.32 \text{ \AA}$ and $c = 5.22 \text{ \AA}$. We created crystal structure of Wurtzite ZnO writing code at C++ program language at size $5 \times 5 \times 5$ as Fig.3.4. The primitive wurtzite ZnO unit cell structures occur from 4 atoms, which their position at Cartesian coordinates (x, y, z) are $(0,0,0)$ $(0,0,\frac{3}{8})$ $(\frac{1}{3},\frac{2}{3},\frac{1}{2})$ $(\frac{1}{3},\frac{1}{3},\frac{7}{8})$ [80, 81].

We created the crystal structure of ZnO with some Co (1-5-10-20-50 and 100 %) concentration in Fig.3.5. In summary, in order to our understanding magnetic properties of TM doped ZnO, we need to created these crystal for Monte Carlo and Spin dynamic theory.

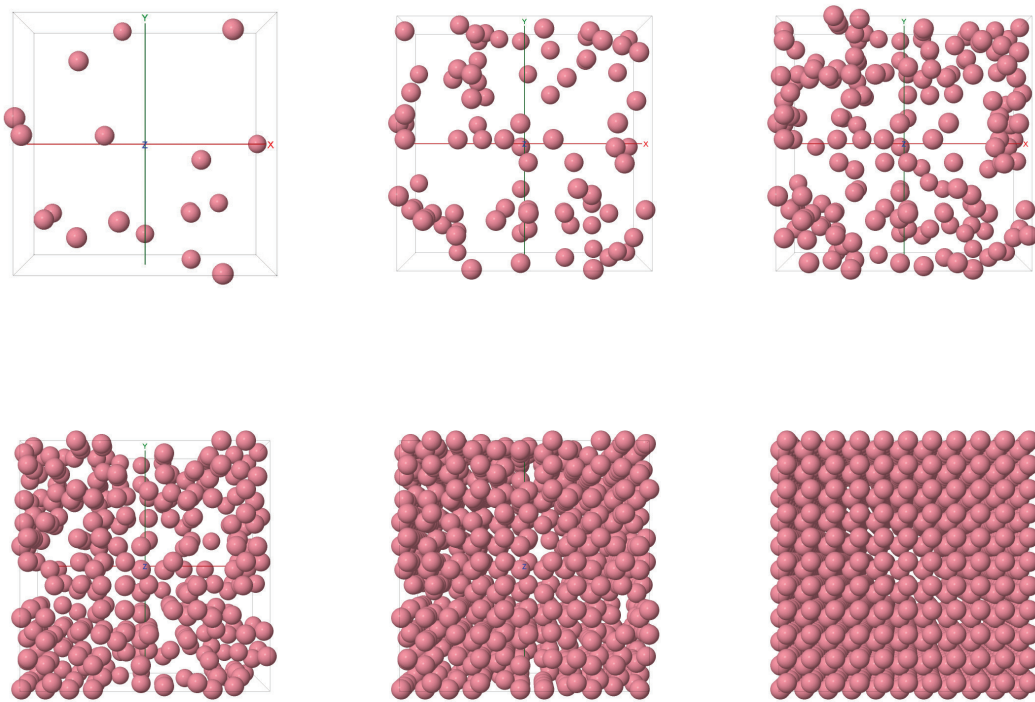


Fig. 3.5 Crystal visualization of DMS structures according to doping concentration. We illustrated CoZnO wurtzite structure in some doped percent in size $4 \times 4 \times 4$. From left to right, Co concentration inside ZnO are 1-5-10-20-50-100%, respectively. In fact last figure is CoO crystal structure

3.4 Exchange Interactions between Local Spins-RKKY

Indirect exchange interaction sometimes called superexchange for antiferromagnetic systems between non-neighboring magnetic ions. In particular, this kind of exchange interaction play an important role in (III,V) and (II,VI) ferromagnetism. Ruderman-Kittel-Kasuya-Yosida (RKKY) model is present for the magnetic impurities. The RKKY interaction is generally ferromagnetic at low electron densities depending some condition. However at higher densities, these interactions will provide many negative (AFM) and positive(FM) exchange bonds, and the system becomes a spin glass. Though there are many controversial models that have been used to describe the properties of magnetism in DMS. For example the Zener exchange model has been useful in explaining many experimental results [46]. The Zener model is a mean field approach that describes ferromagnetism in (Ga,Mn)As for calculating indirect exchange energy between the magnetic moments of manganese or other metal atoms. The most important feature of diluted magnetic semiconductors is the correlation among magnetic properties of the exchange interaction in Fig.3.6. In general the RKKY interaction gives rise to ferromagnetism if k_F is small (nearly empty bands) and to antiferromagnetism when $k_F \sim \pi/a$ (half-filled band).

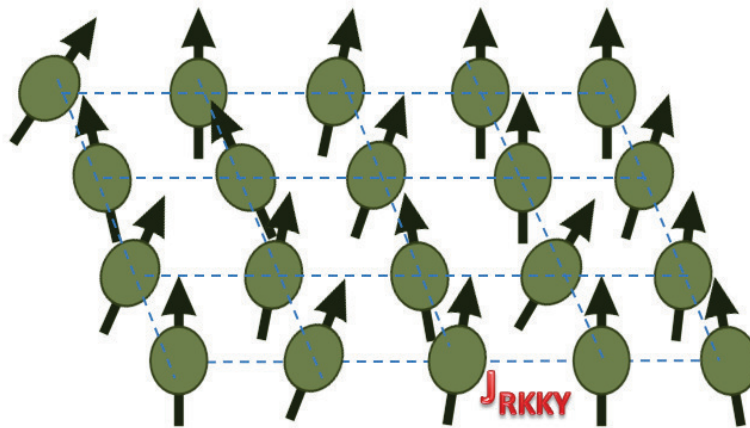


Fig. 3.6 Schematic representation RKKY exchange interactions among atomistic spins

RKKY interaction between the localized magnetic ions the exchange interaction is indirect, because they do not involve direct coupling between magnetic moments. The theory

is used in rare-earth metals, or in alloys of magnetic ions in a non-magnetic metallic host with each other directly [82–84]. The interaction between the conduction electrons and unfilled inner shell electrons suggested by Zener [85] in 1951 for ferromagnetism with incomplete d-shells. This phenomenon known as Zener or s-d interaction model. Later, Ruderman and Kittel showed how localized spins in a metal can couple through polarization and spread of carrying electrons in 1954, the electron wave function depends on the orientation and the distance between the two localized spins [86]. The function generally describe the form of an distance (r) dependent exchange interaction $J_{RKKY}(r)$ given by

$$J_{RKKY}(r) \propto \frac{\cos(2k_F r)}{r^3} \quad (3.1)$$

where k_F Fermi wave factor and r is distance between the two localized magnetic spins. The RKKY interaction can explain electron spin correlations between unpaired electrons in different atoms. Because of this, function of RKKY theory has oscillatory motion such as Fig.3.7

In transition metal oxides, the exchange energy is not always ferromagnetic such as NiO, FeO and CoO. Therefore antiferromagnets has zero net moment. However, the numbers of spin up and spin down electrons are not always equal. Because the moments are aligned with specific crystallographic sites in metal oxides. This phenomenon is known as ferrimagnetism.

3.4.1 Model Description

The main aim of this section is to demonstrate how spin interactions in diluted magnetic semiconductors depend on band structure and types of magnetic ions. Therefore, Ruderman-Kittel-Kasuya-Yosida (RKKY) interaction plays an important role in diluted magnetic alloys, rare earth metals and their metallic compounds. The nearest neighbouring interaction between the magnetic ions tend to align either ferromagnetic or antiferromagnetic, depending on the distance between the ions. The interaction is known as the RKKY interaction by Ruderman, Kittel, Kasuya, and Yosida, and was first developed to explain the indirect exchange coupling

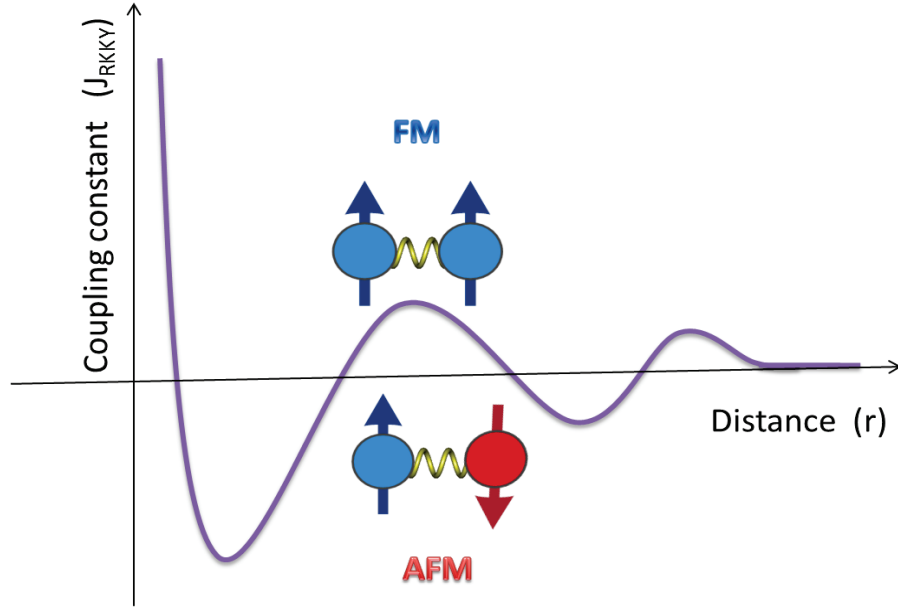


Fig. 3.7 Schematic of the dependence of the coupling constant on distance in Ruderman-Kittel-Kasuya-Yosida model. The RKKY exchange integral plotted as a function of distance. The interaction type is between ferromagnetic (FM) and antiferromagnetic (AFM) coupling. This oscillation depend on Fermi wave factor k_F .

by conduction electrons [86–88]. In the our first step, we determine nearest neighbours interactions among Zn and O atoms. This interaction given by [82–84]:

$$J_{RKKY}(r) = -j_0 \left[\frac{2k_F r \cos(2k_F r) - \sin(2k_F r)}{(2k_F r)^4} \right] e^{-r/l} \quad (3.2)$$

where $j_0 = 2.2 \times e^{-22}$ joule is average exchange energy on RKKY interaction and varies with " r " distance. " l " is damping scale of RKKY interaction due to the localization of the carriers. " $e^{-r/l}$ " term comes from limited conductivity limiting the range of the RKKY interaction since electrons are unable to hop large distances, unlike a metal is given in Eq.3.1.

$$r = \sqrt{(x_2 - x_1)^2 + (y_2 - y_1)^2 + (z_2 - z_1)^2} \quad (3.3)$$

r is distance between two the nearest neighbour spins in three dimension. x , y and z are the components of spin coordinates.

$$k_F = \frac{1}{\hbar} \sqrt{2m\epsilon_F} : \quad (3.4)$$

k_F is Fermi momentum or Fermi wave vector, m is electron's mass. Its value depends on concentration:

$$\varepsilon_F = \frac{\hbar^2 k_F^2}{2m}. \quad (3.5)$$

where ε_F is Fermi energy. Volume is $\frac{(2\pi)^3}{V}$ and sum k , $\sum_k \rightarrow \frac{V}{(2\pi)^3} \int d\vec{k}$ in \vec{k} space, this one gets

$$N = 2 \frac{V}{(2\pi)^3} \int_0^{k_F} 4\pi k^2 dk = \frac{V}{3\pi^2} k_F^3 \Rightarrow n = \frac{N}{V} = \frac{k_F^3}{3\pi^2} \quad (3.6)$$

where n is electron density. If we combine Eq. 3.5 and Eq.3.6, we can obtain new Fermi energy equation as the following.

$$\varepsilon_F = \frac{\hbar^2}{2m} (3\pi^2 n)^{2/3} n^{2/3} \quad (3.7)$$

where

$$p_F = \hbar k_F = \hbar (3\pi^2 n)^{1/3} \quad (3.8)$$

is called the momentum with

$$k_F = (3\pi^2 n)^{1/3}. \quad (3.9)$$

As the distance from the localized spin position increases, Fermi wave vector increase for spin position of the wave functions. In our RKKY indirect interaction calculations for different doping rating, we used different k_F value in the RKKY equation. For different value of TM concentration, they shown ferromagnetic properties in the range 0-15% range, paramagnetic properties in the range 15-50% range, antiferromagnetic properties in the range 50-100% range in Table 3.2 and Fig.3.8. RKKY interaction is always ferromagnetic at low concentration and for small Fermi wave vector k_F . At higher concentration, the interactions can be spin glass, paramagnetic or antiferromagnetic [57]. Because Fermi energy and momentum increase with density of electrons in Eq.3.2.

At small Fermi wave vector k_F , the ground state is ferromagnetic RKKY interaction for diluted magnetic semiconductor. As k_F increases, the system exhibits spin glass (SG) and antiferromagnetic (AFM) phases with different k_F wave vector value. According to results given the below, we created FM, SG and AFM RKKY interaction graphs in the Fig.3.9. The

Concentration(%)	k_F	Concentration(%)	k_F
1	0.8545	25	0.9625
2	0.8590	30	0.9850
3	0.8635	35	1.0075
4	0.8680	40	1.0300
5	0.8725	60	1.1200
10	0.8950	80	1.2100
15	0.9175	90	1.2550
20	0.9400	100	1.3000

Table 3.2 Some Fermi wave vector constant according to different doping concentrations. We used the theoretically calculated k_F parameters.

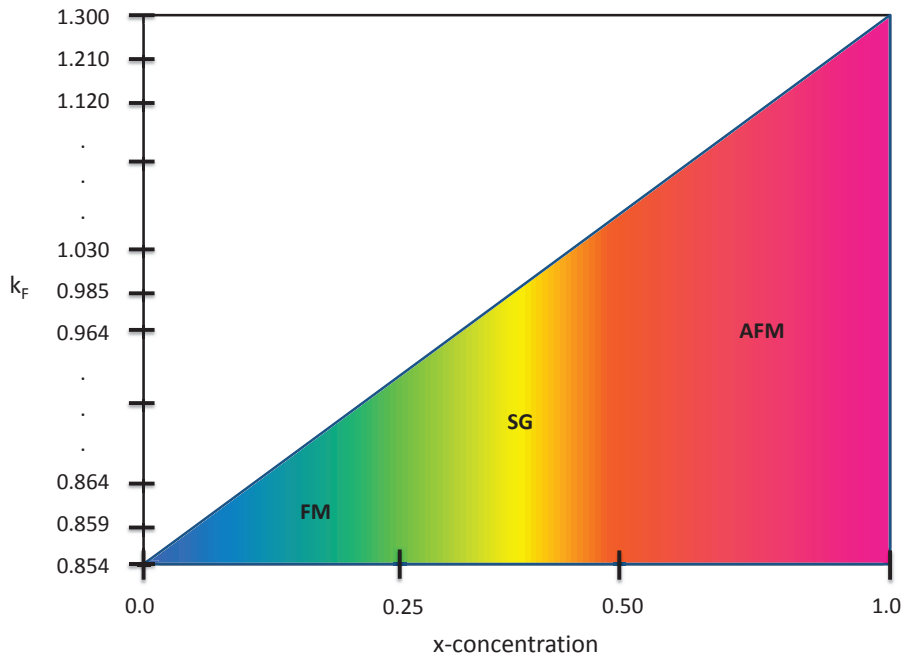


Fig. 3.8 The system is spin-glass (SG) and paramagnetic (PM) phases at middle concentrations. Our results suggest that the spin-glass phase. According to our calculations, while the system is antiferromagnetic at high concentrations and temperatures, it is a ferromagnet (FM) at low concentrations and temperatures

oscillation period does not exceed a few Å. These k_F values are shown Table 3.2 for different concentration.

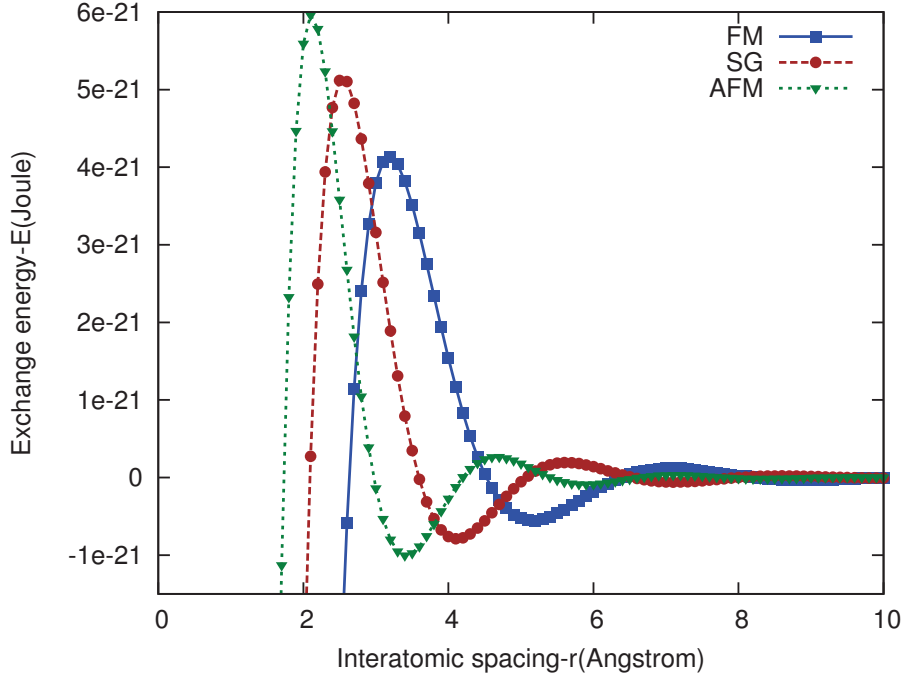


Fig. 3.9 Ruderman-Kittel-Kasuya-Yosida interactions distance dependence in non-magnetic metals

Actual neighbour interactions are from Fig.3.10. Where id : Number identifier of atom in unit cell. cx, cy, cz : Unit cell coordinates as a fraction of unit cell size. mat : Material id of the atom. lc : Category id of the atom, used for calculating properties not categorised by material, hc : height category id, used for calculating properties as a function of height. i : Atom number of atom in local unit cell, j : Atom number of atom in local/remote unit cell. dx, dy, dz : Relative integer coordinates of unit cell for atom j . J_{ij} : Exchange values (Joules)

3.4.2 Spin Glass

Long range interactions can take many forms in magnetic systems, for example, dipole-dipole, direct and RKKY exchange. In recent years, RKKY magnetic interaction has been drawing attention in terms of its important role in giant magnetoresistance, multilayer structures and in diluted magnetic semiconductors [62]. Due to the long range of the RKKY interaction

```

# Unit cell size:
3.32  3.32  5.22
# Unit cell vectors:
1.0 0.0 0.0
0.0 1.0 0.0
0.0 0.0 1.0
# Atoms num, id cx cy cz mat lc hc #
4
0      0      0      0      0      0      0
1      0      0      0.375  1      1      1
2      0.33333 0.33333 0.5    2      2      2
3      0.33333 0.33333 0.875  3      3      3
#Interactions n exctype, id i j dx dy dz Jij
776  0
0      0      2      3      2      1      1.34729e-24
1      0      2      3      2      0      1.34729e-24
2      0      2      3      1      2      1.98884e-24
3      0      0      3      1      1      4.23085e-25
4      0      2      3      1      1      -2.79859e-24
5      0      0      3      1      0      1.91886e-24
.      .      .      .      .      .      .
.      .      .      .      .      .      .
.      .      .      .      .      .      .

```

Fig. 3.10 Used actual neighbour interactions from our simulations of ZnO. Where J_{ij} is variable according to nearest neighbour.

via conduction electrons, these metallic spin glasses can exist even at strong dilution and uniaxial magnetic anisotropy. The strongest evidence for spin-glass properties can be found $Zn_{1-x}Mn_xTe$ [89] and $Zn_{1-x}Mn_xIn_2Te_4$ [90] among the II-VI DMS systems. General method of studying dynamics of spin glasses is via Monte Carlo simulations [91–94]. Thus, spin glasses have great importance in terms of our understanding of magnetic materials whether are disordered or frustrated magnetic systems arises from complex systems through a ferromagnetic or an antiferromagnetic interaction in Fig.3.9.

Spin glass based on Ising model with long range interactions where the coupling constant, J_{ij} , varies from site to site, introduces frustration to the lattice in Fig.3.11. In many diluted magnets that these magnetic ions like Fe, Co, Ni are randomly distributed in the host, the interaction is RKKY which may suggest ferromagnetic and antiferromagnetic interactions. Neighbours magnetic moment interaction is either ferromagnetic or antiferromagnetic in RKKY interaction. For example, interactions of the nearest neighbour distance are ferromagnetic ($J_{ij} > 0$), whilst next-nearest neighbours are antiferromagnetic ($J_{ij} < 0$). And then,

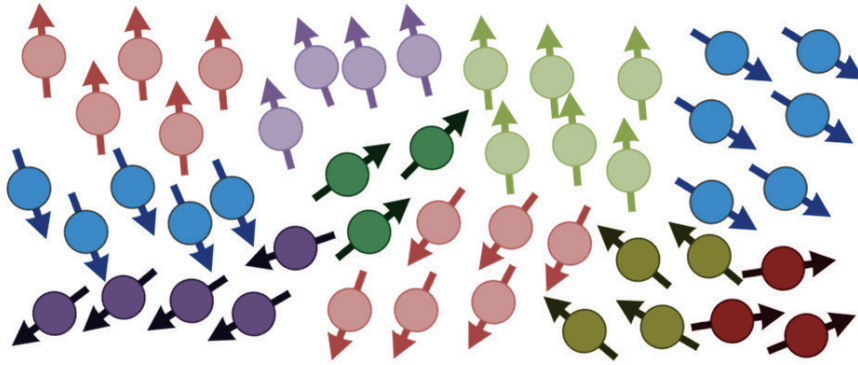


Fig. 3.11 Schematic representation of the random spin structure of a spin glass

further neighbour exchange interactions can be small. So, phase transition can be from the paramagnetic to the spin glass state. The total exchange energy is then the sum over all pairs, J_{ij} .

At first, the theory of spin glasses was posed by Edwards and Anderson [95]. Later, many scientists attract attention for spintronic devices. Their main aim was to examine disorder in microscopic interactions. This phenomenon called dilute magnetic alloys that can be observed a very small concentration (at a few percent) of a magnetic element, transition metal, such as iron or manganese, mixture inside magnetic materials of non-magnetic materials [96]. The combination of both can lead to spin glass behaviour all the magnetic systems. In fact spin glass is magnetic disorder. So, the RKKY interaction is always ferromagnetic at low electron densities for small value of Fermi wave vector k_F . At higher densities, the RKKY interaction due to nearest neighbour suggests a spin glass or ferromagnetic behaviour. In addition, spin glasses are important for variety of applications such as at solving of problems in physics, material science, in computer science, chemistry and other areas. Due to interactions, spin glasses can be uniaxial or isotropic situation; they can be crystalline or amorphous in structure.

3.5 Ground State Spin Configuration

In the first section, we deal with problem related to the magnetic ground state. To determine the magnetic ground state, we need to calculate the energy of several configurations. They can be calculated with molecular dynamics calculations, spin dynamics calculations of magnetic degrees by exploring the ground state configuration [30, 97].

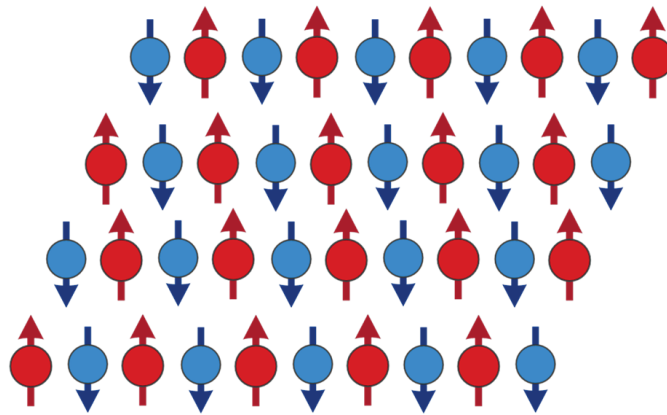


Fig. 3.12 Ground-state spin configuration of an antiferromagnet. The spin configuration is relevance with the spin state.

For Monte Carlo simulation, Heisenberg spins with RKKY interaction were randomly aligned. Diluted magnetic semiconductors occur randomly distributed and have localized spins which become paramagnet at high temperature. In the absence of applied magnetic field, the spins are oriented randomly because of thermal fluctuations. These thermal motions are the order of picoseconds in diluted systems. Spin glasses have many ground states in Fig.3.11, i.e., spin configurations with the lowest total energy. Thus, the system can change randomly between different ground states. At higher densities an antiferromagnetic ground state is apparent, arising from the oscillating distant dependent nature of the exchange interactions Fig.3.13.

The ground state is formed after a transition from ferromagnetic to antiferromagnetic state. Magnetic behaviour associate with magnetic moments that are strongly coupled. Physics of

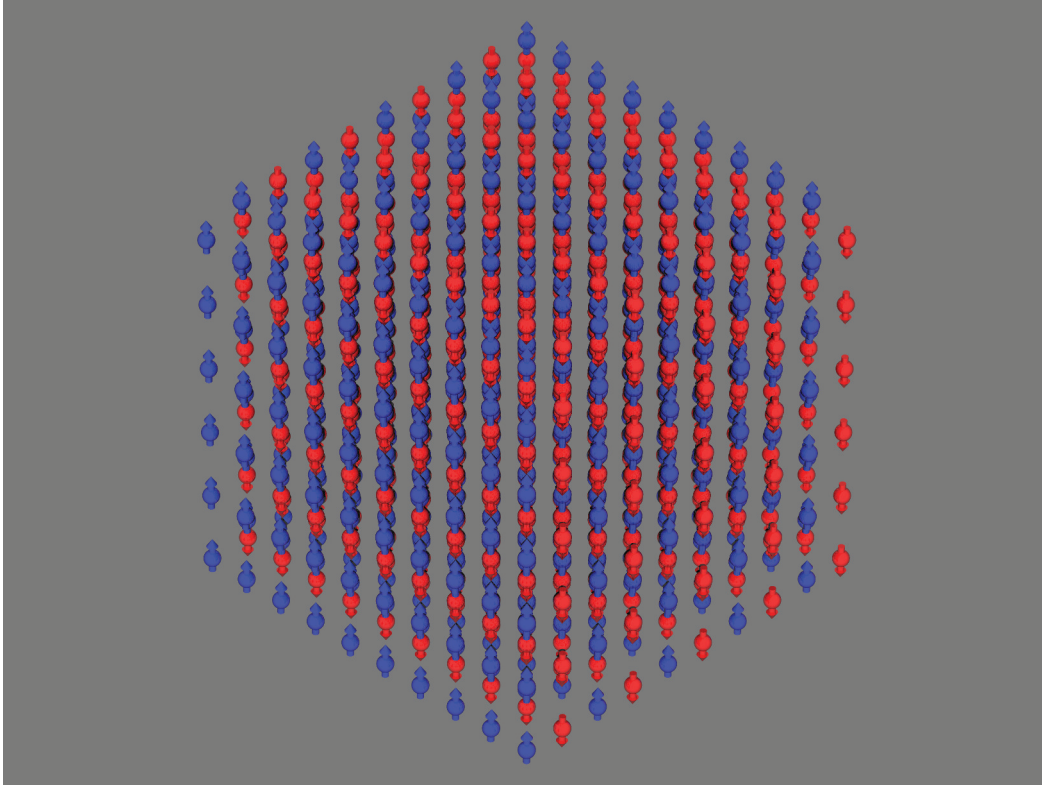


Fig. 3.13 Visualization of antiferromagnetic ground state magnetic structure.

such systems can be described by a Heisenberg spin model. This model describe interacting spins on lattice two spin operators are given as the below.

$$H = -\frac{1}{2} \sum_{r \neq r'} J(r-r') S(r) \cdot S(r'), \quad J(r-r') = J(r'-r) \quad (3.10)$$

If the exchange integral, J , is positive, the model describes ferromagnetic order. Because spins tend to same direction and give positive value.

3.6 Correlations between Spin Magnetic Moments

Spin-spin correlation function revealed some short range order between atomic moments. The dynamic of diluted magnetic semiconductors have a great importance and can be described by means of atomistic spin dynamics simulations. The magnetization curve, $M(T)$, by Monte Carlo simulations obtained[27], additionally, equilibrium and non-equilibrium behaviour of

correlation function have been solved for magnetic systems [25, 98–101]. Therefore, the dynamics have drawn attraction generally for DMS systems in the low concentration limit for a few TM percent doping. Atomistic simulations of the dynamic properties of diluted magnetic semiconductors demonstrate that magnetic order above the ordering temperature, with a non-disappearance pair correlation function, statistically extends till several atomic shells. We observed for a spin-glass behaviour for a low concentration in our simulations.

The partition function is given by

$$Z = \sum_{\mu} \exp\left(\frac{-U_{\mu} + \sum_i h_i s_i}{k_B T}\right) \quad (3.11)$$

where exchange energy or internal energy given by $U_{\mu} = -\frac{1}{2} \sum_{ij} J_{ij} s_i s_j$ and local field $h_i = \mu_0 \mu_B H_i$.

$$\langle s_i \rangle = \frac{k_B T}{Z} \frac{\partial Z}{\partial h_i} \quad (3.12)$$

and the quadratic average

$$\langle s_i s_j \rangle = \frac{k_B^2 T^2}{Z} \frac{\partial^2 Z}{\partial h_i \partial h_j} \quad (3.13)$$

The magnetic susceptibility is $\chi = \partial \langle s_i \rangle / \partial H_i$. An important result of statistical thermodynamics is take into account thermal fluctuations characterize the behaviour of a magnetic system. The fluctuation that relates the magnetic susceptibility of a ferromagnet in thermal-equilibrium given with fluctuations of the magnetization by

$$\chi = \frac{\mu}{k_B T} (\langle M^2 \rangle - \langle M \rangle^2). \quad (3.14)$$

Correlation function is related with a given distance to center of a particle from the center of another particle or possibility density of some particle. Magnetic susceptibility is as in the following.

$$\chi_{ij} = \frac{\partial \langle s_i \rangle}{\partial H_j} = \frac{\mu_0 \mu_B}{k_B T} (\langle s_i s_j \rangle - \langle s_i \rangle \langle s_j \rangle) \quad (3.15)$$

We can write as the Eq. 3.15 for fluctuations of the local magnetization. This important equation known as the correlation function for the magnet's equilibrium response. The

correlation function can be written in Eq.3.16 using the properties of the Ising model and calculating the spin-spin correlation function. In brief, The pair (spin-spin) correlation function $G(r_i - r_j)$ between two spins i and j is defined as the following:

$$G(r_i - r_j) = \langle (s_i - \langle s_i \rangle)(s_j - \langle s_j \rangle) \rangle = \langle s_i s_j \rangle - \langle s_i \rangle \langle s_j \rangle \quad (3.16)$$

In this system, the correlations decay exponentially, and the correlation length ξ is defined as $\lim_{r \rightarrow \infty} G(r_i - r_j) \sim e^{(-r/\xi)}$. Where ξ is given by

$$\xi = -\frac{1}{\ln(\tanh \beta J_{ij})} \quad (3.17)$$

If the system is homogeneous, Eq. 3.16 becomes

$$\langle s_i \rangle = \langle s_j \rangle \equiv \langle s \rangle \quad (3.18)$$

Above T_c ,

$$\langle s \rangle = 0 \Rightarrow G(i, j) = \langle s_i s_j \rangle \quad (3.19)$$

The larger the fluctuations is the higher the susceptibility. The high susceptibilities shown large fluctuations near the Curie temperature point. The spin-spin correlation function $G(r_i - r_j)$ is a measure correlated of a spin one site with a spin at another site. In the system, If the spins are not correlated, then $G(r_i - r_j) = 0$. Interactions between spins are overcome by thermal agitation at high temperatures. Therefore the spins are randomly oriented in the absence of an external magnetic field or other effect and $G(r_i - r_j) \rightarrow 0$ for fixed r . $\langle s_i \rangle = \langle m_i \rangle$

3.7 Role of the Anisotropy

Although a change in the magnetic anisotropy with temperature is a well-known physical phenomenon in magnetic materials, magnetic anisotropy depends on the temperature. As consequence of lattice disorder or defects, anisotropy has important in DMS. They can be comparable (even if even dominate) with the exchange interaction. The magnetic energy

depends on the orientation of the magnetization with regard to the crystal axes, which is known as magnetic anisotropy. Particularly, in wide gap DMS wurtzite structure. when the system crystal field combined with spin orbit interaction, it has strong magnetic anisotropy. A simple model of spin Hamiltonian occur from exchange interaction. If you include anisotropy effect, you can write as follows. This Hamiltonian given by

$$E_{exc+ani} = - \sum_{i \neq j} J_{ij} S_i \cdot S_j - d_e \sum_i (S_i \cdot e)^2. \quad (3.20)$$

Permanent magnets need a high magnetic anisotropy in order to keep the magnetization in a desired direction in magnetic systems. Soft magnets are characterized by a very low anisotropy, whereas materials with intermediate anisotropies are used in the magnetic recording media and industry.

3.8 Summary

Dynamic of Diluted magnetic semiconductor exhibit semiconducting properties. Magnetic semiconductors (ZnO, GaAs, etc) combined with, such as among of a transition metal dopant like Cr, Mn, Fe, Co, Ni and Cu are diluted magnetic semiconductors. However we are interested only in the ZnO wurtzite structure. These properties can be show paramagnetic, ferromagnetic, antiferromagnetic and spin glass order due to some condition. These conditions can be environment temperature, material size, external applied field or laser pulse. Therefore, they have lots of properties for compare the spintronic devices.

DMS identify generally as II-VI and III-V semiconductors and transition metal alloys. These materials have ferromagnetic Curie temperatures, antiferromagnetic Neel temperature and superparamagnetism blocking temperature according to some conditions. These properties were evidenced in some investigations both theoretically and experimentally. Therefore, we need to development some theoretical approach for semiconductor spintronic materials. The most important feature of diluted magnetic semiconductors is the interaction among magnetic properties of the exchange interaction with respect to nearest neighbouring .

- TM doped semiconductors are still controversial and a very active in the research field.
- Many scientist have been interested both experimentally and theoretically.
- DMS are significant in respect to application in industry.
- Magnetic behaviour of ZnO in terms of applications.
- RKKY theory in long and short range for diluted magnetic semiconductors.
- Importance of spintronic materials and technology in industry.

Chapter 4

SIMULATIONS OF DILUTED MAGNETIC SEMICONDUCTORS

4.1 Theoretical Background

Computational methods have great importance for the atomistic simulations of magnetic materials. They are capable of describing two important characteristics physical properties of DMS that their semiconductor property and the magnetic property. When we have look at literature, we see that different methods have been used for magnetic systems. In terms of quantum mechanics these calculations are density functional theory (DFT) by solving the time-independent Schrödinger equation, screened Korringa-Kohn-Rostoker (SKKR) method using Green's functions or Spanish Initiative for Electronic Simulations with Thousands of Atoms (SIESTA) ab initio molecular dynamics simulations of molecules and solids. DFT is a computational quantum mechanical modelling method used in condensed-matter physics, computational physics, and computational chemistry to investigate the electronic structure of basically the ground state of many body systems.

This thesis introduces the main theoretic information about general properties of magnets. According to some researchers, transition metal(TM) doped ZnO exhibit ferromagnetism properties at room temperature [49]. However other researchers reported only at room temperature paramagnetic or ferromagnetic owing to transition metal clusters. Moreover in low Ni concentration 1, 4.3, 7.4 % TM doped ZnO systems exhibits superparamagnetic behavior at room temperature, but this system becomes ferromagnetic at room temperature

at 22,5 % [102]. Moreover, according to Sato [103] some TM doped ZnO films showed spin glass like behaviour. This magnetic properties are still controversial in the literature, as ferromagnetism has not been clearly elucidated yet. II-VI based DMS have drawn much attention for new investigation. Thus, magnetic properties of TM-doped ZnO have attracted the attention of scientists both theoretically and experimental [104, 105].

In this context, we focused to study on the magnetic properties of diluted magnetic semiconductors. It is very important to calculate the exchange integrals between localized spins in the semiconductor host. Calculations of exchange integrals (Eq.3.2) are the RKKY method which rotation of localized spins obtained from the electronic structure, and is a classical Heisenberg Hamiltonian with the magnitude of the local magnetic moment.

4.2 Magnetization Measurements

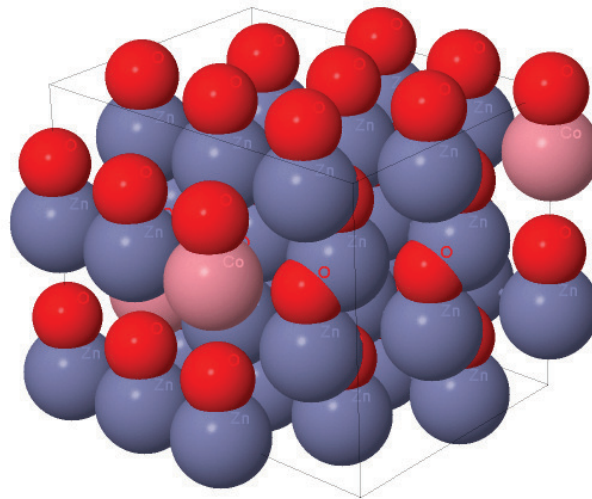


Fig. 4.1 General visulation of Co doped ZnO used our the calculations

In the present work, we calculated some magnetization properties using VAMPIRE software package for ferromagnets, antiferromagnets, paramagnetic, spin glass properties by obtaining hysteresis loops and magnetization dependent temperature using Stochastic Landau

Lifshitz Gilbert equation (spin dynamics-Heun method) and Monte Carlo method. As well as these, we have studied ultrafast laser induced spin dynamics for DMSs materials. General structure of our system shown in Fig.4.1. We have calculated using standard calculations which they are hysteresis loops, $M(T)$, temperature dependent anisotropy, zero field cooling, field cooling, laser induced spin dynamics, demagnetization for a range of transition metal concentrations.

4.2.1 Magnetization Calculations Depending on Temperature

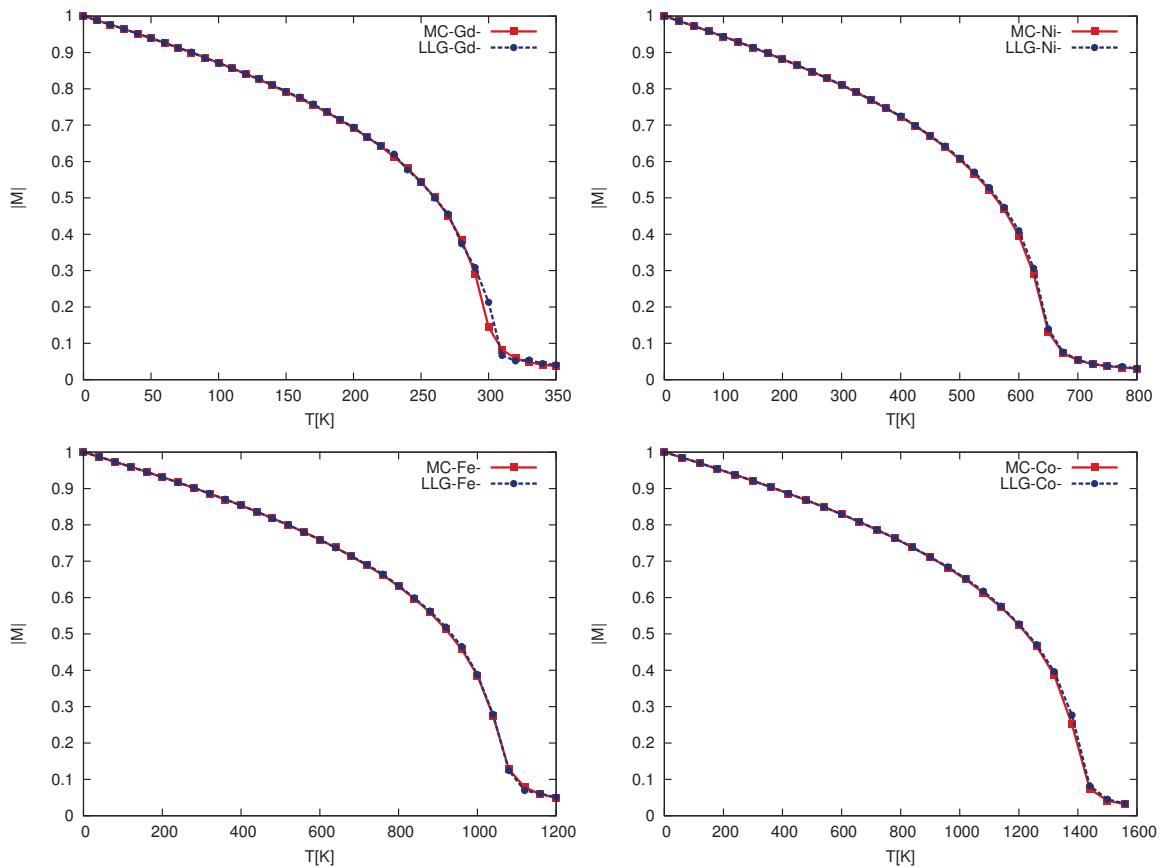


Fig. 4.2 Curie temperature of some ferromagnetic materials. Calculated temperature dependent magnetization and Curie temperature for Gd, Ni, Fe and Co. In this figure, these Curie temperatures are approximately $Gd = 291K$, $Ni = 630K$, $Fe = 1043K$ and $Co = 1388K$ at $5 \times 5 \times 5$ nm particle size. Comparison of equilibrium magnetization versus temperature for a periodic $20 \times 20 \times 20$ FCC-Gd, FCC-Ni, BCC-Fe and BCC-Co system by using spin dynamic and Monte Carlo method

The Curie temperature is a primary temperature for a ferromagnetic material. First of all, we calculated Curie temperature of some ferromagnetic metals for our test simulations. We tested some detail to the correct implementation of the our code. When we compared simulation of temperature dependent magnetization for Monte Carlo and LLG simulations, we obtained using parameter at the paper[8] Curie temperature of some ferromagnetic materials like Gd, Ni, Fe and Co in Fig.4.2. In this figure, the Curie temperature of Gadolinium, Nickel, iron, and Cobalt is 293 K, 631 K, 1043 K, and 1388 K, respectively.

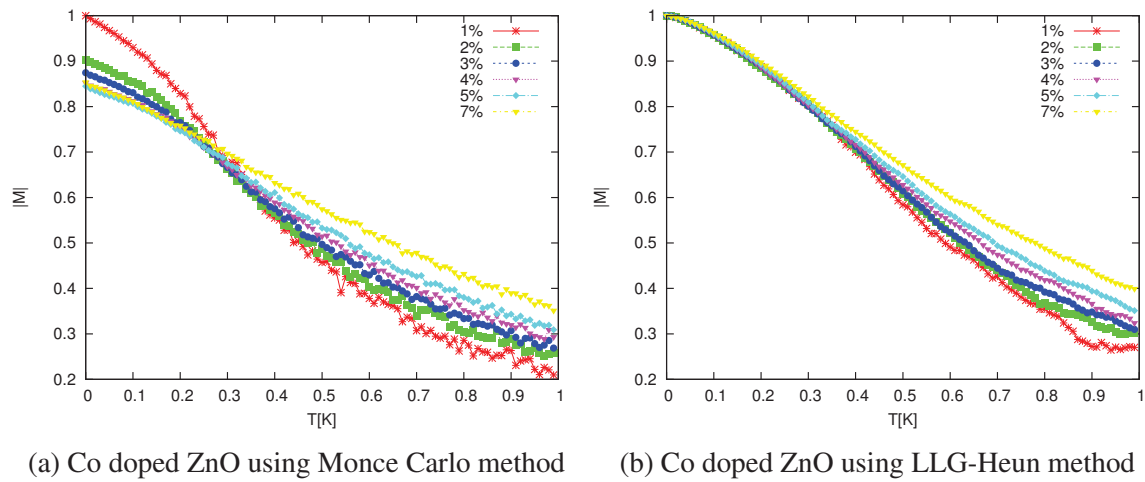


Fig. 4.3 Magnetization measurements of Co doped ZnO at different Co concentration from 1% to 7% using Monte Carlo and LLG-Heun method. Comparison of simulation by using different method.

We used VAMPIRE atomistic spin models software for these calculations at different doping rate. These results demonstrated graphs below of the M-T curves in Fig.4.3. In this section, critical temperatures are estimated with Monte Carlo simulations and Heun method (Spin dynamics).

4.2.2 Zero Field Cooled and Field Cooled Magnetization

The temperature dependent magnetization measured in zero-field-cooled (ZFC) and field-cooled (FC). Measurements of zero-field-cooled and field-cooled magnetizations (M_{ZFC}) and (M_{FC}), respectively, showed different magnetic behaviour for different external applied field in like Fig.4.4. These figures present applied magnetic field dependences of ZFC and

FC magnetization. Usually, at high temperature, most materials are paramagnetic. These two curves are significant because they are easy to estimate two important properties which are blocking temperature and strength of interaction between spins from the temperature dependence. The temperature dependence of the ZFC and FC magnetization is usually measured in a small magnetic field. In order to determine the Curie temperature at which the system becomes ferromagnetic. We used $L \times L \times L$ ($L=10, 15,$ and 20) size wurtzite ZnO materials with periodic boundary conditions. The Hamiltonian of the system was described at chapter-2 by Eq.2.2.

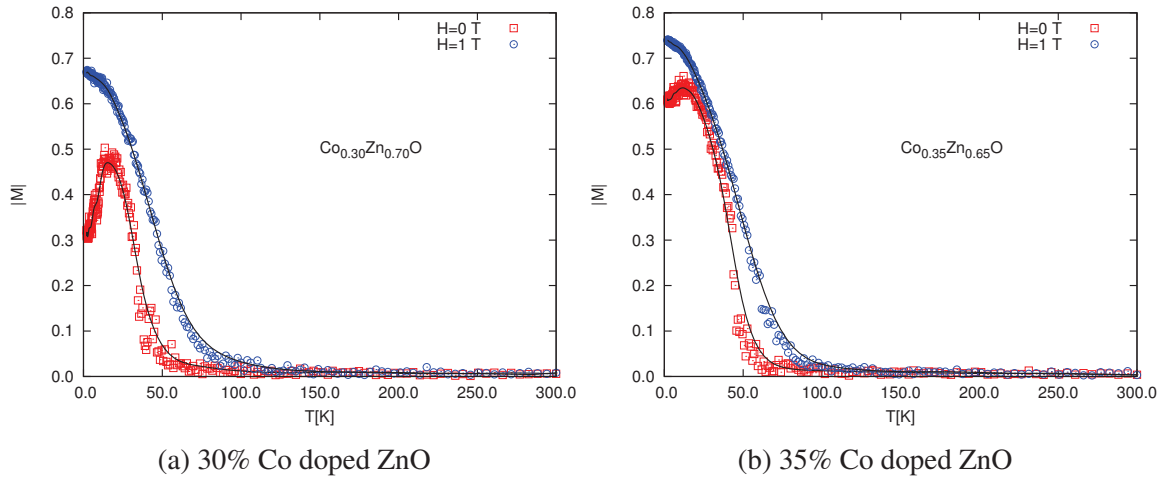


Fig. 4.4 Zero field cooled and field cooled magnetization curves for the $Co_{0.3}Zn_{0.7}O$ and $Co_{0.35}Zn_{0.65}O$ samples at different applied fields at room temperatures. Where we have plotted $M(T)$ for the samples cooled down from room temperature to 0 K measured in an external magnetic field at 0 T (ZFC) or 1 T (FC), respectively. For both samples, there is a clear difference between the ZFC and the FC data at different applied field. In figure, blocking temperature is around 20 K for our parameter.

Theoretically, ZFC and FC calculations were studied in diluted magnetic semiconductor [106]. Recently, superparamagnetic properties in magnetic nanoparticles have attracted considerable attention because they are importance for instability of magnetic recording devices in the new generation magnetic devices. Fig.4.4 shows temperature dependences of magnetizations. Both of figures exhibit spin glass in the zero-field-cooled and field-cooled magnetizations among 30-35%. These samples shows Ising spin glass behaviour with the long range RKKY interaction. $M(T)$ curves of CoZnO were measured under $H=1$ T after

ZFC measurements done. The permanent magnetization as a function of temperature in CoZnO was measured from 300 K to 0 K. In order to obtain the ZFC magnetization curve, the sample is firstly cooled in a zero field from a high temperature above blocking temperature T_B where particles are in a superparamagnetic state, down to a low temperature below T_B .

ZFC measurements were started at low temperature after cooling the sample in zero external field. Then, magnetization was measured as the temperature slowly increases. FC measurements start at high temperature where a field is applied and the magnetization is measured as the temperature slowly decreases. In Fig.4.4, range 30-35% Co content in zero field cooled magnetization around $T = 20$ K a spin glass like, field cooled magnetization a superparamagnetic behavior. The results of the simulations of field-cooled and zero field cooled in a dilute systems of superparamagnetic nanoparticles with uniaxial anisotropy was presented. Quantitative analysis of FC and ZFC experiments for a dilute assembly of uniaxial nanoparticles is given. So, superparamagnetic particles have a blocking temperature T_B , and in this point they can show superparamagnetic behaviour. Below T_B spontaneous magnetization and magnetic hysteresis is observed. You can see these properties between zero field cooled and field cooled magnetization curves. Generally, ZFC magnetization is seen at low temperatures. Zero field cooled and field cooled measurement have been performed using Monte Carlo method in VAMPIRE for 25%, 30%, 35% and 40% Co:ZnO samples. FC and ZFC measurements were cooled down from room temperature to 0 K. Blocking temperatures obtained at around 20 K Fig.4.4. By taking into account, we examined magnetic behaviour of material different doping rating.

We can sum up three group all these calculations for ZFC/FC measurements. First of all, in the lower concentration (1-5%), material shown ferromagnetic properties for small k_F value such as in Fig.4.3. Secondly, in the range 25-35%, material shown superparamagnetic and spin glass properties. Finally, >65% it shown antiferromagnetic properties. Because, samples do not have long-range magnetic order, but it is a spin glass. The behaviour of the system around the blocking temperature shown spin glass properties superparamagnetism from a canonical spin-glass at the field cooled curve in the measurements. Due to the different magnetic anisotropy we have obtained some figures in the our studies.

Anisotropy effect

Long range RKKY Ising spin glasses connect with uniaxial magnetic anisotropy by means of conduction electrons. The effect of uniaxial anisotropy on the hysteresis behaviour or magnetization depend on temperature is great important for magnetization behaviour. The magnetization behaviour is one of the important properties which have received much attention for properties of nanoscale magnetic materials. Magnetic field connect with applied and the magnetization as a function of temperature. The FC curve is obtained by measuring the magnetization when cooling the sample to the low temperature in the same field [107]. In the ZFC and FC measurements the field must be weak enough to be able to compare with the anisotropy field in Fig.4.5. Magnetization behaviour was shown different magnetic properties at high anisotropy energy value. Therefore, we compared FC-ZFC behaviour according to anisotropy effect [108].

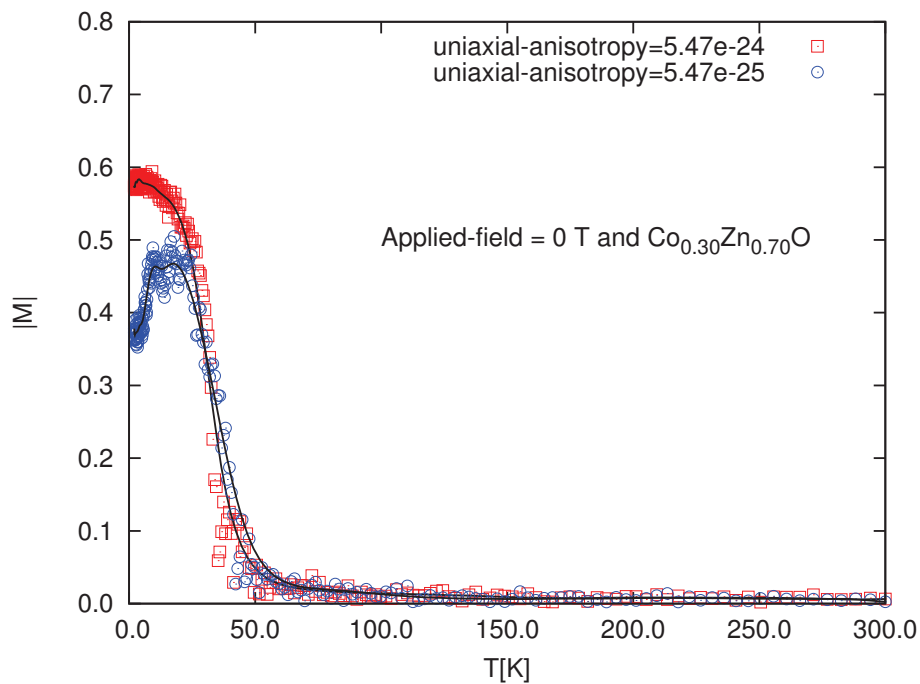


Fig. 4.5 Effect of uniaxial anisotropy in magnetization behaviour from zero field cooled magnetization measurements.

The importance of whole results can be used in examining of magnetic properties with several important applications at different temperature, size, applied field and so on.

Ferromagnetic properties

We developed some models a for ferromagnetic ordering in diluted magnetic semiconductors by taking doped amount into account. Owing to indirect RKKY exchange interaction among the magnetic moment, we found magnetization temperature behaviour. In the low percent, low temperature and low k_F value in RKKY equation, CoZnO diluted semiconductor shown ferromagnetic properties. If you use different k_F value, you can obtain different the magnetization curves. Ferromagnetic interactions are always important for short range

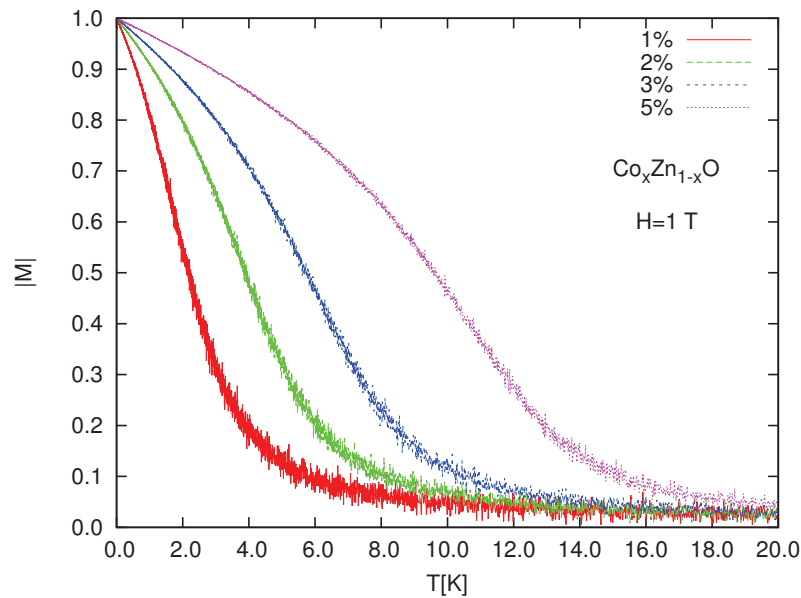


Fig. 4.6 Ferromagnetic properties of CoZnO at low density and temperature. k_F value is 0.1 in RKKY equation. This figure is shown magnetization depend on temperature which it part view from size $20 \times 20 \times 20$ and 1-2-3-5% Co doped ZnO. This calculation is field cooled magnetization

distance or among nearest neighbour spins. We obtain this ferromagnetic properties shown as in Fig.4.6. $Zn_{1-x}Co_xO$ ferromagnetic semiconductors, finding that all magnetic properties, from the significantly predictions of the used RKKY theory. Particularly, feature of our results is the strong theoretical correlation between T_c and the system experimentally observed of DMS saturation magnetization.

Size effect

The zero field cooled and field cooled magnetization measurements show that the blocking temperature increases with increasing of the system size. We show magnetization behaviour of size effect in system for different size in Fig.4.7 and Fig.4.8.

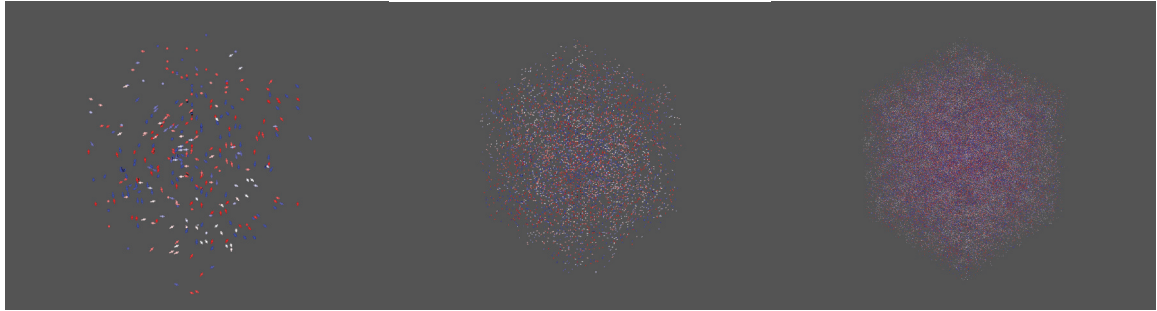


Fig. 4.7 The zero field cooled magnetizations of $Zn_{0.98}Co_{0.02}O$ at different size. Size $7 \times 7 \times 7$, $20 \times 20 \times 20$ and $50 \times 50 \times 50$ as a function of temperature.

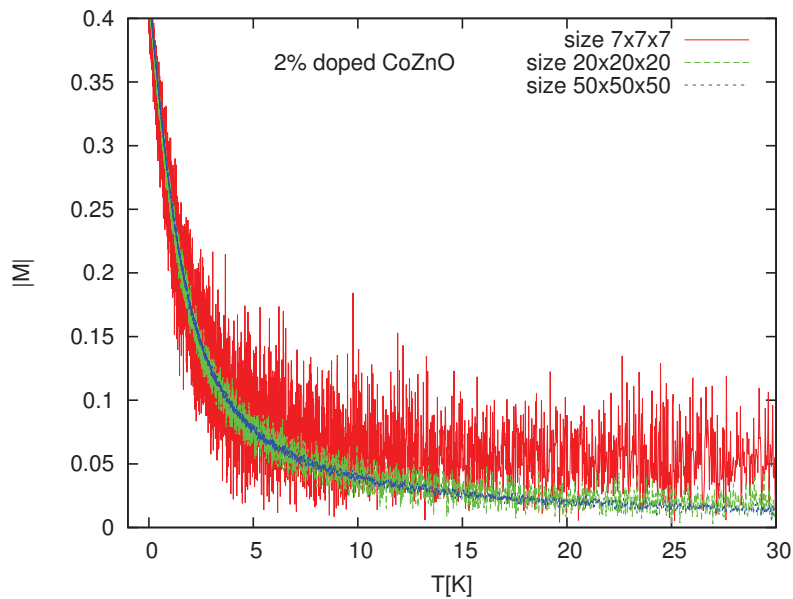


Fig. 4.8 Temperature dependence of field cooled magnetizations for different size of CoZnO. FC calculations 2% Co doped ZnO. The system was cooled at 1 T from 300 K to 0 K.

For example, if you want to obtain Blocking temperature, you have to take the system size into account. Because, we have observed disorder at magnetization temperature behaviour in some crystal size for Co doped ZnO. Since, size effect has a great important for system order.

Spin Glass properties

Spin glass is a magnetic system that exhibit ferromagnetic and antiferromagnetic properties with interactions distributed at random throughout material. Spin glasses display normal magnetic properties above T_c . They also display distinct transport properties depending on field cooled or zero field cooled. In fact, ZFC and FC magnetic behaviour is one of the characteristic features of a spin glass. Thus RKKY theory is important in order to understanding spin glass behaviour. Spin glasses disorder in magnetic systems with frustrated interactions, that exhibits a phase transition to a low temperature state. Spins have no magnetic long range order. In general, spin glasses exhibit characteristics of both equilibrium and non-equilibrium at statistical mechanics. But, it does not all systems.

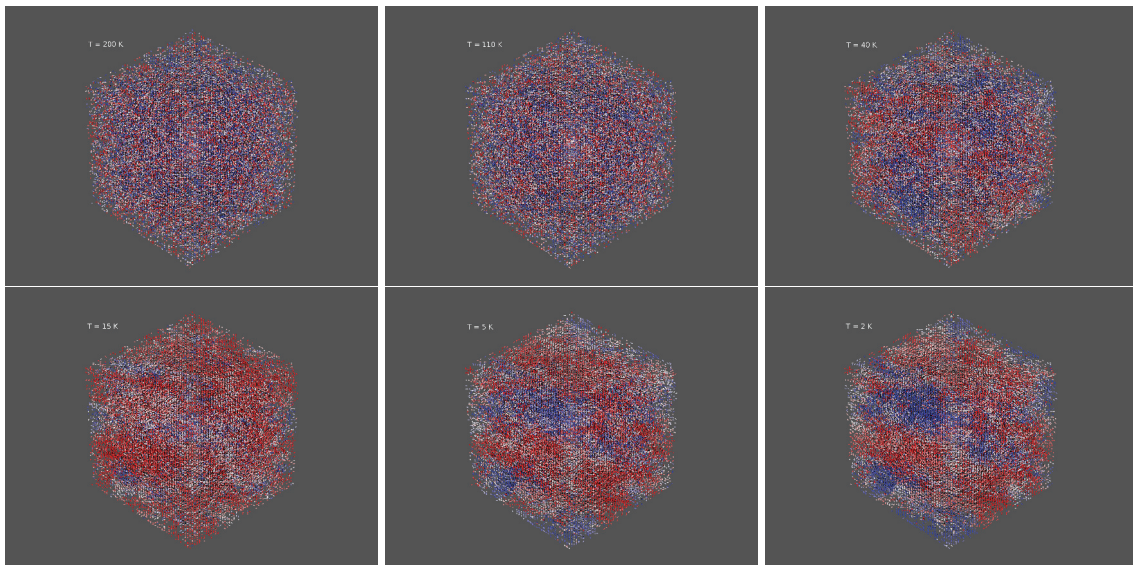


Fig. 4.9 Crystal visualization of DMSs $Co_{0.3}Zn_{0.7}O$ spin glass properties from ZFC calculations. System of $15 \times 15 \times 15$ cubic lattice of atomic magnetic moments.

The crystal is randomly doped with Co atoms with the desired percentage, to give a diluted magnetic semiconductor. The exchange interactions are given by the oscillatory RKKY interaction between spins, leading to a spin-glass like behaviour at between 25-35% densities in Fig.4.4 and Fig.4.9 at 0 T. All the visualisations combined with POV-Ray software.

Paramagnetic properties

Paramagnetic materials have a small, positive susceptibility to magnetic fields and have random spin directions in magnetic systems. The zero field cooling and field cooling magnetization curves exhibit paramagnetic, superparamagnetic and spin glass properties under 100 K with increasing Co concentration around 30 % doped ZnO diluted semiconductor in the our simulations. Fig.4.4 shown that the FC curves display typical superparamagnetic (SPM) behaviour at between 25-35 % samples in the around 20 K and 0 T. But, Fig.4.10 shown paramagnetic properties from samples at 1 T and around 70 K. It is known that the Blocking temperature is associated with the particle size, anisotropy and applied field.

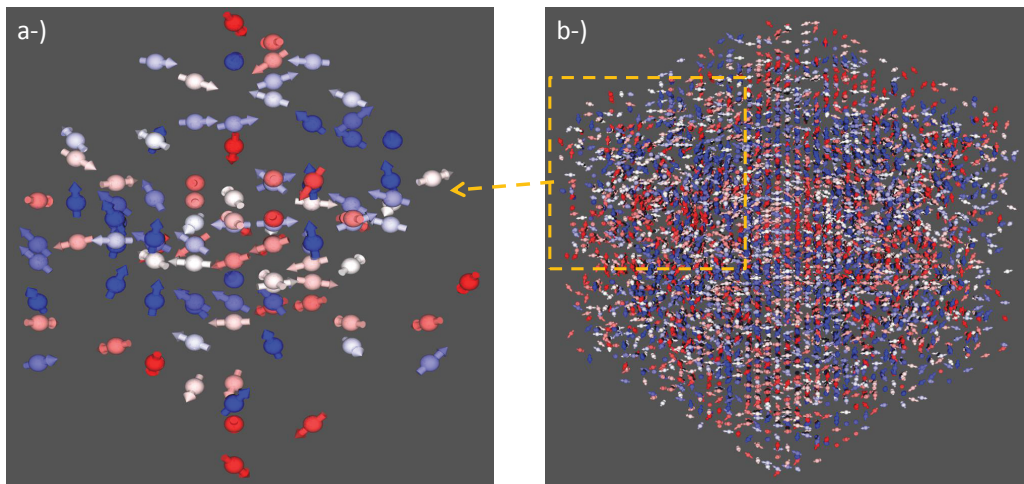


Fig. 4.10 Paramagnetic spin direct visulation zero field cooling and field cooling measurements. Snapshot from an atomistic spin dynamics simulation of ZnO doped with 30% Co. $Co_{0.3}Zn_{0.7}O$ atomic magnetic moments structure obtained by PovRoy at temperature $T=300$ K ZFC-FC magnetization.

Antiferromagnetic properties

Antiferromagnetic properties is spin up and spin down array of the magnetic moments of atoms with neighboring spins. Antiferromagnetic materials are commonly among transition metal oxides compounds that they spontaneously align their magnetic moments antiparallel below the critical temperature. This antiparallel state remains constant when the external

field is removed. CoZnO thin films with high Co concentration do not show ferromagnetic behaviour. For example, at higher percent like 70 or 100 % Co doped ZnO diluted semiconductor an antiferromagnetic ground state is apparent, arising from the oscillating distant dependent nature of the exchange interactions as shown 4.11.

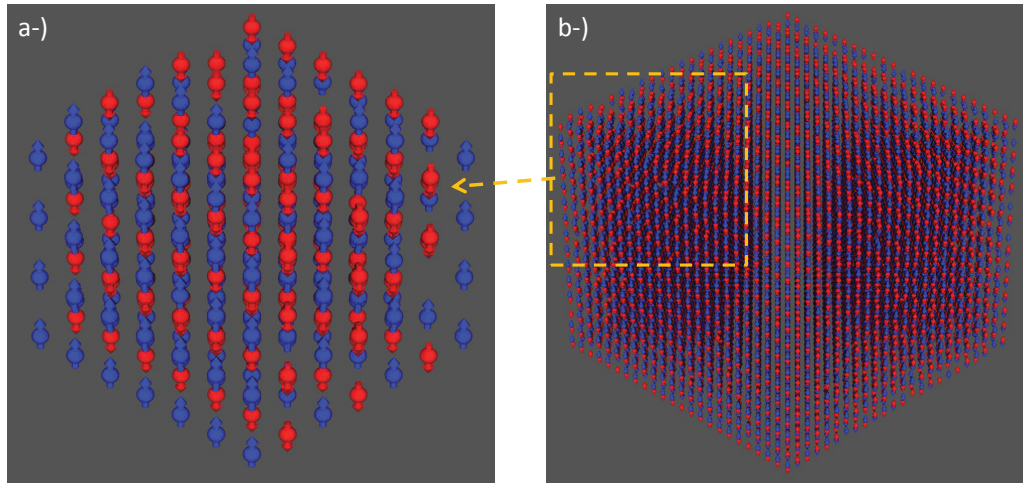


Fig. 4.11 Antiferromagnetic ground state visulation doping zero field cooled and field cooled magnetization measurements of CoO

4.2.3 Hysteresis Calculations

In this section, we examine the analysis of the magnetic field of a diluted magnetic semiconductor such as magnetic hysteresis. The hysteresis calculation is the standard magnetic characterisation technique to determine application properties of magnetic materials. This application is use in the solving problems and the engineering applications. Magnetic properties acquired from the hysteresis loop are important a properties of ferromagnet. Because they describe the real structure of the magnet. Hysteresis loops are obtained by monitoring the volume-averaged magnetization M as a function of the external magnetic field H . Flux density can be written $B = \mu(H + M)$ as a function of H and M . Two important properties derived from M - H loops are the coercive force or coercivity H_c and the remanent magnetization or remanence M .

Hysteresis curves, that is the dependence of the magnetization M on the external field strength H , provide important information on various ferromagnetic magnetic properties. Flux density as a function of magnetization field strength for a range of Cobalt densities is shown in Fig.4.12. We also examined hysteresis curves according to applied field effect, magnetic properties of hysteresis curves connected with external applied field as shown Fig.4.13.

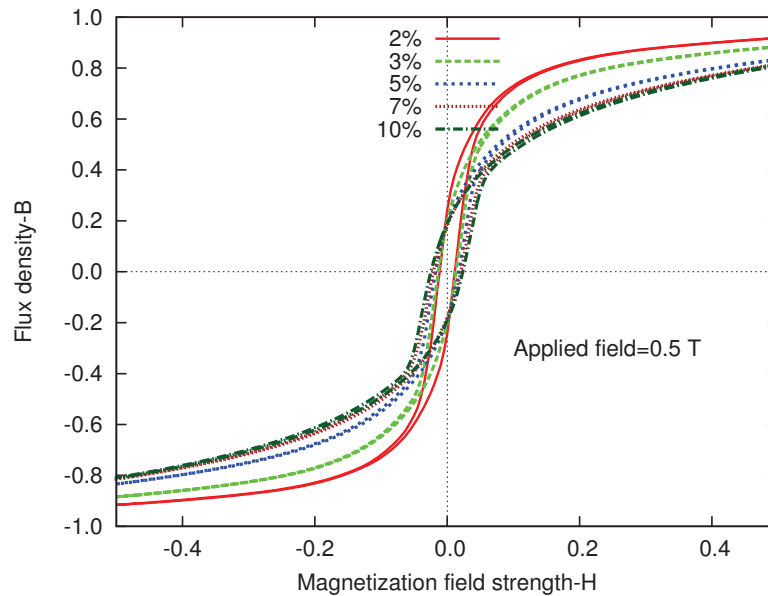


Fig. 4.12 The hysteresis loops of the CoZnO thin films with different cobalt concentrations. As densities is increased, magnetization decreased.

Field dependence

Hysteresis measurement generally measures with the magnetic field dependence of the magnetization at a constant temperature in order to characterize ferromagnetic materials. Magnetization of ferromagnets connect with the coercive field, the saturation and the permanent magnetization. In this type of measurements, the magnetic field is increased from zero to a large value value. Fig.4.13 shows the magnetic hysteresis loops of the CoZnO thin films at 0 K temperature with different cobalt concentrations. All the samples exhibit ferromagnetic ordering with clear hysteresis loops. As applied field decreased, coercive field

increased. These figures lead to stronger clusters at higher densities and more resistance. Therefore it is lower saturation and remanence.

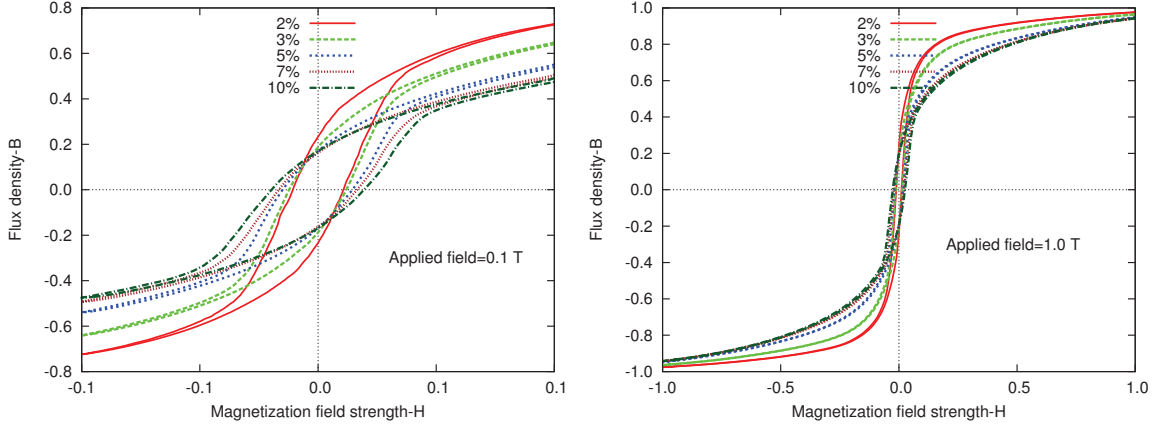


Fig. 4.13 The hysteresis loops of the CoZnO thin films with different external applied field. We measurement among $0.1T \leq B \leq 1T$ external applied field in figure samples. Higher densities lead to stronger clusters - more resistance to applied field so lower saturation and remanence

Anisotropy dependence

To investigate the anisotropy dependence of the coercivity, in recent years, DMSs have attracted much attention in term of for spintronic applications, magnetic recording and media. Because Co has unique physical properties such as high Curie temperature and magnetic high coercivity. In fact, many ways were used for improving the magnetic properties of DMSs. As one of these methods is Co doped ZnO, other methods are Ni-Fe doped ZnO or Mn doped GaAs which these most studies materials. We examined effect only of the uniaxial anisotropy, with different anisotropy constant. In order to understand anisotropy effects in a system consisting of about several hundred to several thousand atoms we used as systems size $20 \times 20 \times 20$ nm. Magnetic coercivity is increased, permanent magnetization is increased in Fig.4.14.

The coercive field given by

$$H_c \sim \frac{2k_u}{\mu_0 M_s} \quad (4.1)$$

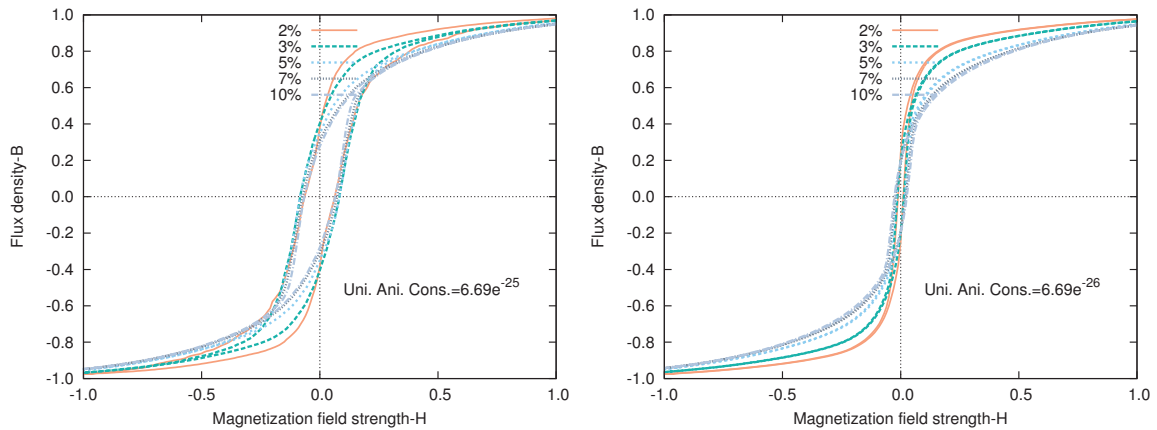


Fig. 4.14 Effects of uniaxial anisotropy constant on hysteresis curves. As anisotropy is increased, coercivity increased.

where k_u is the anisotropy constant. Coercivity of cobalt is more higher than other transition metals like Ni, Fe. We couldn't try different element except for Co transition element. As anisotropy is increased, coercive field is increase according to Eq.4.1.

4.3 Summary

Spin electronics on diluted magnetic semiconductors could offer many advantages for commercial spintronic devices which they can be made in form ferromagnetic metal thin films. Their advantages are microelectronics, a better sensitivity to magnetic fields, and a possibility to fabricate multifunctional devices. In this section we have presented Co doped ZnO as the semiconductor material, because the ZnO device technology is a new field, the physical properties of ZnO. We theoretically investigate the magnetic properties of Co doped ZnO crystals nanostructure for Co concentrations at different percentages with Monte Carlo method using the Vampire software. According to concentrations, we have observed many magnetic properties like ferromagnetic, antiferromagnetic, paramagnetic and spin glass. We also examined applied field, uniaxial anisotropy energy value at different size.

- Hysteresis analysis for ferromagnetic properties of Co doped ZnO in many parameter.

- Zero field cooling and field cooling measurement dependent on temperature. As a result of these, we have examined many magnetic properties.
- Field dependence of the coercive field, this allows permanent of the magnetization to be controlled by magnetic field strength
- Magnetization dependence of anisotropy, applied field, temperature and size.

Chapter 5

LASER DYNAMICS IN MAGNETISM

5.1 Introduction

Laser dynamics or ultrafast magnetic processes is a new research field of femtomagnetism: using pico/femto second laser pulses to demagnetize ferromagnetic metallic thin films. This research field has become the origin of a new field in modern magnetism that is referred as femtosecond magnetism and dawn of a new era for future research in magnetism[38, 109–111]. The fundamental length and time scales are nanometers (nm) and femtoseconds (fs). Therefore, ultrafast laser control of magnetism is one of the most exciting topics in physics and technology.

The general aim of the laser dynamics is to investigate the dynamical properties of magnetic materials and magnetic order of nanostructures accruing in a time scale shorter than the switching time of magnetic devices, therefore at a length scale below a few hundreds of nanometers Fig.5.1. This field extremely motivates to develop new magnetic structures with high performances used in the technologies of recording and processing the information. Typically, 1 Tb/cm^2 or more area information is written on a time scale from a few femtoseconds to a few nanoseconds. We need the specific information on the structure or electronic properties of the magnetic material to compare some magnetic properties. This is of great importance when specific information about the spin dynamics is desired such as the dynamical behaviour about the effect of doping on the magnetization damping. In this

chapter, we investigate how an ultrashort laser pulse couples with to the spin of electrons in magnetic metals.

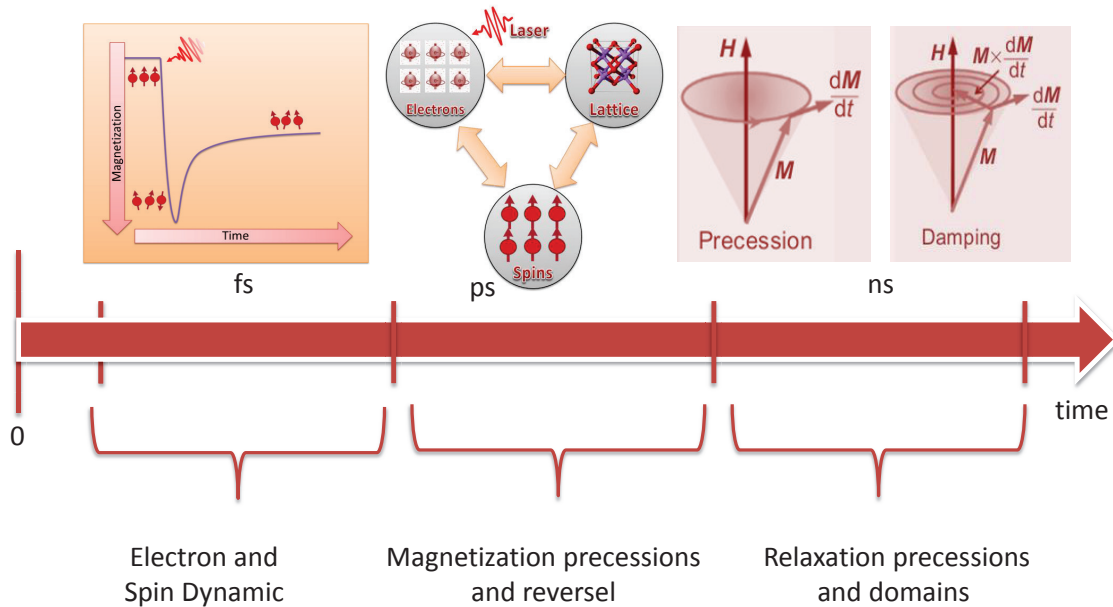


Fig. 5.1 The flow diagram of ultrafast spin dynamics. This figure is the characteristic time scales of the magnetization dynamic.

The dynamics of results indicate that the material polarization induced by the photon field interacts coherently with the spins. The corresponding mechanism has its origin in relativistic quantum electrodynamics, beyond the spin-orbit interaction including the ionic potential. In addition, this coherent interaction is clearly distinguished from the incoherent ultrafast demagnetization connected with the thermalization of the spins. We predicted that the corresponding coherent self-induced processes are the dawn of a new area for future research in magnetism.

5.2 Research Motivation of Ultrafast Dynamics in DMS

In modern magnetism, femtosecond lasers are new approaches to study the ultrafast spins dynamics in magnetic nanostructures. During the past few years, the significance of laser-induced ultrafast spin dynamics in ferromagnetic metals has been intensively increased.

Therefore, one of the most exciting topics in today's field of magnetism in advanced technology is the dynamics of spin systems in ultrafast timescales. These phenomena described by a short laser pulse are ultrafast demagnetization, optical effects and laser-induced precession. In this section, we will discuss magnetism in the ultrafast regime by comparing quantitative experiments and theory in the literature on ferromagnetic transition metals(TM), rare earth(RE) elements and the magnetization dynamics of diluted semiconductor metals.

Spin dynamics include the spin-orbit interaction, the exchange interaction, the spin-phonon interaction and the dipolar interaction. Therefore, there are elementary questions; what happens to the ferromagnetic material with a sudden change in the applied magnetic field? What happens if a the ferromagnet or the electrons are heated above the Curie temperature within tens of femtoseconds? What happens if other timescales are involved? Answers to all of these questions will be discussed. Time-scales of magnetization process is the following.

- 10^6 years: Earth field.
- 10^1 years: Magnetic storage devices such as tape, disk.
- $10^{-3} - 10^{-6}$ seconds: Electronic circuits.
- 10^{-9} seconds: Readable and writeable of hard-disks.
- $10^{-9} - 10^{-12}$ seconds: Magnetization processions and reversal.
- $10^{-12} - 10^{-15}$ seconds: Ultrafast Spin Dynamics

Ultrafast magnetic processes of spintronic devices play an important role, such as magnetic tunneling junctions, spin transistors in the magnetic data storage or processing. Such structures have different magnetic properties of different coupled layers either through direct or indirect exchange coupling. This coupling mechanism depend on the time scale of the magnetic excitation. Advances of this area are storage capacity and energy efficiency depending of the limits of magnetic switching speed and storage density. In particular, the effect of fs pulse on spins of $Co_xZn_{1-x}O$ are investigated at low magnetic fields up to 1 Tesla.

5.3 Laser Induced Spin Dynamics

Laser induced ultrafast spin dynamics has become important for ferromagnetic metals. The switching of magnetization from one state to the other is under the impact of an external magnetic field, temperature or laser pulse during the dynamic process [74]. These processes are shown in detail in Fig.5.2. Characteristic properties of materials depend on the material parameters as well as dimensions of the magnetic system. The dynamics of the magnetization processes can be described by the Landau and Lifshitz with a mathematical definition in the Eq.2.26. This equation was later extended by Gilbert equation of motion for the magnetization dynamics, which has currently known as the Landau-Lifshitz-Gilbert equation, i.e. Eq.2.31. In fact, the equilibrium orientation of magnetization causes with a balance between exchange energy, the applied magnetic field and magnetic anisotropy.

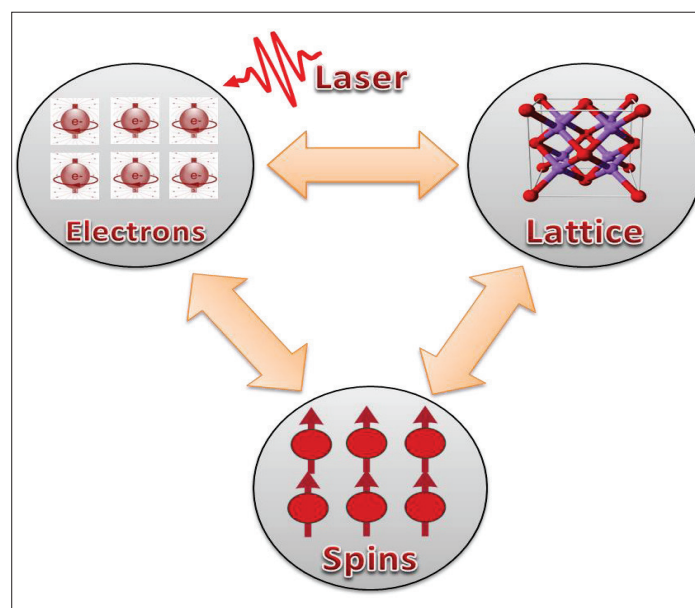


Fig. 5.2 Schematic representation of ultrafast spin dynamics. The three-temperature model suggested by Agranat *et. al* [112] some of the possible behaviour of a magnetic interactions for a ferromagnetic metal, such as spin-lattice, electron-spin and electron-lattice interactions in the picosecond laser pulse. The dynamic behaviour of a magnetic can be understood in terms of three thermodynamic reservoirs and interactions in the figure.

During the past few years, laser induced (laser pump) magnetisation dynamics has become one of the most exciting topics in today's magnetism on ultrafast timescales for applications

in magnetic storage devices, spintronics, and quantum computation [113–116]. They enable us to do new magnetic media with ultrashort, like femtosecond laser pulses and picosecond magnetic field pulses which are the process faster than 100 ps. These techniques led to observations of magnetization changes on a few femtosecond or a sub-picosecond timescale. In this chapter, we have presented an overview of the latest developments in methods based on fast laser excitation [28, 29, 117]. Spin dynamics are modelled using the LLG equation. In particular, the best known ferromagnetic materials are the 3d transition metals and rare earth metals: Fe, Ni, Co and Gd, Dy, respectively. Materials such as Nickel and Cobalt show a spontaneous magnetization at room temperature.

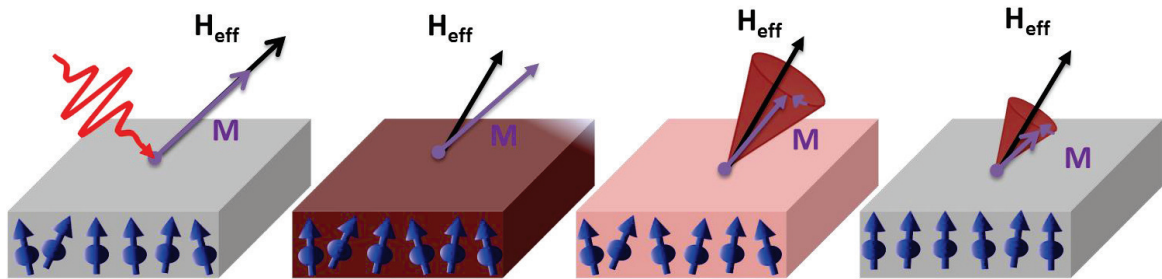


Fig. 5.3 Schematic representation of laser-induced magnetization dynamics of the excitation mechanism of the ferromagnetic and exchange spin precession modes with an external magnetic field. Before from the laser pump, the magnetization of the dominating sublattice align with the effective field (left). After the pump, other figures show behaviour of both the effective field and magnetization within few ps time scale. Consequently, the magnetization precess connected with the effective field, H_{eff} , and the magnetization, M , in magnetic systems.

The introduction of ultrafast laser pulse enables time durations of only a few tens of femtoseconds. Even some scientists prove the presence of attosecond pulses [39, 118–120]. Spin lattice relaxation time is different for any magnetic materials such as rare earth [121] Ni [113]. In particular, RE-TM alloys have magnetic properties which make them suitable for ultrafast magnetic recording in the absence of a magnetic field. A surprising discovery of ultrafast demagnetization of a Ni film by Beaurepaire *et al.* demonstrated remarkable results on laser induced demagnetization with 60 fs laser pulses using a time resolved pump probe set-up. They reported that the magnetic order of Ni was quenched on a sub-ps timescale

when Ni induced with an ultrafast laser pulse. Their aim was to control reverse magnetism on picosecond time-scales with ultrafast laser pulses Fig.5.3.

Firstly, before the induced pulse implement, the magnetic system in equilibrium magnetization is aligned with the effective field H_{eff} . We can consider the signal sent by the laser pulse. The energy preserved by the laser induced pulse increases the temperature of the sample under the laser light which takes place on a timescale smaller than a few femtosecond.

5.4 Demagnetization

Demagnetization is the loss of magnetization as a result of laser excitation in the ultrafast field. In 1996 Beaurepaire *et al.* found the demagnetization in nickel element using the time resolved Magneto Optical Kerr Effect (MOKE) technique to measure magnetization dynamics. They observed a reduction in the magnetization on a picosecond time scale in laser pump. In fact, most ferromagnets have shown demagnetization properties in a ~ 100 fs [29] duration. The influence of an ultrafast laser pulse on a ferromagnetic magnetic

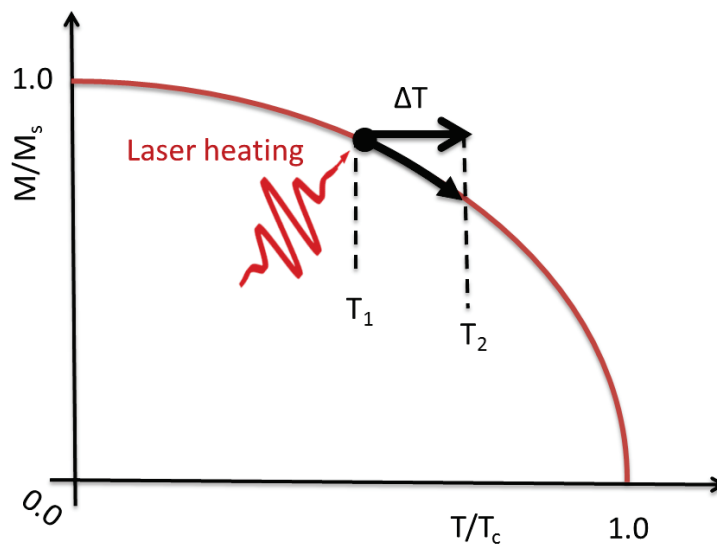


Fig. 5.4 Schematic illustration of a conventional magnetization-temperature diagram and the effect of laser

material has shown in equilibrium at temperature T_1 in Fig.5.4. After the laser pulse, the

material equilibrates to a new state at temperature T_2 . This figure is known as $M(T)$ curves. As the temperature is increased, magnetization is reduced. This process can be called demagnetization in the laser induced spin dynamics [29].

First ultrafast studies on the impact of laser pulses were found for Ni element using picosecond laser pulses, and this pioneering result has shown in Fig.5.5(Symbolic demagnetization) and Fig.5.6b. Their works opened a new curiosity field in ultrafast magnetization dynamics for Ni atom [34], Fe/FePt [110], for Co [122], GdFeCo [38, 41], $CoPt_3$ [109, 123] Fe [124, 125]. This area is called 'femtomagnetism', 'ultrafast-magnetism' or 'ultrafast magnetization(spinn) dynamics'. However, some results are still being debated both theoretically and experimentally.

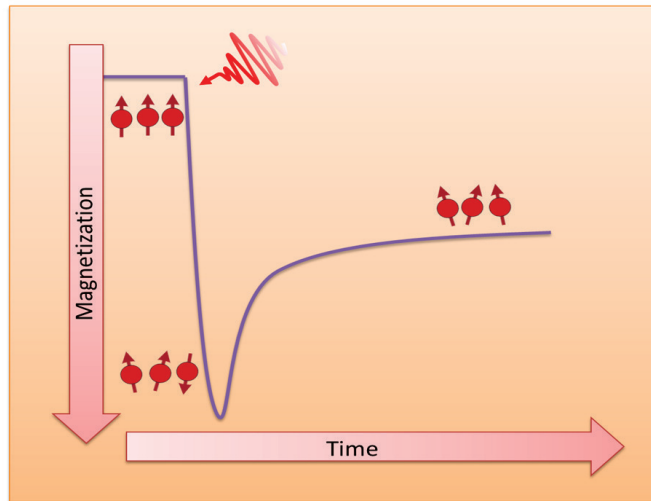
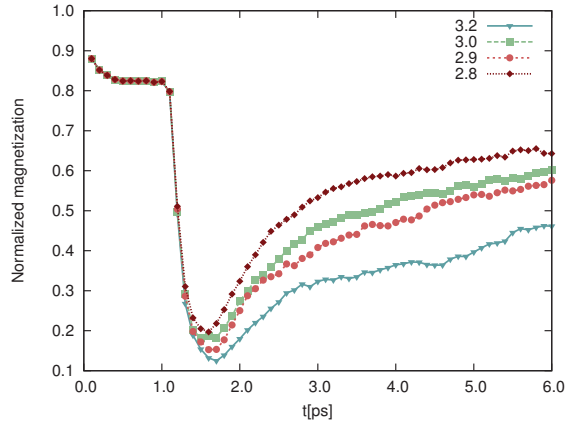
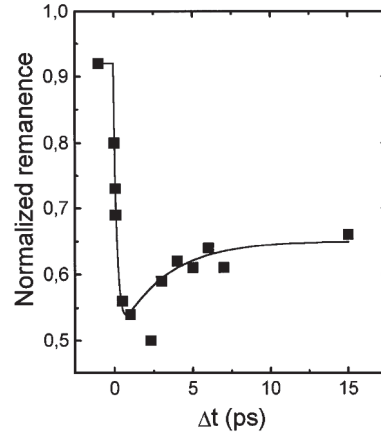


Fig. 5.5 Schematic summary of ultrafast magnetization dynamics.

The Landau-Lifshitz-Gilbert equation known as the classical model for magnetization dynamics is the basis of magnetization dynamics with a fixed magnitude. Therefore, the validity of this model is controversial for ultrafast phenomena. Later, some of the experimental results were investigated by different groups [113, 123, 126, 127], and other ultrafast phenomena in magnets was reported such as spin orientation [35, 128, 129], innovation of magnetic structure [130, 131], and by inverse Faraday effect [132–134]. We simulated the behaviour of demagnetization on the time scale of picoseconds.



(a) Ni demagnetization from our calculation. In figure 3.2, 3.0, 2.9 and 2.8×10^{21} watt is laser pulse power



(b) Ni demagnetization from ref. [34]

Fig. 5.6 (a) Calculated time-resolved magnetisation dynamics of Nickel obtained using the atomistic spin dynamics model. (b) Experimental measurements of the ultrafast demagnetisation dynamics measured using the MOKE in Nickel by Beaurepaire *et al.*. This measurement was the first example of ultrafast demagnetisation in a ferromagnetic material. Several processes have been obtained for ultrafast magnetization dynamics.

5.5 Reversal in a Field

The dynamics of femtosecond laser pulse induced magnetization reversal is controlled by both temperature-induced changes and field-induced rotational dynamics. Spin-lattice relaxation times are under of 50 ps. Reversal of magnetization which is simply heating the electron system above the Curie temperature is not enough. However, in combination with either a static or pulsed magnetic field, optical excitation by femtosecond laser pulses induces magnetization reversal that can be drastically fast [135, 136]. Recent experiments have also shown a new generation ultrashort field pulses in a Schottky diode [137]. Hereby, approach of magnetization reversal is using a short magnetic field pulse by struggling a torque on magnetization M , following precession of M at nanoscale regime [29, 138]. Therefore, precessional switching faces two challenges: generation of short magnetic field pulses and suppression of the precession at a suitable time.

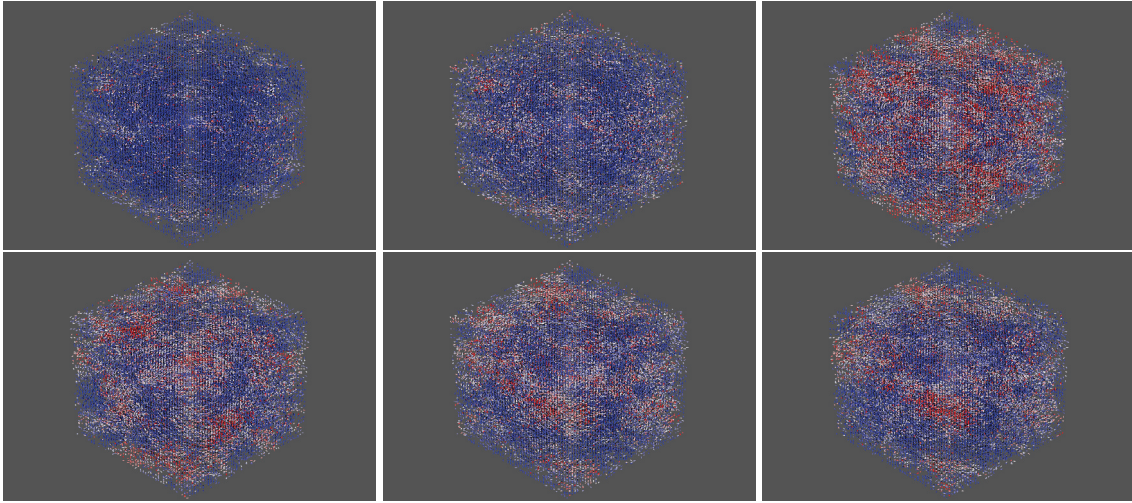


Fig. 5.7 Crystal visualization of $Co_{0.3}Zn_{0.7}O$ magnetic reversal properties. System of $15 \times 15 \times 15$ cubic lattice of atomic magnetic moments.

5.6 Ultrafast Spin Dynamics in DMS

The main emphasis in this section will be on ultrafast magnetization dynamics in ferromagnetic transition metals doped ZnO induced by femtosecond laser pulses. An ultrashort laser pulse may create excitation in the form of free electron hole pairs in the semiconductor. This phenomenon is coherent with phase relationship decayed a few femtoseconds due to electron-electron, hole-hole, and electron-hole scattering processes. As it was mentioned in the introduction section, a novel work in laser induced demagnetization has been demonstrated by Beaurepaire *et al.* using a 60 fs laser pulse demagnetization in a Ni element. After this discovery, laser induced demagnetization has been significant in ferromagnetic transition metals and rare earth metals and their alloys.

Demagnetization attracted researchers after the discovery of ferromagnetism in III-V (In,Mn)As and (Ga,Mn)As diluted magnetic semiconductors [33, 139, 140]. By taking exchange interactions of III-V ferromagnetic semiconductors into account, such as GaMnAs and InMnAs, a small concentration of Mn ions exhibit ferromagnetic state at Curie temperature 50 K. Also, we have examined magnetization behaviour at different laser powers and doping rates in Fig.5.8 and Fig.5.9.

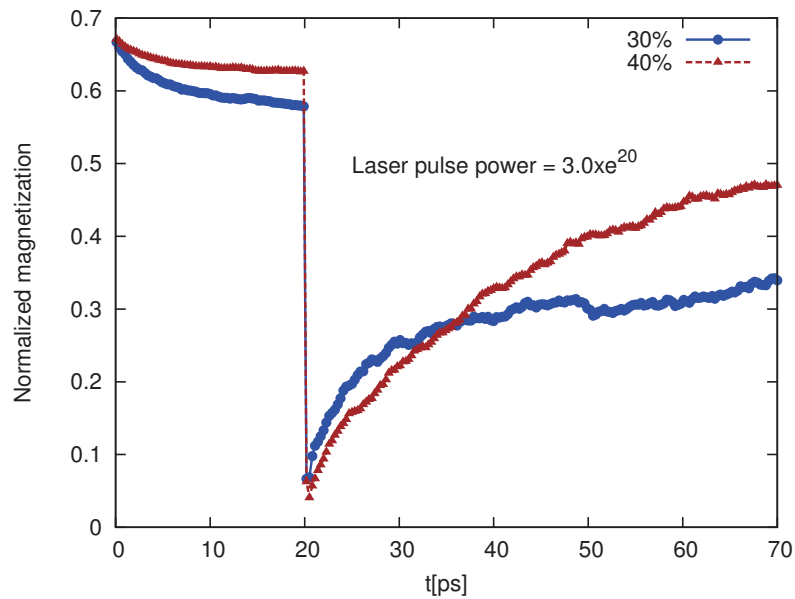


Fig. 5.8 Laser pulse calculations at concentration and pulse power Co doped ZnO. System size is $15 \times 15 \times 15$. Magnetization decreased sharply around 20 ps, and then magnetization is balanced.

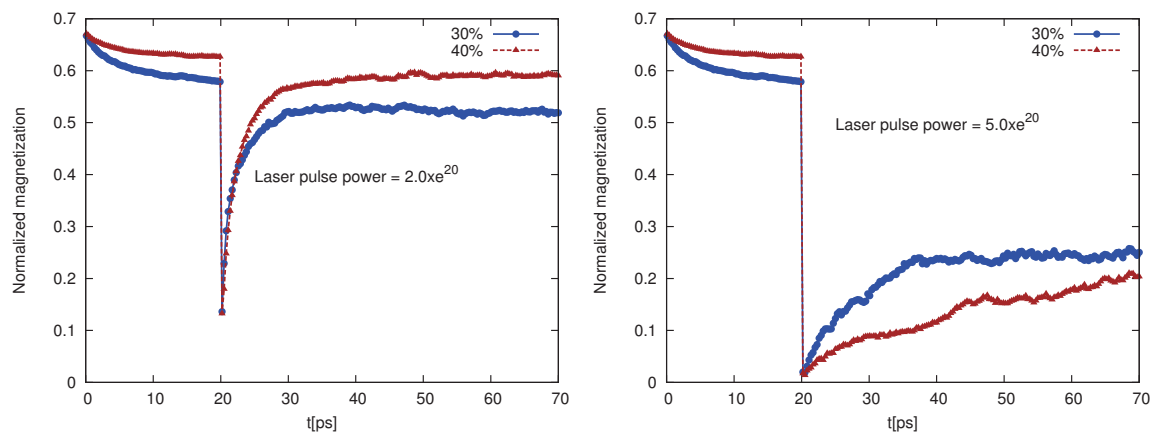


Fig. 5.9 Two temperature model calculations at constant concentration and at different pulse power CoZnO. System size is $15 \times 15 \times 15$. This process is called demagnetization by increase of temperature.

The field of ultrafast magnetization dynamics concerned with energy and angular momentum in a magnetic system. Basically, in terms of usage, these studies highly relevant in technological applications and electronic industry in nano-world. They are used in manufacturing fast data storage, magnetic random access memory devices and in the field of

spintronics at ultrafast technology. Recently, the ultrafast spin dynamics in a magnetically doped ZnO and GaN wide band gap semiconductor has been investigated [75, 141]. According to some damping parameter in LLG equation, we have obtained magnetization behaviour for different damping constant values in Fig-5.10.

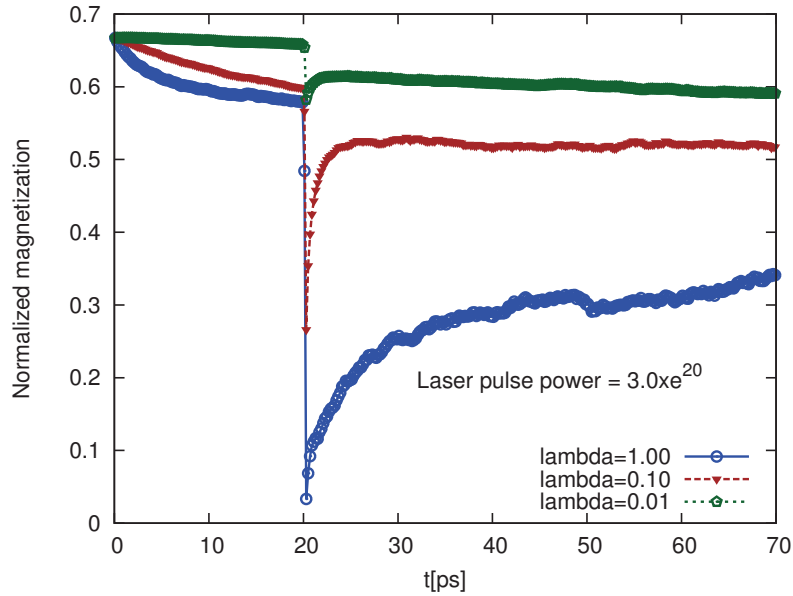


Fig. 5.10 Laser pulse calculations at concentration and pulse power Co doped ZnO. System size is $15 \times 15 \times 15$. Magnetization decreased sharply at around 20ps, and then magnetization balanced.

5.7 Two Temperature Model

The Two Temperature Model (TTM) has been widely used to predict the temporal and spatial evolution of the lattice temperature distributions, T_l , and electron temperatures distributions, T_e , in ultrafast laser processing of metals at femtosecond or picosecond time frames using LLG-Heun method. In order to understand this model, we should ask the question, what the characteristic timescale for the demagnetization process and the processes is involved? TTM can be considered a metallic sample photoexcited by a femtosecond laser pulse because there is a large difference between the electronic (C_e) and lattice or phononic (C_p) heat capacities with $C_p \gg C_e$ at room temperature. The femtosecond laser pulse reveals non-

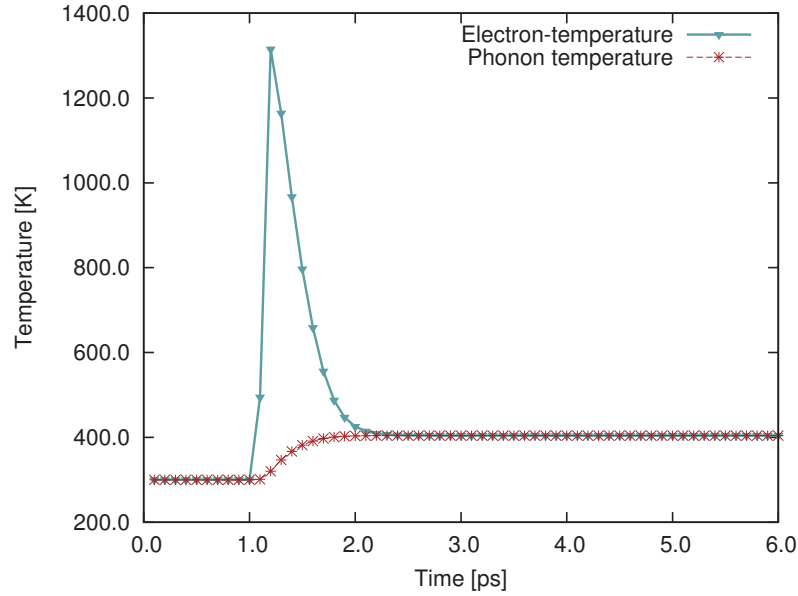


Fig. 5.11 Temperature-time behaviour using two temperature model calculations of Ni

equilibrium electron distribution in materials. Then, at different femtosecond time-scales, the non-equilibrium electrons redistribute their energies due to electron-electron Coulomb interactions. In a laser pulse system, temperature excitation is called Two Temperature Model which is the heat transfer through the electronic and atomic systems. Energy transport within the electronic system is solved according to the heat diffusion equation. Basic form of the TTM, in terms of relation between electron and phonon, is given by

$$\begin{aligned} C_e \frac{\partial T_e}{\partial t} &= G(T_e - T_l) + S(t) \\ C_l \frac{\partial T_l}{\partial t} &= G(T_l - T_e) \end{aligned} \quad (5.1)$$

where $S(t)$ represents the laser field pulse energy, C_e and C_l are the electron heat capacity and the lattice heat capacity, respectively, and G is the electron-lattice coupling factor. T_e and T_l are electron and phonon temperature. This is estimated by

$$G = \frac{\pi^2 m_e n_e c_s^2}{6\pi\tau(T_e)T_e} \quad (5.2)$$

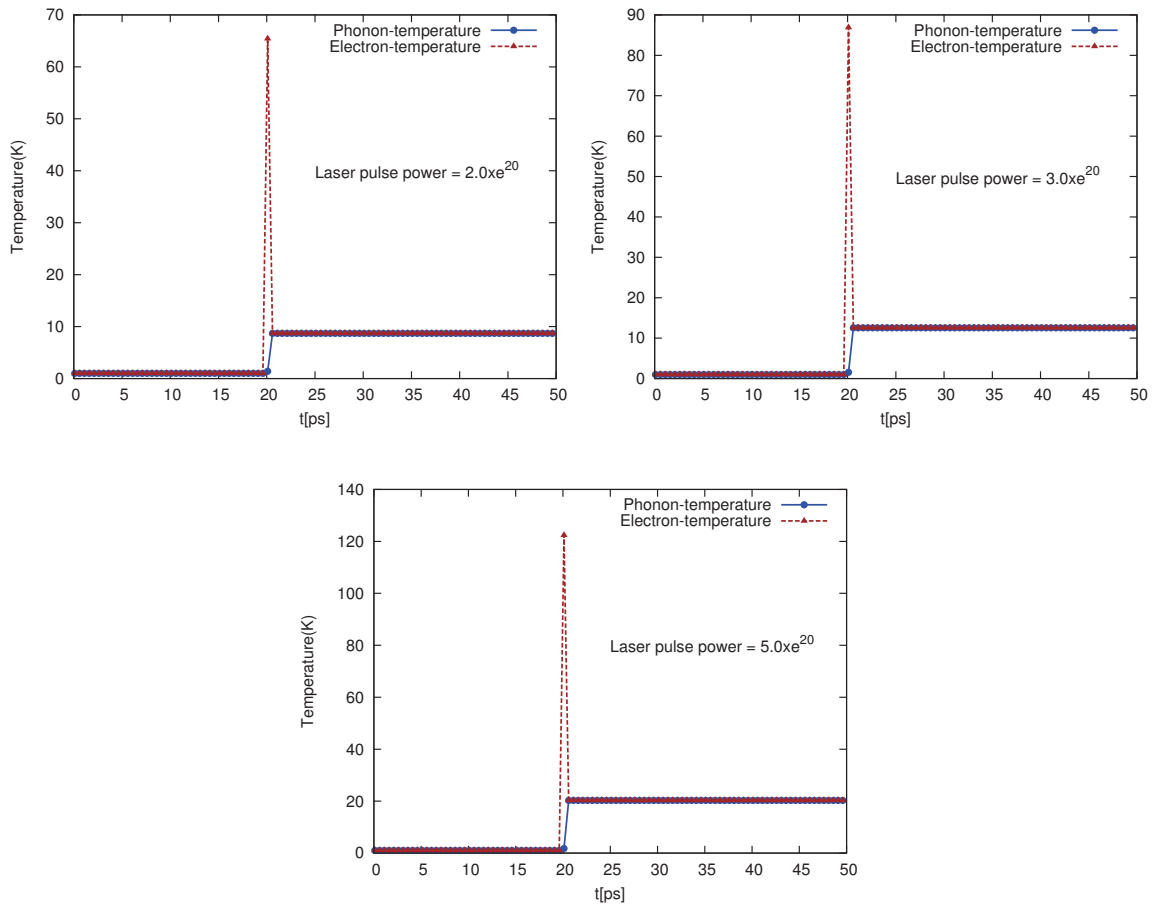


Fig. 5.12 Temperature-time behaviour using two temperature model calculations of CoZnO. Two temperature model calculations at constant concentration and at different pulse power CoZnO. Sytem size is $15 \times 15 \times 15$. This process is called demagnetization by the increase of temperature.

5.8 Summary

In summary, diluted magnetic semiconductors films were widely used in spintronic devices. As previously discussed, these materials are used in both the electronic and process of the information, processes that are strongly dependent on the magnetization dynamics. In this chapter, we have investigated the laser induced demagnetization with two temperature model in CoZnO with various concentrations of cobalt in order to answer some of the fundamental questions at the different temperatures.

We aimed to introduce and summarize comparing some the experimental and theoretical studies of ultrafast spins dynamics studies. We present an overview of using different theoretical approaches to the net magnetization, magnetic anisotropy, and magnetic structure. Simulated Curie temperature and demagnetization dynamics in CoZnO.

- Magnetic behaviour of Co against their exchange interaction when excited with an intense 20 ps laser pulse. The magnetization of CoZnO decreases after 20 ps, under the influence of the externally applied magnetic field.
- The demagnetization of the CoZnO with some doping rates becomes more efficient.
- The laser-induced ultrafast demagnetization takes place on the picosecond time-scale for spintronic materials.
- How fast can a magnetic change of structure displaying a magnetic order?
- Importance of laser induced precessional dynamics and processes is crucial for magnetization dynamics on the elementary length- and time-scales.

Chapter 6

CONCLUSIONS AND OUTLOOK

6.1 Overview

The main results of this thesis is related the development and application of an atomistic model of diluted magnetic semiconductors. A model of ZnCoO was stated on experimental observations and successfully compared by using Langevin dynamic and Monte Carlo method. New methods was developed based on literature values of the physical constants and experimental observations. This work provides new insights into magnetisation processes on the femtosecond timescale, possible for new engineering, industry and spintronic devices. Moreover, it has been made clear that any model of femtosecond laser induced dynamics for magnetic semiconductor. The calculations is able to reverse magnetisation is scientifically curious and potentially technologic important.

We detail given some information about magnetization and used simulation methods in chapter 1-2. We used RKKY indirect exchange interaction at spin Hamiltonian for our all calculations in chapter 3. By using zero field cooling and field cooling, we observed different magnetic properties at different parameter n chapter 4. Finally, we examined demagnetization on the laser-pulse behaviour of ZnCoO in chapter 5. In fact, this field is new resources area of magnetic semiconductor.

6.1.1 Spintronic Applications

In recent years, dilute magnetic oxides including ZnO based DMS and non-oxide ferro-magnetic semiconductors like Mn doped GaMnAs have been the subject of numerous experimental and computational investigations. So, they become today's most popular devices and online applications in Fig.6.1. Many scientists are interested in the investigation of

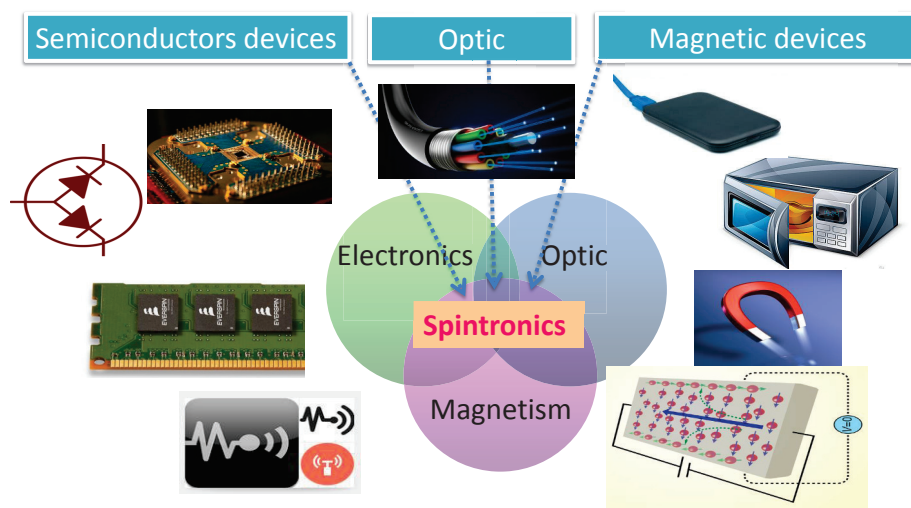


Fig. 6.1 Schematic representation of spintronic devices illustrated dependent as electronic, optic and magnetic devices

the nanostructured magnetic materials after the discovery of giant magnetoresistance, which Nobel Prize in Physics by Albert Fert and Peter Gronberg in 2007. So, many observations showed that the research in magnetism has been increasing due to increasing demand for faster and more dense magnetic storage. Fundamental properties of magnets which have served as one of the cornerstones of magnetic data storage. Due to the demand in industry for 'faster' and 'smaller' magnetic bits, the field of nano-magnetism is one of the greatest in condensed matter physics. In terms of writing and reading in the faster times, we need to development new models.

6.2 Computational Methods and Test Simulations

We have performed a detailed literature survey for existing studies/models on the magnetic behaviour of diluted magnetic semiconductor. Most studies suppose that the RKKY interaction leads to frustrations and spin glass state. However, our simulations showed that this interaction in the system not only lead to the formation of the ferromagnetic, antiferromagnetic and paramagnetic structure but also spin glass due to exchange interactions.

In the our studies, first of all, we examined magnetic behaviour of the coupling constant which depends on distance in Fig.3.9. And then, by using Monte Carlo-Heisenberg Metropolis algorithm and LLG-Heun method we observed a different magnetization behaviour in transition metal doped ZnO. Monte Carlo simulations, fully connected with Ising model, were studied for spin lattice systems with indirect exchange interaction. If one wants to compare with other computational methods, LLG-Heun method is the best way for magnetic systems. We have presented magnetic properties of $Zn_{1-x}Co_xO$ ($0 \leq x \leq 1$) by performing MC simulations. The theory of ferromagnetism in (II-VI) and (III-V) semiconductors by Dietl et al. [46] is based on Zener's model of ferromagnetism [85, 142] in (II-VI) $Zn_{1-x}Mn_xTe$ and (III-V) $Ga_{1-x}Mn_xAs$.

The atomistic spin dynamics simulations presented in this thesis have been performed with VAMPIRE [1], a software developed at Department of Physics, University of York-UK. During this thesis, we have used two techniques which are Monte Carlo method and LLG-Heun method. The main outcome of this thesis is that a new method has been presented for magnetic properties of diluted magnetic semiconductors. In this thesis, calculations of magnetization phenomena are performed at University of York and Marmara University.

6.3 Magnetic Properties of Transition Metal Doped ZnO

So far most diluted magnetic semiconductor materials have low T_c values, thus they are not suitable for spintronics applications. They include transition metal doped II-VI or III-V group semiconductors, which have been the most studied DMS materials for spintronic in investigations. For example, $Ga_{1-x}Mn_xAs$ at 110 K T_c Curie temperature has shown

ferromagnetic properties[46]. These reports were later experimentally confirmed for several other materials, such as, CoAlN, GaMnP. In particular, dilute magnetic oxides, such as, ZnO are promising towards novel applications, such as, transparent spintronics devices. Importance of diluted magnetic semiconductors have been increasing [27]. Spin dynamic came from ferromagnetic resonance experimentally time dependent behaviour of a magnetic materials was described by the Landau and Lifshitz equation. So we presented technological applications of diluted magnetic semiconductors as well.

Most of II-VI diluted magnetic semiconductors have shown spin glass phase or antiferromagnetic phase at low temperatures, which depends on the concentration of the transition metal ion. Spins are randomly oriented in the absence of an external magnetic field since diluted magnetic semiconductors always exhibit very weak magnetization due to small doped ferromagnetic materials like Co, Fe. In the our calculations shown different magnetic properties according to some input parameters. Chapter 4 predicted that a TM alloy such as ZnCoO would have different magnetization rates.

6.3.1 Time Scales of Magnetization Dynamics

Spintronic materials are used in navigation, power generation, medicine, electronics and more. Last decade, these magnetic applications have been increasing rapidly. New generation of spintronics applications is called magnetoresistive random access memory (MRAM) devices. MRAM have major importance with respect to other solid state memory types like static RAM (SRAM), dynamic RAM (DRAM) and Flash memory. However MRAM is a promising candidate for universal memory, which works as both random access memory and storage devices like hard disk drives. Moreover, the read/write speed increases day by day. All of them are used for store data according to magnetic hysteresis or magnetization behaviour. Ferromagnetic properties depends on some magnetization conditions, such as, in the presence of an external applied field. In this thesis, we examined the theory of magnetic behaviour and ultrafast magnetization dynamics on diluted magnetic materials in light of new ideas.

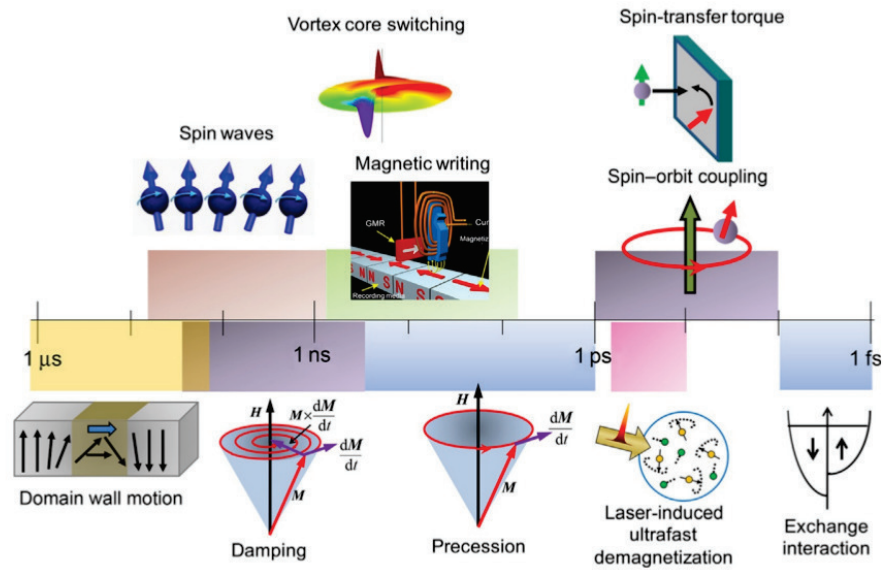


Fig. 6.2 Characteristic time scales of magnetization dynamics taken from ref[143]

6.3.2 Ultrafast Magnetization

The introduction of femtosecond lasers in magnets have enabled new areas of ultrafast phenomena. It has crucial properties to understand the ultrafast time scale of the magnetization dynamics and reversal processes in magnetic materials. In this thesis both the spin dynamics and classical spin Hamiltonian were studied for some transition metals doped ZnO systems. We are interested in the magnetization dynamics on the ultrafast time scales. In the last decades, importance of time-scale magnetism have been increasing from the nanosecond to the picosecond and even further to the femtosecond time scale to satisfy the need of today's electronics devices. Due to these circumstances, we have focused on ultrafast magnetization dynamics.

Moreover, in the industry or market, solid state memory are much ahead in what concerns the writing speed. Therefore, alternative ways of changing and controlling the magnetization on ultrafast time scale are subject of intense interest during the last decade. Along with alternative techniques to generate short magnetic field pulses, such as electro-optical current switches, searches and studies of fundamentally different mechanisms to influence spins are actively conducted. The time scale is still much longer than 100 ps at magnetization process. Interestingly, the latter time has been recommended below this time which the processes

in a magnetic systems can be referred to as "ultrafast magnetization dynamics". Actually, this time is a classic spin lattice relaxation time. First experimental results were published in 1996, showing the picosecond demagnetization of a Ni film induced by 60 fs laser pulses. This evidence of demagnetization occur within the first picosecond after the laser excitation according to some experimental and theoretical studies of laser induced magnetization dynamics. Since 1996, many observations of ultrafast light-induced magnetization dynamics resulted in different areas. We have discussed spin dynamics in Chapter 5 starting from ultrafast demagnetization.

6.4 Demagnetization at Transition Metal Doped ZnO

Ultrafast magnetization dynamics in Ni element has been explored for the past 20 years, starting with the pioneering discovery of Beaurepaire et al. in 1996 [34]. This area has led to a wide variety of novel and ultrafast applications for laser controlled writing of magnetic information. A general overview of ultrafast spin dynamics is given in the second chapter. In Chapter 5, we have studied the ultrafast spin dynamics. Feasibility to reverse the magnetization of GdFeCo discovered in 2007 by Stanciu et al was given inspiration to many scientist [37–41]. This provides great opportunities for the application of ultrafast magnetic system. The simulations and new findings described in this thesis may give new opportunities for the spintronic devices.

We have developed a theoretical method by controlling the precessional motion of a paramagnetic system on a picosecond timescale. High laser pulse excitation showed straight line after reversal. Diluted magnetic semiconductors have the potential to serve as an alternative technique for the storage of information and have significant advantages in data storage in terms of both speed and cost. In terms of applications, this study is a comparatively cheap and easy alternative method to measure ultrafast magnetization dynamics. Therefore, this area contributes to a better understanding of ultrafast processes and interactions in diluted magnetic semiconductors. The work provides new insights into magnetization processes on the femtosecond timescale, potentially important for engineering new devices.

Appendix A

A.1 Code's Development and Properties

The atomistic spin dynamics simulations calculated in this thesis have been performed with VAMPIRE. The software developed by R. F. L. Evans *et al.* [1, 8] Computational Magnetism group at Department of Physics, University of York. This software is a simulation method such as Monte Carlo metropolis and spin dynamics with standard calculations which they Curie temperature, field cooling, hysteresis loops and ultrafast spin dynamics.

A.2 Table of Parameters Used for Simulations

Parameter	Value	Unit
μ_s -Atomistic spin moment	1.73	μ_B
k_u -Anisotropy energy	6.69×10^{-24}	Joule/atom
J_{ij} -Exchange integral	2.0×10^{-22}	joule/link
M -Applied field	0.1 - 0.5 - 1.0 and 3.0	Tesla
Unit cell size	SC	3.524 Å
Crystal structure	SC, BCC, FCC, WZ and ZB	nm
System Size	10x10x10 and 20x20x20 Unit cell	nm ³
Time	t	Second(sn)
Applied field	H	Tesla(T)
Temperature	T	Kelvin(K)
Gyromagnetic ratio	γ	$1.76 \times 10^{11}/\text{Tsn}$

Table A.1 Used physical parameters for CoZnO in this thesis

$$\mu_B = \frac{e\hbar}{2m_e} : \text{Bohr magneton} = 9.2740 \times 10^{-24} \text{ J/T}$$

$$m_e : \text{Mass of electron} = 9.1 \times 10^{-31} \text{ kg}$$

$$\hbar : \text{Planck constant} = 6.62606957 \times 10^{-34} \text{ m}^2 \text{ kg/s}$$

$$e : \text{Elementary charge} = 1.6022 \times 10^{-19} \text{ Coulomb}$$

$$k_B \text{ is Boltzmann constant} = 1.3807 \times 10^{-23} \text{ J/K}$$

A.3 Code

```
#include <iostream>
#include <fstream>
#include <string>
#include <vector>
#include <cmath>
#include <cstdlib>
struct interaction_t{
double rij;
double Jij;
};
double Jijr(double rij)
{
const double j0=2.4e-18;
const double pi = 3.141592653589793238462;
// kf value 1.3 (AFM, 100 % Co doping)
// kf value 0.859 (FM, 0% Co doping)
const double kf=0.8635;
double x = 2.0*kf*rij;
double factor = exp(-rij/3.0)*j0*(x*cos(x)-sin(x))/ &
                (x*x*x*x);

return factor;
}
int main(){
// unit cell size in Angstroms
double a=3.32;
double b=3.32;
double c=5.22;
//atom counter
int i=0;
double xi, yi, zi, xj, yj, zj;
//the number of unit cells in x,y,z
int nuc[3]={7,7,7};
//the number of atoms (*4 atoms in unit cell)
int natom=nuc[0]*nuc[1]*nuc[2]*4;
std::vector<double> x(natom,0.0);
std::vector<double> y(natom,0.0);
std::vector<double> z(natom,0.0);
//this stores the "unit cell" displacement from the origin
//in x,y and z.
std::vector<int> dx(natom,0);
std::vector<int> dy(natom,0);
```

```
std::vector<int> dz(natom,0);
//The arguement here is the atom number (from 0->natoms)
//and it returns the atom number within the unit cell.
std::vector<int> aiuc(natom,4);
std::vector<std::string> atom_type(natom);
// index positions of atom Zn and atom O
for (int n=0; n<nuc[0]; n++){
for (int m=0; m<nuc[1]; m++){
for (int l=0; l<nuc[2]; l++){
//atom 0 in unit cell
atom_type[i] = "Zn";
x[i] = (0*a + n*a) + (0*b + m*b)*0.57735026919;
y[i] = 0*b + m*b;
z[i] = 0*c + c*l;
//store the number of the atom within &
the unit cell (this first atom is always zero)
aiuc[i]=0;
//store the unit cell displacement in x,y,z
dx[i]=n;
dy[i]=m;
dz[i]=l;
i++;
//atom 1 in unit cell
atom_type[i] = "O";
x[i] = (0*a + n*a) + (0*b + m*b)*0.57735026919;
y[i] = 0*b + m*b;
z[i] = 3*c/8 + c*l;
aiuc[i]=1;
dx[i]=n;
dy[i]=m;
dz[i]=l;
i++;
//atom 2 in unit cell
atom_type[i] = "Zn";
x[i] = (a/3 + n*a) + (b/3 + m*b)*0.57735026919;
y[i] = 2*b/3 + m*b;
z[i] = c/2 + c*l;
aiuc[i]=2;
dx[i]=n;
dy[i]=m;
dz[i]=l;
i++;
//atom 3 in unit cell
```



```
atom_type[i] = "O";
x[i] = (a/3 + n*a) + (b/3 + m*b)*0.57735026919;
y[i] = 2*b/3 + m*b;
z[i] = 7*c/8 + c*1;
aiuc[i]=3;
dx[i]=n;
dy[i]=m;
dz[i]=1;
i++;
}
}
}
//for writing neighbourlist
std::ofstream neighbourlist("CoZnO.ucf");
//do some error checking
if(!neighbourlist.is_open())
{
std::cerr << "Error opening neighbourlist file , &
              exiting" << std::endl;
exit(0);
}
neighbourlist << "# Unit cell size:" << std::endl;
neighbourlist << "3.32\t3.32\t5.22" << std::endl;
neighbourlist << "# Unit cell vectors: " << std::endl;
neighbourlist << "1.0 0.0 0.0 " << std::endl;
neighbourlist << "0.0 1.0 0.0 " << std::endl;
neighbourlist << "0.0 0.0 1.0 " << std::endl;
neighbourlist << "# Atoms num, id cx cy cz mat lc hc" &
              << std::endl;

neighbourlist << "4" << std::endl;
neighbourlist << "0\t0\t0\t0\t0\t0" << std::endl;
neighbourlist << "1\t0\t0\t0.375\t1\t1\t1" << std::endl;
neighbourlist << "2\t0.33333\t0.33333\t0.5\t2\t2\t2" &
              << std::endl;
neighbourlist << "3\t0.33333\t0.33333\t0.875\t3\t3\t3" &
              << std::endl;
neighbourlist << "#Interactions n exctype, &
              id i j dx dy dz\tJij" << std::endl;
neighbourlist << "776\t0" << std::endl;
std::vector<interaction_t> interactions(0);
std::string zinc="Zn";
int counter=0;
//loop over the atoms
```

```

for(int i = 0 ; i < natom ; i++)
{
// check only for central cell
if(dx[i]==3 && dy[i]==3 && dz[i]==3){
//loop over atom i's neighbours
for(int j = 0 ; j < natom ; j++)
{
// determine positions of atom i and atom j
xi=x[i];
yi=y[i];
zi=z[i];
xj=x[j];
yj=y[j];
zj=z[j];
// determine separation vector
double separation_x = xj-xi;
double separation_y = yj-yi;
double separation_z = zj-zi;
// determine |separation vector|
double rij;
rij= sqrt((xj-xi)*(xj-xi) + (yj-yi)*(yj-yi) + &
          (zj-zi)*(zj-zi)); // distance between two points
//if the distance between two atoms is less than &
some small number then it is
//a self interaction and should be neglected &
(or set to zero)
if(rij > 1e-20 && (atom_type[j]==zinc)&&(atom_type[i]==zinc))&
//could have if(i==j)
{
if(rij <=15.0){
neighbourlist << counter << "\t" << aiuc[i]&
          << "\t" << aiuc[j] << "\t" << dx[i]-dx[j] &
          << "\t" << dy[i]-dy[j] << "\t" << dz[i]-dz[j] &
          << "\t" << Jijr(rij) << std::endl;
counter++;
}
interaction_t tmp;
tmp.rij = rij;
tmp.Jij = Jijr(rij);
interactions .push_back(tmp);
}
else
}
}

```

```

}
}
// return (0);
std::cout << counter << std::endl;
// Write material file
std::ofstream matfile("CoZnO.mat");
// set magnetic density
const double density = 0.03;
matfile << "#=====&
=====" << std::endl;
matfile << "# CoZnO material file for vampire V3+" &
<< std::endl;
matfile << "#=====&
=====" << std::endl;
matfile << "" << std::endl;
matfile << "#-----&
-----" << std::endl;
matfile << "# Number of Materials" << std::endl;
matfile << "#-----&
-----" << std::endl;
matfile << "material:num-materials=4" << std::endl;
for(int i=1; i<5; i++){
matfile << "#-----&
-----" << std::endl;
matfile << "# Material " << i << " Co Sublattice "&
<< i << std::endl;
matfile << "#-----&
-----" << std::endl;
matfile << "material[" << i << "]:material-name=Co"&
<< std::endl;
matfile << "material[" << i << "]:damping-constant=&
1.0" << std::endl;
matfile << "material[" << i << "]:atomic-spin-moment=&
1.5 !muB" << std::endl;
matfile << "material[" << i << "]:uniaxial-anisotropy-&
constant=5.47e-26" << std::endl;
matfile << "material[" << i << "]:material-element=Ag"&
<< std::endl;
matfile << "material[" << i << "]:density=" << density&
<< std::endl;
// matfile << "material[" << i << "]:initial-spin-&
direction=random" << std::endl;
}

```

```

std::ofstream Jrijfile("J_rij.dat");
if(!Jrijfile.is_open())
{
std::cerr << "Could not open J_rij.dat for writing&
            unsorted J_ij(r_ij) data, exiting" << std::endl;
}
std::cout << "here" << std::endl;
for(int i=0; i<1000; i++){
Jrijfile << double(i)*0.1 << "\t" << Jijr(double(i)*0.1)&
<< std::endl;
}
//return 0;
// Loop over all atoms in system (i)
for (int i=0; i< 1; i++){
// For each i, loop over all atoms in the system&
(j) and calculate their separation
for (int j=0; j< natom; j++){
// determine positions of atom i and atom j
xi=x[i];
yi=y[i];
zi=z[i];
xj=x[j];
yj=y[j];
zj=z[j];
// determine separation vector
double separation_x = xj-xi;
double separation_y = yj-yi;
double separation_z = zj-zi;
// determine |separation vector|
double rij;
rij= sqrt((xj-xi)*(xj-xi) + (yj-yi)*(yj-yi) + &
          (zj-zi)*(zj-zi)); //distance between two points
if(rij>1e-20)
{
// Jrijfile << rij << "\t" << Jijr(rij) << std::endl;
}
// if separation vector is less than neighbour separation,&
count as nearest neighbour
}
}
}
//return(0);
//write the coordinates

```

```
std::ofstream myfile;
myfile.open("example.xyz");
//myfile << 4000 << std::endl << std::endl;
myfile << natom << std::endl << std::endl;
for(i=0; i<natom; i++){
myfile << atom_type[i] << "\t" <<x[i]<<"\t"&
        <<y[i]<<"\t"<<z[i]<<std::endl;
}
myfile.close();
double summ=0.0;
// Calculate Jij(r)
std::ofstream rJijrfile;
rJijrfile.open("RJijr");
for(int iid=0; iid<interactions.size(); iid++){
rJijrfile << iid << "\t" << interactions[iid].rij &
        << "\t" << interactions[iid].Jij << std::endl;
summ+=interactions[iid].Jij;
}
std::cout << "Sum Jij = " << summ << std::endl;
rJijrfile.close();
return 0;
}
```

A.4 Input and Material File Examples for Simulations

Input File

```
#=====
# Sample vampire input file to perform
# field cooling calculation for v3.0
# Creation attributes:
create:crystal-structure=sc
create:periodic-boundaries-x
create:periodic-boundaries-y
create:periodic-boundaries-z
#-----
# System Dimensions:
#-----
dimensions:unit-cell-size = 3.54 !A
dimensions:system-size-x = 15 !nm
dimensions:system-size-y = 15 !nm
dimensions:system-size-z = 15 !nm
#-----
# Material Files:
```

```
#-----  
material:file=CoZnO.mat  
material:unit-cell-file=CoZnO.ucf  
#-----  
# Simulation attributes:  
#-----  
sim:temperature=300.0  
sim:equilibration-temperature=300.0  
sim:minimum-temperature=0.0  
sim:maximum-temperature=300.0  
sim:temperature-increment=50.0  
sim:time-steps-increment=1  
sim:equilibration-time-steps=1000  
sim:loop-time-steps=1000  
sim:total-time-steps=5000000  
sim:time-step=1.0E-16  
sim:applied-field-strength=1.0 !T  
sim:cooling-time=0.1 !ns  
sim:save-checkpoint=end  
#-----  
# Program and integrator details  
#-----  
sim:program=field-cool  
sim:integrator=monte-carlo  
#-----  
# data output  
#-----  
output:real-time  
output:temperature  
output:magnetisation  
output:mean-magnetisation-length  
output:output-rate=1000  
#output:height-magnetisation  
#screen:real-time  
#screen:temperature  
#screen:mean-magnetisation-length  
#-----  
# Visulation for PovRay  
#-----  
config:atoms  
config:atoms-output-rate=100000
```

Material File

```
#=====
# CoZnO material file for vampire V3+
#=====
# Number of Materials
#-----
material:num-materials=4
#-----
# Material 1 Co Sublattice 1
#-----
material[1]:material-name=Co
material[1]:damping-constant=1.0
material[1]:atomic-spin-moment=1.5 !muB
material[1]:uniaxial-anisotropy-constant=5.47e-26
material[1]:material-element=Ag
material[1]:density=0.02
#-----
# Material 2 Co Sublattice 2
#-----
material[2]:material-name=Co
material[2]:damping-constant=1.0
material[2]:atomic-spin-moment=1.5 !muB
material[2]:uniaxial-anisotropy-constant=5.47e-26
material[2]:material-element=Ag
material[2]:density=0.0
#-----
# Material 3 Co Sublattice 3
#-----
material[3]:material-name=Co
material[3]:damping-constant=1.0
material[3]:atomic-spin-moment=1.5 !muB
material[3]:uniaxial-anisotropy-constant=5.47e-26
material[3]:material-element=Ag
material[3]:density=0.02
#-----
# Material 4 Co Sublattice 4
#-----
material[4]:material-name=Co
material[4]:damping-constant=1.0
material[4]:atomic-spin-moment=1.5 !muB
material[4]:uniaxial-anisotropy-constant=5.47e-26
material[4]:material-element=Ag
material[4]:density=0.0
```

References

- [1] R. F. L. Evans, “Atomistic simulation of magnetic nanomaterials, <http://vampire.york.ac.uk/>,” 2013.
- [2] J. Coey, *Magnetism and Magnetic Materials*. Springer, 2010.
- [3] C.-G. Stefanita, *Magnetism - Basics and Applications*. Cambridge University Press, 2012.
- [4] M. Bandyopadhyay and S. Dattagupta, “Memory in nanomagnetic systems: Superparamagnetism versus spin-glass behavior,” *Phys. Rev. B*, vol. 74, p. 214410, Dec 2006.
- [5] R. F. L. Evans, *Atomistic Modelling of Nanogranular Magnetic Materials*. PhD thesis, The University of York, Department of Physics, <http://www-users.york.ac.uk/~rfl500/resources/thesis.pdf>, 7 2008.
- [6] T. A. Ostler, *Computer Simulations of Ultrafast Magnetisation Reversal*. PhD thesis, The University of York, Department of Physics, <http://tomostler.co.uk>, 7 2012.
- [7] W. Fan, *Atomistic Modelling of Magnetisation Reversal Processes in Recording Media*. PhD thesis, The University of York, Department of Physics, <http://etheses.whiterose.ac.uk/5182/>, 9 2013.
- [8] R. F. L. Evans, W. J. Fan, P. Chureemart, T. A. Ostler, M. O. A. Ellis, and R. W. Chantrell, “Atomistic spin model simulations of magnetic nanomaterials,” *Journal of Physics: Condensed Matter*, vol. 26, no. 10, p. 103202, 2014.
- [9] E. Ising, “Beitrag zur theorie des ferromagnetismus,” *Zeitschrift für Physik*, vol. 31, pp. 253–258, 1925.
- [10] S. Ruta, “Computational modelling of interaction effects in Fe₃O₄ nanoparticle systems for comparison with experiments,” Master’s thesis, The University of York, Department of Physics, York-United Kingdom, 2013.
- [11] B. Újfalussy, X.-D. Wang, D. M. C. Nicholson, W. A. Shelton, G. M. Stocks, Y. Wang, and B. L. Gyorffy, “Constrained density functional theory for first principles spin dynamics,” *Journal of Applied Physics*, vol. 85, no. 8, 1999.

- [12] M. Fähnle, R. Drautz, R. Singer, D. Steiauf, and D. Berkov, “A fast ab initio approach to the simulation of spin dynamics,” *Computational Materials Science*, vol. 32, no. 1, pp. 118 – 122, 2005.
- [13] U. Nowak, O. N. Mryasov, R. Wieser, K. Guslienko, and R. W. Chantrell, “Spin dynamics of magnetic nanoparticles: Beyond brown’s theory,” *Phys. Rev. B*, vol. 72, p. 172410, Nov 2005.
- [14] L. LD and L. EM, “On the theory of the dispersion of magnetic permeability in ferromagnetic bodies,” *Physikalische Zeitschrift der Sowjetunion*, vol. 8(2), pp. 153–169, 1935.
- [15] T. Gilbert, “A lagrangian formulation of the gyromagnetic equation of the magnetization field,” *Physical Review*, vol. 100, p. 1243, 1955.
- [16] A. Makarov, *Modeling of Emerging Resistive Switching Based Memory Cells*. PhD thesis, Technische Universität Wien, <http://www.iue.tuwien.ac.at/phd/makarov/>, 2014.
- [17] K. Vahaplar, *Ultrafast Path for Magnetization Reversal in Ferrimagnetic GdFeCo Films*. PhD thesis, Radboud University, Institute for Molecules and Materials, <http://www.kadirvahaplar.com/>, 2011.
- [18] W. Brown, “Thermal fluctuations of a single-domain particle,” *Phys. Rev.*, vol. 130, pp. 1677–1686, Jun 1963.
- [19] W. T. Coffey, *The Langevin Equation*. Worldscientific, 2004.
- [20] A. Lyberatos and R. Chantrell, “Thermal fluctuations in a pair of magnetostatically coupled particles,” *Journal of Applied Physics*, vol. 73, pp. 6501–6503, May 1993.
- [21] O. Chubykalo, J. Hannay, M. Wongsam, R. Chantrell, and J. Gonzalez, “Langevin dynamic simulation of spin waves in a micromagnetic model,” *Phys. Rev. B*, vol. 65, p. 184428, May 2002.
- [22] J. Garcia-Palacios and F. Lazaro, “Langevin-dynamics study of the dynamical properties of small magnetic particles,” *Phys. Rev. B*, vol. 58, pp. 14937–14958, Dec 1998.
- [23] Y. Nakatani, Y. Uesaka, N. Hayashi, and H. Fukushima, “Computer simulation of thermal fluctuation of fine particle magnetization based on langevin equation,” *Journal of Magnetism and Magnetic Materials*, vol. 168, no. 3, pp. 347 – 351, 1997.
- [24] W. Scholz, T. Schrefl, and J. Fidler, “Micromagnetic simulation of thermally activated switching in fine particles,” *Journal of Magnetism and Magnetic Materials*, vol. 233, no. 3, pp. 296 – 304, 2001.
- [25] J. Hellsvik, *Atomistic Spin Dynamics, Theory and Applications*. PhD thesis, Uppsala University, Faculty of Science and Technology, <http://www.diva-portal.org/smash/get/diva2:358126/FULLTEXT01.pdf>, 12 2010.

- [26] B. Skubic, *Spin Dynamics and Magnetic Multilayers*. PhD thesis, Uppsala University, Faculty of Science and Technology, <http://www.diva-portal.org/smash/get/diva2:170558/FULLTEXT01.pdf>, 9 2007.
- [27] J. Hellsvik, B. Skubic, L. Nordström, B. Sanyal, O. Eriksson, P. Nordblad, and P. Svedlindh, “Dynamics of diluted magnetic semiconductors from atomistic spin-dynamics simulations: Mn-doped GaAs,” *Phys. Rev. B*, vol. 78, p. 144419, Oct 2008.
- [28] R. Skomski, *Simple Models of Magnetism*. Oxford Graduate Texts, 2012.
- [29] O. K. Hillebrands, Burkard, *Spin Dynamics in Confined Magnetic Structures II*. Springer/Topics in Applied Physics, 2003.
- [30] S. P. E. Helmut Kronmüller(Editor), *Handbook of Magnetism and Advanced Magnetic Materials*. Wiley, 2007.
- [31] B. Skubic, J. Hellsvik, L. Nordström, and O. Eriksson, “A method for atomistic spin dynamics simulations: implementation and examples,” *Journal of Physics: Condensed Matter*, vol. 20, no. 31, p. 315203, 2008.
- [32] A. Eschenlohr, M. Battiato, P. Maldonado, N. Pontius, T. Kachel, K. Holldack, R. Mitzner, A. F?hlisch, P. M. Oppeneer, and C. Stamm, “Ultrafast spin transport as key to femtosecond demagnetization,” *Nat Mater*, vol. 12, pp. 332–336, Apr 2013.
- [33] A. Kirilyuk, A. Kimel, and T. Rasing, “Ultrafast optical manipulation of magnetic order,” *Rev. Mod. Phys.*, vol. 82, pp. 2731–2784, Sep 2010.
- [34] E. Beaupaire, J.-C. Merle, A. Daunois, and J.-Y. Bigot, “Ultrafast spin dynamics in ferromagnetic nickel,” *Phys. Rev. Lett.*, vol. 76, pp. 4250–4253, May 1996.
- [35] A. V. Kimel, A. Kirilyuk, A. Tsvetkov, R. V. Pisarev, and T. Rasing, “Laser-induced ultrafast spin reorientation in the antiferromagnet tmFeO_3 ,” *Nature*, vol. 429, p. 850, 2004.
- [36] C. Stanciu, F. Hansteen, A. Kimel, A. Kirilyuk, A. Tsukamoto, A. Itoh, and T. Rasing, “All-optical magnetic recording with circularly polarized light,” *Phys. Rev. Lett.*, vol. 99, p. 047601, Jul 2007.
- [37] C. D. Stanciu, F. Hansteen, A. V. Kimel, A. Tsukamoto, A. Itoh, A. Kirilyuk, and T. Rasing, “Ultrafast interaction of the angular momentum of photons with spins in the metallic amorphous alloy gdfeco ,” *Phys. Rev. Lett.*, vol. 98, p. 207401, May 2007.
- [38] A. T. Ostler and at all, “Ultrafast heating as a sufficient stimulus for magnetization reversal in a ferrimagnet,” *Nat Commun*, vol. 3, p. 666, 2012.
- [39] I. Radu and at all, “Transient ferromagnetic-like state mediating ultrafast reversal of antiferromagnetically coupled spins,” *Nature*, vol. 472, p. 205, 2011.

- [40] T. Ostler, R. Evans, R. Chantrell, U. Atxitia, O. Chubykalo-Fesenko, I. Radu, R. Abrudan, F. Radu, A. Tsukamoto, A. Itoh, A. Kirilyuk, T. Rasing, and A. Kimel, “Crystallographically amorphous ferrimagnetic alloys: Comparing a localized atomistic spin model with experiments,” *Phys. Rev. B*, vol. 84, p. 024407, Jul 2011.
- [41] U. Atxitia, T. Ostler, J. Barker, R. Evans, R. Chantrell, and O. Chubykalo-Fesenko, “Ultrafast dynamical path for the switching of a ferrimagnet after femtosecond heating,” *Phys. Rev. B*, vol. 87, p. 224417, Jun 2013.
- [42] T. Dietl and H. Ohno, “Dilute ferromagnetic semiconductors: Physics and spintronic structures,” *Rev. Mod. Phys.*, vol. 86, pp. 187–251, Mar 2014.
- [43] J. Coey, “Dilute magnetic oxides,” *Current Opinion in Solid State and Materials Science*, vol. 10, no. 2, pp. 83 – 92, 2006.
- [44] T. Fukumura, Y. Yamada, H. Toyosaki, T. Hasegawa, H. Koinuma, and M. Kawasaki, “Exploration of oxide-based diluted magnetic semiconductors toward transparent spintronics,” *Applied Surface Science*, vol. 223, no. 1–3, pp. 62 – 67, 2004. Proceedings of the Second Japan-US Workshop on Combinatorial Materials Science and Technology.
- [45] T. Dietl and H. Ohno, “Ferromagnetic iii–v and ii–vi semiconductors,” *MRS Bulletin*, vol. 28, pp. 714–719, 10 2003.
- [46] T. Dietl, H. Ohno, F. Matsukura, J. Cibert, and D. Ferrand, “Zener model description of ferromagnetism in zinc-blende magnetic semiconductors,” *Science*, vol. 287, no. 5455, pp. 1019–1022, 2000.
- [47] K. Sato and H. Katayama-Yoshida, “Stabilization of ferromagnetic states by electron doping in fe-, co- or ni-doped zno,” *Japanese Journal of Applied Physics*, vol. 40, no. 4A, p. L334, 2001.
- [48] G. Gu, G. Xiang, J. Luo, H. Ren, M. Lan, D. He, and X. Zhang, “Magnetism in transition-metal-doped zno: A first-principles study,” *Journal of Applied Physics*, vol. 112, no. 2, pp. –, 2012.
- [49] K. Ueda, H. Tabata, and T. Kawai, “Magnetic and electric properties of transition-metal-doped zno films,” *Applied Physics Letters*, vol. 79, no. 7, 2001.
- [50] S. Datta, J. Furdyna, and R. Gunshor, “Diluted magnetic semiconductor superlattices and heterostructures,” *Superlattices and Microstructures*, vol. 1, no. 4, pp. 327 – 334, 1985.
- [51] N. Read and D. Green, “Paired states of fermions in two dimensions with breaking of parity and time-reversal symmetries and the fractional quantum hall effect,” *Phys. Rev. B*, vol. 61, pp. 10267–10297, Apr 2000.
- [52] I. Žutić, J. Fabian, and S. Das Sarma, “Spintronics: Fundamentals and applications,” *Rev. Mod. Phys.*, vol. 76, pp. 323–410, Apr 2004.

- [53] M. N. Baibich, J. M. Broto, A. Fert, F. N. Van Dau, F. Petroff, P. Etienne, G. Creuzet, A. Friederich, and J. Chazelas, "Giant magnetoresistance of (001)fe/(001)cr magnetic superlattices," *Phys. Rev. Lett.*, vol. 61, pp. 2472–2475, Nov 1988.
- [54] D. Monroe, "Nobel focus: Sensitive magnetic sandwich," *Phys. Rev. Focus*, vol. 20, p. 13, Oct 2007.
- [55] S. J. Pearton, C. R. Abernathy, M. E. Overberg, G. T. Thaler, D. P. Norton, N. Theodoropoulou, A. F. Hebard, Y. D. Park, F. Ren, J. Kim, and L. A. Boatner, "Wide band gap ferromagnetic semiconductors and oxides," *Journal of Applied Physics*, vol. 93, no. 1, 2003.
- [56] S. A. Wolf, D. D. Awschalom, R. A. Buhrman, J. M. Daughton, S. von Molnár, M. L. Roukes, A. Y. Chtchelkanova, and D. M. Treger, "Spintronics: A spin-based electronics vision for the future," *Science*, vol. 294, no. 5546, pp. 1488–1495, 2001.
- [57] J. M. D. Coey, M. Venkatesan, and C. B. Fitzgerald, "Donor impurity band exchange in dilute ferromagnetic oxides," *Nat Mater*, vol. 4, pp. 173–179, Feb 2005.
- [58] G. T. Thaler, M. E. Overberg, B. Gila, R. Frazier, C. R. Abernathy, S. J. Pearton, J. S. Lee, S. Y. Lee, Y. D. Park, Z. G. Khim, J. Kim, and F. Ren, "Magnetic properties of n-gamnn thin films," *Applied Physics Letters*, vol. 80, no. 21, 2002.
- [59] P. Sharma, A. Gupta, K. V. Rao, F. J. Owens, R. Sharma, R. Ahuja, J. M. O. Guillen, B. Johansson, and G. A. Gehring, "Ferromagnetism above room temperature in bulk and transparent thin films of mn-doped zno," *Nat Mater*, vol. 2, pp. 673–677, Oct 2003.
- [60] R. M. Frazier, J. Stapleton, G. T. Thaler, C. R. Abernathy, S. J. Pearton, R. Rairigh, J. Kelly, A. F. Hebard, M. L. Nakarmi, K. B. Nam, J. Y. Lin, H. X. Jiang, J. M. Zavada, and R. G. Wilson, "Properties of co-, cr-, or mn-implanted aln," *Journal of Applied Physics*, vol. 94, no. 3, 2003.
- [61] F. J. Owens, "Ferromagnetism above room temperature in bulk sintered gallium phosphide doped with manganese," *Journal of Physics and Chemistry of Solids*, vol. 66, no. 5, pp. 793 – 796, 2005.
- [62] K. Sato, L. Bergqvist, J. Kudrnovský, P. H. Dederichs, O. Eriksson, I. Turek, B. Sanyal, G. Bouzerar, H. Katayama-Yoshida, V. A. Dinh, T. Fukushima, H. Kizaki, and R. Zeller, "First-principles theory of dilute magnetic semiconductors," *Rev. Mod. Phys.*, vol. 82, pp. 1633–1690, May 2010.
- [63] X. Liu, F. Lin, L. Sun, W. Cheng, X. Ma, and W. Shi, "Doping concentration dependence of room-temperature ferromagnetism for ni-doped zno thin films prepared by pulsed-laser deposition," *Applied Physics Letters*, vol. 88, no. 6, pp. –, 2006.

- [64] S. K. Nayak, M. Ogura, A. Hucht, H. Akai, and P. Entel, “Monte carlo simulations of diluted magnetic semiconductors using ab initio exchange parameters,” *Journal of Physics: Condensed Matter*, vol. 21, no. 6, p. 064238, 2009.
- [65] T. Dietl, “Spintronics and ferromagnetism in wide band gap semiconductors,” *AIP Conference Proceedings*, vol. 772, no. 1, pp. 56–64, 2005.
- [66] H. Munekata, H. Ohno, S. von Molnar, A. Segmüller, L. L. Chang, and L. Esaki, “Diluted magnetic iii-v semiconductors,” *Phys. Rev. Lett.*, vol. 63, pp. 1849–1852, Oct 1989.
- [67] H. Ohno, A. Shen, F. Matsukura, A. Oiwa, A. Endo, S. Katsumoto, and Y. Iye, “(ga,mn)as: A new diluted magnetic semiconductor based on gaas,” *Applied Physics Letters*, vol. 69, no. 3, 1996.
- [68] H. Saeki, H. Tabata, and T. Kawai, “Magnetic and electric properties of vanadium doped zno films,” *Solid State Communications*, vol. 120, no. 11, pp. 439 – 443, 2001.
- [69] S.-J. Han, J. Song, C.-H. Yang, S. Park, J.-H. Park, Y. Jeong, and K. Rhie, “A key to room-temperature ferromagnetism in fe-doped zno: Cu,” *Applied Physics Letters*, vol. 81, pp. 4212–4214, Nov 2002.
- [70] P. V. Radovanovic and D. R. Gamelin, “High-temperature ferromagnetism in ni²⁺-doped zno aggregates prepared from colloidal diluted magnetic semiconductor quantum dots,” *Phys. Rev. Lett.*, vol. 91, p. 157202, Oct 2003.
- [71] C. J. Cong, L. Liao, J. C. Li, L. X. Fan, and K. L. Zhang, “Synthesis, structure and ferromagnetic properties of mn-doped zno nanoparticles,” *Nanotechnology*, vol. 16, no. 6, p. 981, 2005.
- [72] M. Tsai, T. Jiang, and C. Huang, “Competition between ferromagnetic and anti-ferromagnetic couplings in co doped zno with vacancies and ga co-dopants,” *Journal of Magnetism and Magnetic Materials*, vol. 324, no. 9, pp. 1733 – 1738, 2012.
- [73] J. H. Kim, H. Kim, D. Kim, Y. E. Ihm, and W. K. Choo, “Magnetic properties of epitaxially grown semiconducting zn_{1-x}co_x thin films by pulsed laser deposition,” *Journal of Applied Physics*, vol. 92, no. 10, 2002.
- [74] M. Wu, J. Jiang, and M. Weng, “Spin dynamics in semiconductors,” *Physics Reports*, vol. 493, no. 2–4, pp. 61 – 236, 2010.
- [75] M. Raskin, T. Stiehm, A. W. Cohn, K. M. Whitaker, S. T. Ochsenbein, S. M. de Vasconcellos, M. S. Brandt, D. R. Gamelin, and R. Bratschitsch, “Ultrafast spin dynamics in magnetic wide-bandgap semiconductors,” *physica status solidi (b)*, vol. 251, no. 9, pp. 1685–1693, 2014.

- [76] A. Murayama, K. Seo, K. Nishibayashi, I. Souma, and Y. Oka, "Spin dynamics in a diluted magnetic semiconductor quantum well studied by pump-probe absorption spectroscopy: Magnetic-field-induced suppression of electron-spin relaxation," *Applied Physics Letters*, vol. 88, no. 26, pp. –, 2006.
- [77] G. K. Z. WILAMOWSKI, R. BUCZKO, "Ultra-fast spin dynamics in diluted magnetic semiconductors," *Proceedings of the XXV International School of Semiconducting Compounds*, vol. 90, no. 5, pp. 1685–1693, 1996.
- [78] B. Koopmans and W. de Jonge, "Ultrafast spin dynamics in magnetic semiconductor quantum wells studied by magnetization modulation spectroscopy," *Applied Physics B*, vol. 68, no. 3, pp. 525–530, 1999.
- [79] B. Koopmans, M. van Kampen, and W. J. M. de Jonge, "Electron and hole spin dynamics in magnetic semiconductors," *physica status solidi (b)*, vol. 215, no. 1, pp. 217–222, 1999.
- [80] M. C. Gibson, *Implementation and Application of Advanced Density Functionals*. PhD thesis, Durham University, Department of Physics, <http://etheses.dur.ac.uk/2938/>, 2006.
- [81] T. S. Heng, A. Kumar, C. S. Ong, Y. P. Feng, Y. H. Lu, K. Y. Zeng, and J. Ding, "Investigation of the non-volatile resistance change in noncentrosymmetric compounds," *Sci. Rep.*, vol. 2, Aug 2012.
- [82] K. Szałowski and T. Balcerzak, "Rkky interaction with diffused contact potential," *Phys. Rev. B*, vol. 78, p. 024419, Jul 2008.
- [83] A. F. Jalbout, H. Chen, and S. L. Whittenburg, "Monte carlo simulation on the indirect exchange interactions of co-doped zno film," *Applied Physics Letters*, vol. 81, no. 12, 2002.
- [84] L. Drissi, A. Benyoussef, E. Saidi, and M. Bousmina, "Monte carlo simulation of magnetic phase transitions in mn-doped zno," *Journal of Magnetism and Magnetic Materials*, vol. 323, no. 23, pp. 3001 – 3006, 2011.
- [85] C. Zener, "Interaction between the d shells in the transition metals," *Phys. Rev.*, vol. 81, pp. 440–444, Feb 1951.
- [86] M. Ruderman and C. Kittel, "Indirect exchange coupling of nuclear magnetic moments by conduction electrons," *Phys. Rev.*, vol. 96, pp. 99–102, Oct 1954.
- [87] T. Kasuya, "A theory of metallic ferro- and antiferromagnetism on zener's model," *Progress of Theoretical Physics*, vol. 16, no. 1, pp. 45–57, 1956.
- [88] K. Yosida, "Magnetic properties of cu-mn alloys," *Phys. Rev.*, vol. 106, pp. 893–898, Jun 1957.

- [89] P. M. Shand, A. D. Christianson, T. M. Pekarek, L. S. Martinson, J. W. Schweitzer, I. Miotkowski, and B. C. Crooker, "Spin-glass ordering in the diluted magnetic semiconductor $\text{zn}_{1-x}\text{mn}_x\text{Te}$," *Phys. Rev. B*, vol. 58, pp. 12876–12882, Nov 1998.
- [90] G. F. Goya and V. Sagredo, "Spin-glass ordering in $\text{zn}_{1-x}\text{mn}_x\text{in}_2\text{te}_4$ diluted magnetic semiconductor," *Phys. Rev. B*, vol. 64, p. 235208, Nov 2001.
- [91] L. Berthier and J.-P. Bouchaud, "Geometrical aspects of aging and rejuvenation in the ising spin glass: a numerical study," *Phys. Rev. B*, vol. 66, p. 054404, Aug 2002.
- [92] A. T. Ogielski, "Dynamics of three-dimensional ising spin glasses in thermal equilibrium," *Phys. Rev. B*, vol. 32, pp. 7384–7398, Dec 1985.
- [93] B. Skubic, O. E. Peil, J. Hellsvik, P. Nordblad, L. Nordström, and O. Eriksson, "Atomistic spin dynamics of the cu-mn spin-glass alloy," *Phys. Rev. B*, vol. 79, p. 024411, Jan 2009.
- [94] R. E. Blundell, K. Humayun, and A. J. Bray, "Dynamic exponent of the 3d ising spin glass," *Journal of Physics A: Mathematical and General*, vol. 25, no. 12, p. L733, 1992.
- [95] S. F. Edwards and P. W. Anderson, "Theory of spin glasses," *Journal of Physics F: Metal Physics*, vol. 5, no. 5, p. 965, 1975.
- [96] K. Binder and A. P. Young, "Spin glasses: Experimental facts, theoretical concepts, and open questions," *Rev. Mod. Phys.*, vol. 58, pp. 801–976, Oct 1986.
- [97] A. Deák, L. Szunyogh, and B. Ujfalussy, "Thickness-dependent magnetic structure of ultrathin fe/ir(001) films: From spin-spiral states toward ferromagnetic order," *Phys. Rev. B*, vol. 84, p. 224413, Dec 2011.
- [98] K. Chen and D. P. Landau, "Spin-dynamics study of the dynamic critical behavior of the three-dimensional classical heisenberg ferromagnet," *Phys. Rev. B*, vol. 49, pp. 3266–3274, Feb 1994.
- [99] S.-H. Tsai, A. Bunker, and D. P. Landau, "Spin-dynamics simulations of the magnetic dynamics of rbmnf_3 and direct comparison with experiment," *Phys. Rev. B*, vol. 61, pp. 333–342, Jan 2000.
- [100] X. Tao, D. P. Landau, T. C. Schulthess, and G. M. Stocks, "Spin waves in paramagnetic bcc iron: Spin dynamics simulations," *Phys. Rev. Lett.*, vol. 95, p. 087207, Aug 2005.
- [101] J. Hellsvik, "Atomistic spin dynamics simulations on mn-doped gaas and cumn," *Journal of Physics: Conference Series*, vol. 200, no. 7, p. 072040, 2010.
- [102] M. El-Hilo, A. Dakhel, and A. Ali-Mohamed, "Room temperature ferromagnetism in nanocrystalline ni-doped zno synthesized by co-precipitation," *Journal of Magnetism and Magnetic Materials*, vol. 321, no. 14, pp. 2279 – 2283, 2009. Current Perspectives: Modern Microwave Materials.

- [103] K. Sato and H. Katayama-Yoshida, “First principles materials design for semiconductor spintronics,” *Semiconductor Science and Technology*, vol. 17, no. 4, p. 367, 2002.
- [104] D.-L. Hou, R.-B. Zhao, Y.-Y. Wei, C.-M. Zhen, C.-F. Pan, and G.-D. Tang, “Room temperature ferromagnetism in ni-doped zno films,” *Current Applied Physics*, vol. 10, no. 1, pp. 124 – 128, 2010.
- [105] B. Pandey, S. Ghosh, P. Srivastava, D. Avasthi, D. Kabiraj, and J. Pivin, “Synthesis and characterization of ni-doped zno: A transparent magnetic semiconductor,” *Journal of Magnetism and Magnetic Materials*, vol. 320, no. 24, pp. 3347 – 3351, 2008.
- [106] R. W. Chantrell and E. P. Wohlfarth, “Rate dependence of the field-cooled magnetisation of a fine particle system,” *physica status solidi (a)*, vol. 91, no. 2, pp. 619–626, 1985.
- [107] S. D. S. D. Liu, Yi, *Handbook of Advanced Magnetic Materials*. Springer, 2006.
- [108] N. A. Usov, “Numerical simulation of field-cooled and zero field-cooled processes for assembly of superparamagnetic nanoparticles with uniaxial anisotropy,” *Journal of Applied Physics*, vol. 109, no. 2, pp. –, 2011.
- [109] J.-Y. Bigot, M. Vomir, and E. Beaurepaire, “Coherent ultrafast magnetism induced by femtosecond laser pulses,” *Nat Phys*, vol. 5, pp. 515–520, Jul 2009.
- [110] R. F. L. Evans, T. A. Ostler, R. W. Chantrell, I. Radu, and T. Rasing, “Ultrafast thermally induced magnetic switching in synthetic ferrimagnets,” *Applied Physics Letters*, vol. 104, no. 8, pp. –, 2014.
- [111] M. O. A. Ellis, T. A. Ostler, and R. W. Chantrell, “Classical spin model of the relaxation dynamics of rare-earth doped permalloy,” *Phys. Rev. B*, vol. 86, p. 174418, Nov 2012.
- [112] A. M.B.Agranat, S.I.Ashitkov and G.I.Rukman, “Interaction of picosecond laser pulses with the electron, spin, and phonon subsystems of nickel,” *Zh. Eksp. Teor. Fiz*, vol. 86, pp. 1376–1379, 1984.
- [113] J. Hohlfeld, E. Matthias, R. Knorren, and K. Bennemann, “Nonequilibrium magnetization dynamics of nickel,” *Phys. Rev. Lett.*, vol. 78, pp. 4861–4864, Jun 1997.
- [114] B. Koopmans, J. Ruigrok, F. Longa, and W. de Jonge, “Unifying ultrafast magnetization dynamics,” *Phys. Rev. Lett.*, vol. 95, p. 267207, Dec 2005.
- [115] U. Atxitia, O. Chubykalo-Fesenko, R. W. Chantrell, U. Nowak, and A. Rebei, “Ultrafast spin dynamics: The effect of colored noise,” *Phys. Rev. Lett.*, vol. 102, p. 057203, Feb 2009.
- [116] N. Kazantseva, U. Nowak, R. W. Chantrell, J. Hohlfeld, and A. Rebei, “Slow recovery of the magnetisation after a sub-picosecond heat pulse,” *EPL (Europhysics Letters)*, vol. 81, no. 2, p. 27004, 2008.

- [117] C. D. Stanciu, *Laser-Induced Femtosecond Magnetic Recording*. PhD thesis, Radboud University, Institute for Molecules and Materials, <http://www.stanciu.nl/thesis.htm>, 2008.
- [118] T. Popmintchev and at all., “Bright coherent ultrahigh harmonics in the kev x-ray regime from mid-infrared femtosecond lasers,” *Science*, vol. 336, pp. 1287–1291, Dec 2012.
- [119] A. Vaterlaus, T. Beutler, and F. Meier, “Spin-lattice relaxation time of ferromagnetic gadolinium determined with time-resolved spin-polarized photoemission,” *Phys. Rev. Lett.*, vol. 67, pp. 3314–3317, Dec 1991.
- [120] P. B. Corkum, N. H. Burnett, and M. Y. Ivanov, “Subfemtosecond pulses,” *Opt. Lett.*, vol. 19, pp. 1870–1872, Nov 1994.
- [121] W. Hübner and K. Bennemann, “Simple theory for spin-lattice relaxation in metallic rare-earth ferromagnets,” *Phys. Rev. B*, vol. 53, pp. 3422–3427, Feb 1996.
- [122] B. Koopmans, G. Malinowski, F. Dalla Longa, D. Steiauf, M. Fahnle, T. Roth, M. Cinchetti, and M. Aeschlimann, “Explaining the paradoxical diversity of ultrafast laser-induced demagnetization,” *Nat Mater*, vol. 9, pp. 259–265, Mar 2010.
- [123] L. Guidoni, E. Beaurepaire, and J.-Y. Bigot, “Magneto-optics in the ultrafast regime: Thermalization of spin populations in ferromagnetic films,” *Phys. Rev. Lett.*, vol. 89, p. 017401, Jun 2002.
- [124] T. Kampfrath, R. G. Ulbrich, F. Leuenberger, M. Münzenberg, B. Sass, and W. Felsch, “Ultrafast magneto-optical response of iron thin films,” *Phys. Rev. B*, vol. 65, p. 104429, Feb 2002.
- [125] E. Carpena, E. Mancini, C. Dallera, M. Brenna, E. Puppini, and S. De Silvestri, “Dynamics of electron-magnon interaction and ultrafast demagnetization in thin iron films,” *Phys. Rev. B*, vol. 78, p. 174422, Nov 2008.
- [126] B. Koopmans, M. van Kampen, J. Kohlhepp, and W. de Jonge, “Ultrafast magneto-optics in nickel: Magnetism or optics?,” *Phys. Rev. Lett.*, vol. 85, pp. 844–847, Jul 2000.
- [127] J.-Y. Bigot, L. Guidoni, E. Beaurepaire, and P. Saeta, “Femtosecond spectrotemporal magneto-optics,” *Phys. Rev. Lett.*, vol. 93, p. 077401, Aug 2004.
- [128] M. Vomir, L. Andrade, L. Guidoni, E. Beaurepaire, and J.-Y. Bigot, “Real space trajectory of the ultrafast magnetization dynamics in ferromagnetic metals,” *Phys. Rev. Lett.*, vol. 94, p. 237601, Jun 2005.
- [129] J. de Jong, I. Razdolski, A. Kalashnikova, R. Pisarev, A. Balbashov, A. Kirilyuk, T. Rasing, and A. Kimel, “Coherent control of the route of an ultrafast magnetic phase

- transition via low-amplitude spin precession,” *Phys. Rev. Lett.*, vol. 108, p. 157601, Apr 2012.
- [130] J.-U. Thiele, M. Buess, and C. H. Back, “Spin dynamics of the antiferromagnetic-to-ferromagnetic phase transition in ferri on a sub-picosecond time scale,” *Applied Physics Letters*, vol. 85, no. 14, 2004.
- [131] G. Ju, J. Hohlfeld, B. Bergman, R. van de Veerdonk, O. Mryasov, J.-Y. Kim, X. Wu, D. Weller, and B. Koopmans, “Ultrafast generation of ferromagnetic order via a laser-induced phase transformation in ferri thin films,” *Phys. Rev. Lett.*, vol. 93, p. 197403, Nov 2004.
- [132] F. Hansteen, A. Kimel, A. Kirilyuk, and T. Rasing, “Nonthermal ultrafast optical control of the magnetization in garnet films,” *Phys. Rev. B*, vol. 73, p. 014421, Jan 2006.
- [133] F. Hansteen, A. Kimel, A. Kirilyuk, and T. Rasing, “Femtosecond photomagnetic switching of spins in ferrimagnetic garnet films,” *Phys. Rev. Lett.*, vol. 95, p. 047402, Jul 2005.
- [134] A. V. Kimel, A. Kirilyuk, P. A. Usachev, R. V. Pisarev, A. M. Balbashov, and T. Rasing, “Ultrafast non-thermal control of magnetization by instantaneous photomagnetic pulses,” *Nature*, vol. 435, pp. 655–657, Jun 2005.
- [135] T. Gerrits, H. A. M. van den Berg, J. Hohlfeld, L. Bar, and T. Rasing, “Ultrafast precessional magnetization reversal by picosecond magnetic field pulse shaping,” *Nature*, vol. 418, pp. 509–512, Aug 2002.
- [136] J. Hohlfeld, T. Gerrits, M. Bilderbeek, T. Rasing, H. Awano, and N. Ohta, “Fast magnetization reversal of gdfco induced by femtosecond laser pulses,” *Phys. Rev. B*, vol. 65, p. 012413, Dec 2001.
- [137] Y. Acremann, M. Buess, C. H. Back, M. Dumm, G. Bayreuther, and D. Pescia, “Ultrafast generation of magnetic fields in a schottky diode,” *Nature*, vol. 414, pp. 51–54, Nov 2001.
- [138] T. Silva and T. Crawford, “Methods for determination of response times of magnetic head materials,” *Magnetics, IEEE Transactions on*, vol. 35, pp. 671–676, Mar 1999.
- [139] R. R. Subkhangulov, H. Munekata, T. Rasing, and A. V. Kimel, “Laser-induced spin dynamics in ferromagnetic (in,mn)as at magnetic fields up to 7 t,” *Phys. Rev. B*, vol. 89, p. 060402, Feb 2014.
- [140] O. Morandi, P.-A. Hervieux, and G. Manfredi, “Laser induced ultrafast demagnetization in diluted magnetic semiconductor nanostructures,” *The European Physical Journal D*, vol. 52, no. 1-3, pp. 155–158, 2009.

-
- [141] K. M. Whitaker, M. Raskin, G. Kiliani, K. Beha, S. T. Ochsenbein, N. Janssen, M. Fonin, U. Rüdiger, A. Leitenstorfer, D. R. Gamelin, and R. Bratschitsch, “Spin-on spintronics: Ultrafast electron spin dynamics in zno and zn_{1-x}co_x sol-gel films,” *Nano Letters*, vol. 11, no. 8, pp. 3355–3360, 2011. PMID: 21749121.
- [142] C. Zener, “Interaction between the *d*-shells in the transition metals. iii. calculation of the weiss factors in fe, co, and ni,” *Phys. Rev.*, vol. 83, pp. 299–301, Jul 1951.
- [143] A. Barman and A. Haldar, *Solid State Physics, Vol.65 Time-Domain Study of Magnetization Dynamics in Magnetic Thin Films and Micro- and Nanostructures*. Academic Press, 2014.

Publications and Presentations

Publications

- *A Computational Study on Magnetic Effects of $Zn_{1-x}Cr_xO$ Type Diluted Magnetic Semiconductor* (Submitted)
- *Atomistic spin model simulations of Co doped ZnO* (In preparation)
- *Ultrafast laser pulse atomistic spin simulations in transition metal doped ZnO* (In preparation)

Presentations

- *Atomistic spin model simulations on the indirect exchange interactions of Co-doped ZnO.* M Arucu, R F L Evans, T A Ostler, R W Chantrell and S Aktas; Magnetism Conference 2015, 30-31 March 2015, Leeds–UK
- *Using VAMPIRE atomistic spin simulations: Magnetic properties of Ni doped ZnO DMS film.* M Arucu, R F L Evans, T A Ostler, R W Chantrell and S Aktas; FEM-TOMAG Radboud Summer School; 3–15 August 2014; Nijmegen-The Netherlands
- *Atomistic spin model simulations of the magnetic properties of Ni doped ZnO.* M Arucu, R F L Evans, T A Ostler, R W Chantrell and S Aktas; Magnetism Conference 2014, 7-8 April 2014, Manchester–UK
- *“Size effect on magnetic stability of Nano-Particles”.* S Aktas, M Arucu, I P Duru; 3rd International Conference on Superconductivity and Magnetism–ICSM2012, 29 April - 4 May 2012, İstanbul, Turkey

Curriculum Vitae

Personal Information

Address: Department of Physics, University of Marmara, Goztepe Campus 34722 / Kadikoy Istanbul / TURKEY *e-mail:* muhammetarucu@gmail.com *Skype:* muhammetarucu

Education

- **Ph.D:** Department of Physics, Institute of Pure and Applied Sciences, University of Marmara Istanbul-Turkey, 2009-2015, My Supervisors: Professor Sahin Aktas from Marmara University-Turkey and Professor Roy W. Chantrell from University of York-UK.
- **M.S:** Department of Physics, Institute of Pure and Applied Sciences, University of Marmara, 2003-2006, Istanbul-Turkey, “Thesis Title: Investigation of the effects of conducting currents on the phase transition of the magnetic vortex lattice”, My Supervisor: Professor Şahin Aktaş.
- **B.S:** Department of Physics, Faculty of Arts and Sciences, Trakya University 1999-2003 Edirne-Turkey.

Employment

- **Academic Visitor:** The University of York, Department of Physics, Computational Magnetism group at under the supervision of Professor Roy Chantrell. September 2013-May 2015
- **Research Fellow:** Department of Physics, Faculty of Arts and Sciences ,University of Marmara, June 2013-August 2013, Istanbul-Turkey
- **Research Fellow:** Department of Physics, Faculty of Arts and Sciences, Ağrı Ibrahim Çeçen University, September 2010-May 2013, Ağrı-Turkey
- **Lecturer:** Department of educational sciences, Faculty of Education, University of Marmara, September 2006-June 2010, Istanbul-Turkey
- **Physics Teacher:** High School, Ministry of Education Ministry of Education, September 2003-June 2006, Istanbul-Turkey

